Volume 14 | Number 1 | January-December 2025

JCB | Journal of Circulating Biomarkers

ABOUTSCIENCE

JCB

GENERAL INFORMATION

Aims and Scope
Journal of Circulating Biomarkers is an international, peer-reviewed, open access, scientific, online only journal, published continually. It focuses on all aspects of the rapidly growing field of circulating blood-based biomarkers and diagnostics using circulating protein and lipid markers, circulating tumor cells (CTC), circulating cell-free DNA (cfDNA) and extracellular vesicles, including exosomes, microvesicles, microparticles, ectosomes and apoptotic bodies. The journal publishes high-impact articles related to circulating biomarkers and diagnostics, ranging from basic science to translational and clinical applications, circulation protein and lipid markers, CTC, cfDNA and extracellular vesicle.

Included within the scope are a broad array of specialties:
Oncology
Immunology
Neurology
Metabolic diseases
Cardiovascular medicine
Diagnostics and therapeutics
Infectious diseases

Abstracting and Indexing
CNKI Scholar
CrossRef
DOAJ
Ebsco Discovery Service
Embase
Google Scholar
J-Gate
OCLC WorldCat
Opac-ACNP (Catalogo Italiano dei Periodici)
Opac-SBN (Catalogo del servizio bibliotecario nazionale)
PubMed Central
ROAD (Directory of Open Access Scholarly Resources)
ScienceOpen Scilit
Scimago
Scopus
Sherpa Romeo
Transpose

Publication process
Peer review
Papers submitted to JCB are subject to a rigorous peer review process, to ensure that the research published is valuable for its readership. JCB applies a single-blind review process and does not disclose the identity of its reviewers.

Lead times
Submission to final decision: 6-8 weeks
Acceptance to publication: 2 weeks

Publication fees
All manuscripts are submitted under Open Access terms. Article processing fees cover any other costs, that is no fee will be applied for supplementary material or for colour illustrations. Where applicable, article processing fees are subject to VAT.

Author information and manuscript submission
For full author guidelines and online submission visit
www.aboutscience.eu

ABOUTSCIENCE

Aboutscience Srl
Piazza Duca d'Aosta, 12 - 20124 Milano (Italy)

Editorial and production enquiries
jcb@aboutscience.eu

Supplements, reprints and commercial enquiries
Lucia Steele - email: lucia.steele@aboutscience.eu

Publication data
eISSN: 1849-4544
Continuous publication
Vol. 14 is published in 2025

JCB
J Circ Biomark 2025; 14: 1-4
ISSN 1849-4544 | DOI: 10.33393/jcb.2025.3396
ORIGINAL RESEARCH ARTICLE

Irisin and Insulin Interplay in Thyroid Disorders: A Pilot Study

Amisha Malhotra, Gayathri M Rao, Aradhana Marathe, Sowmya Ananda Jothi, Vinod Chandran

Department of Biochemistry, Kasturba Medical College Mangalore, Manipal Academy of Higher Education, Manipal, India

ABSTRACT

Background: This research was performed to evaluate Irisin and Insulin concentrations in Thyroid patients.
Material and methods: This investigation was performed as a cross-sectional study within the Biochemistry Department at KMC, Mangalore, and the Central Lab at KMCH-AT, Mangalore. Participants were classified into two cohorts: those having regular thyroid function as well as those having thyroid disorder, including both hypothyroid and hyperthyroid patients, with 28 individuals (n = 28) in each category based on thyroid stimulating hormone (TSH) levels obtained during thyroid dysfunction screenings. Socio-demographic variables like height, weight, and body mass index were calculated, along with the assessment of hypertensive or hypotensive conditions. Insulin levels were quantified using an automated analyzer system. Statistical analyses were performed utilizing Easy-R (EZR) version 1.55, developed by Jichi Medical University in Saitama, Japan. The normal distribution of the parameters was evaluated through normality tests, with t-tests and Kruskal-Wallis tests applied as appropriate.
Results: Irisin levels significantly declined in hypothyroid individuals while showing an insignificant rise in hyperthyroidism. Insulin levels significantly increased in hyperthyroid patients compared to normal and hypothyroid groups. A positive correlation between insulin and irisin was found in hypothyroidism, while a negative correlation was observed in hyperthyroidism.
Conclusion: Preliminary findings of this study indicate a potential interdependence between Irisin and thyroid levels. Investigating the interaction between the thyroid profile and irisin can pave the way for considering irisin as a biomarker for novel treatment strategies in thyroid disorders and metabolic conditions.

Keywords: Adipose tissue, Irisin, Metabolic changes, Thyroid disorders

Introduction

Sedentary behavior is related to a greater likelihood of various health disorders like obesity, diabetes, cardiac disorder, certain cancers, as well as neurological disorders. Irisin, a hormone produced during exercise, is derived from the proteolysis of FNDC5, a cell membrane protein, and plays a crucial role in connecting muscles with other tissues. Recent research has highlighted the numerous beneficial effects of irisin, including the browning of adipocytes, modulation of metabolic processes, and regulation of bone metabolism. White adipocytes, which are associated with endocrine functions, can impact various metabolic processes. The uncoupling protein 1 (UCP1), also called thermogenin, is responsible for distinguishing cellular respiration from heat production and is found in the mitochondrial membranes of brown adipose tissue. Beige or brown fat cells produce thermogenic cells, which can help prevent obesity (1).

Thyroid hormones appear to function as natural thermogenins by disrupting the process of mitochondrial ATP synthesis, thereby generating heat instead of producing ATP. These hormones significantly influence lipid profiles and insulin sensitivity, with one potential outcome being obesity (2,3). The incidence of hyperthyroidism is notably higher in Asian populations compared to European populations. Both hyperthyroidism and hypothyroidism are common medical conditions, with spontaneous hypothyroidism occurring in approximately 1% to 2% of the population. Individuals exhibiting clinically or subclinically impaired thyroid function are at an increased risk for cardiovascular issues, complications associated with abnormal lipid metabolism, and disorders of the musculoskeletal system (4).

Received: November 22, 2024
Accepted: May 20, 2025
Published online: June 9, 2025

Corresponding author:
Vinod Chandran
email: vinod.chandran@manipal.edu

Brown adipocytes and skeletal muscle cells, which are derived from myf5-expression, are under the regulation of transcriptional regulators such as PRDM16, PGC1a, and others. A recent animal model study demonstrated that chronic rosiglitazone, a PPARγ agonist, activation of mouse preadipocytes from epididymal white adipose tissue revealed that UCP1-expressing adipocytes have the ability for thermogenesis but lack the expression of BAT transcription factors like ZIC1 and PRDM16. These cells are known as "brute" (brown-in-white) adipocytes. The transition from PGC1 overexpression in mouse skeletal muscle, as well as exercise-induced expression of the FNDC5 gene, has been previously overlooked despite the initial reports of the mouse sequence of FNDC5 in 2002 by two distinct groups. FNDC5 is highly expressed in adult murine tissues but to a lesser extent in skeletal muscle. The protein FNDC5 is a precursor peptide, which, upon proteolytic cleavage, gives rise to irisin. Previous studies have shown that the FNDC5 gene is also associated with the development of myoblasts and neurons (5).

Recent research has shown that irisin has the capacity to impact the functionality of pancreatic islets. More specifically, irisin has been proven to boost insulin production as well as hasten glucose-stimulated insulin release in pancreatic cells by means of a process that relies on protein kinase A (PKA). In situations marked by elevated levels of glucose or fat, irisin has displayed the capability to enlarge cell size while decreasing cell death within pancreatic islets. Additionally, it promotes cell growth, enhances insulin production and secretion, and has the ability to affect insulin signaling. For example, in mouse C2C12 myoblasts, the overexpression of irisin led to heightened glucose absorption, glycogen synthesis, and activation of AMPK/insulin receptor subunit/ERK1/2 following insulin administration. Another recent investigation demonstrated that irisin counteracts the inhibition of insulin signaling caused by palmitic acid in rat cardiomyocytes, underscoring its potential to amplify insulin-triggered glucose absorption through activation (6).

Material and methods

Inclusion criteria

Age group 18-35 years, both male and female, non-alcoholic, non-smoking individuals. Newly diagnosed thyroid disorder patients were included in the study.

Exclusion criteria

Known diabetics, known malignancies, patients with cancer therapy, women with pregnancy, lactation, menopause or on oral contraceptives were excluded.

This investigation was performed as a cross-sectional study within the patients who were referred for thyroid stimulating hormone (TSH) investigations to the Biochemistry laboratory section at the Central Lab at KMCH-AT, Mangaluru. Participants were classified into two groups based on their TSH levels: those with normal thyroid function and those with thyroid disorders, both hypothyroid and hyperthyroid patients, constituting 28 individuals (n = 28) in each group.

Socio-demographic variables like height and weight were recorded, and Body Mass Index was calculated, along with the assessment of hypertensive or hypotensive conditions using medical records. Insulin levels were quantified using ELISA kits obtained from DRG diagnostics. Irisin levels were measured using ELISA kits procured from Origin Labs. (The detection range was 15.63-1000 pg/ml, and sensitivity was 6.9 pg/ml) TSH levels were analyzed by ECLIA using Roche-COBAS Pro Immunomodule autoanalyzer at KMC hospital Attavar. Statistical analysis was performed using EZR (Easy-R) version 1.55, developed by Jichi Medical University in Saitama, Japan. The normal distribution of the parameters was evaluated through normality tests, with t-tests and Kruskal-Wallis tests applied as appropriate.

Results

TABLE 1 - Descriptive statistics of study groups with parameters expressed as Mean ± SD for normal data and median with (Q1, Q3) for skewed data

Parameters	Normal	Hypothyroid	Hyperthyroid
Age	25.89 ± 6.2	26.8 ± 5.09	28.5 ± 4.71
Weight	66.0 ± 13.4	73.0 ± 14.01	62.3 ± 11.33
BMI	23.9 ± 5.17	27.2 ± 4.68	22.6 ± 4.11
Irisin	1.01 (0.44, 1.26)	1.57 (1.27, 1.86)	0.98 (0.5, 1.22)
TSH	2.23 (1.51, 3.08)	6.94 (5.41, 14.4)	0.24 (0.03, 0.40)
Insulin	29.39 (15.35, 67.57)	9.54 (3.72, 33.03)	32.79 (14.43, 87.06)

TABLE 2 - Inter-group comparisons showing p-values (only)

Statistical Analysis	Hyperthyroid vs Hypothyroid	Normal vs Hyperthyroids	Normal vs Hypothyroids	Hyper-Hypo-Normal
TSH	<0.001	<0.001	<0.001	<0.001
Insulin	0.0287	0.954	0.0047	<0.001
Irisin	<0.001	1	<0.001	<0.001
BMI	<0.001	0.307	0.0156	0.00138

The above table shows the level of significance obtained between the three groups ($p < 0.01$). Parametric Independent sample t-test and non-parametric Mann-Whitney U test were done to analyze the data between the two groups.
One-way ANOVA and Kruskal-Wallis were done to find the significant change between all three groups.

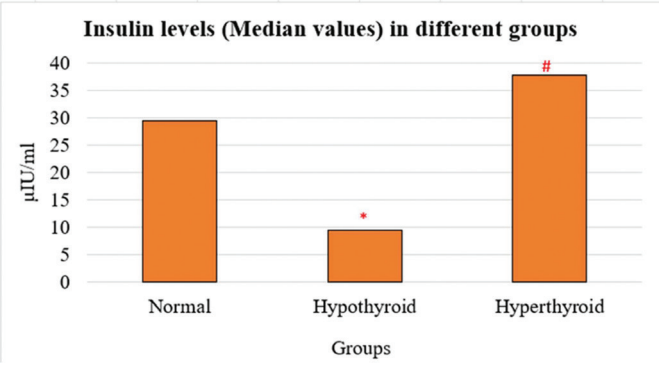

FIGURE 1 - Median values for insulin levels. * denotes $p < 0.005$ in comparison with the normal group. # denotes $p < 0.005$ in comparison with the hyperthyroid group.

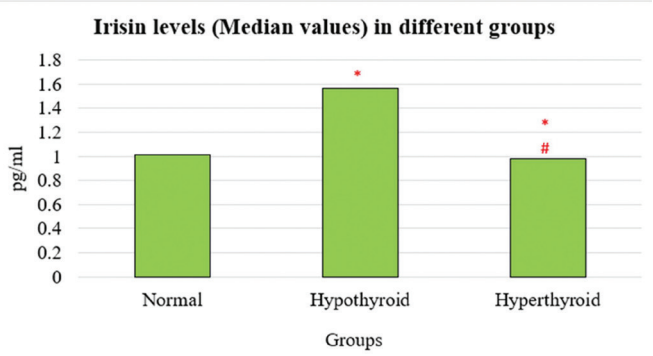

FIGURE 2 - Median values for Irisin levels. * denotes p < 0.005 in comparison with the normal group. # denotes p < 0.005 in comparison with the hyperthyroid group.

There had been a marked decline in irisin concentrations in individuals with hypothyroidism, while there was a statistically insignificant rise in irisin concentrations in those having hyperthyroidism. The difference in irisin levels among the three groups was deemed significant. On the other hand, the insulin levels exhibited a highly significant increase in the hyperthyroid group when compared to both the normal and hypothyroid groups. Additionally, there had been a positive association between insulin as well as irisin concentrations in individuals with hypothyroidism, whereas a negative correlation was noted in those with hyperthyroidism.

Discussion

Thyroid disorders represent chronic endocrine conditions that impact individuals globally. These disorders typically necessitate lifelong management and are linked to greater fatality rates as well as morbidity, especially among older populations. Balance in the circulating thyroid hormones is disturbed, leading to alterations in metabolic parameters and subsequent metabolic dysfunction. The irisin molecule has emerged as a potential agent for the prevention, monitoring, and management of significant metabolic disorders, including polycystic ovarian syndrome (PCOS), obesity, diabetes, chronic renal disorder, ischemic heart disease, as well as high blood pressure (6).

Despite the prevalence of thyroid diseases, the parameters utilized for monitoring treatment remain insufficient. In 2012, researchers identified irisin as a promising myokine released from its precursor protein FNDC5 in response to physical activity, which facilitates the transformation of white adipose tissue (WAT) into brown adipose tissue (BAT). A variety of studies have highlighted the role of irisin in physiological adaptations, particularly concerning exercise. For example, research conducted on murine models examined the role of irisin in promoting the browning of WAT as a result of exercise (7). There is limited or no proof that physical activity has an impact on WAT browning in humans. This investigation examines the connection between "irisin," insulin, and TSH in hypothyroid and hyperthyroid individuals (8,9).

Irisin has the potential to impact the functioning of the thyroid gland. The communication of thyroid hormones occurs through both central and peripheral pathways, affecting energy expenditure. The central pathway involves the hypothalamus, which secretes "thyrotropin-releasing hormone (TRH)" in response to various stimuli like low levels of thyroid hormones or exposure to cold temperatures. Once released into the bloodstream, T4 is transformed into the more active form, T3, in peripheral tissues like the liver, kidneys, and skeletal muscles. T3 then adheres to particular receptors in target tissues, including adipose tissue, muscle, and the central nervous system, activating genes related to metabolism and leading to increased energy consumption. Irisin influences metabolism by promoting the browning of subcutaneous white adipocytes, resulting in increased expression of UCP1 and subsequent enhancements in oxygen consumption and thermogenesis (9).

It is highly likely that fluctuations in irisin levels are influenced by metabolic status due to the intricate interplay between irisin and thyroid hormones. Undoubtedly, further investigation into the physiology of irisin and its regulatory mechanisms will be imperative in the foreseeable future. Recent studies have indicated a correlation between thyroid function and irisin levels. Specifically, thyroid hormones, particularly T3, have been demonstrated to impact the production and release of irisin in skeletal muscle tissue. Animal research has shown that hypothyroidism is linked to reduced irisin expression, while hyperthyroidism is associated with elevated irisin levels. These results align with our own study, raising intriguing questions about the complex relationship between the thyroid gland and the irisin hormone (10).

Insulin and thyroid disorders have been connected, with interactions between the two systems influencing metabolic equilibrium. Thyroid hormones, such as thyroxine (T4) and triiodothyronine (T3), play a crucial role in energy metabolism and glucose utilization. These hormones affect insulin sensitivity and glucose metabolism in various organs, including the liver, muscle, and adipose tissue. Thyroid dysfunction, such as hypothyroidism (reduced thyroid activity) or hyperthyroidism (excessive thyroid activity), can disrupt insulin signaling and glucose metabolism (11).

Conclusion

In our study, we saw an inverse relationship between TSH levels and irisin. In hypothyroid subjects, irisin levels have significantly decreased, and in hyperthyroid subjects, there is a rise, though insignificant. Evaluation of T3, T4, intermediates and enzymes of the thyroid metabolic pathway would provide more insights into the role of Irisin in the regulation of thyroid profile parameters.

Limitations: Among thyroid profiles, Only TSH was estimated, Detailed thyroid function was not considered**,** and subjects were selected randomly and not classified based on gender. Correlation with lifestyle parameters and other demographic parameters were not evaluated.

Disclosures

Conflict of interest: The authors declare no conflict of interest.
Financial support: This research received no specific grant from any funding agency in the public, commercial, or not-for-profit sectors.

Data Availability statement: The data supporting the findings of this study are available from the corresponding author upon reasonable request.
Authors Contribution: AM, SA**:** Data collection and benchwork; VC**:** Protocol preparation; GMR: Manuscript preparation; AM**:** Statistical analysis and data entry.

References

1. Arhire LI, Mihalache L, Covasa M. Irisin: a hope in understanding and managing obesity and metabolic syndrome. Front Endocrinol (Lausanne). 2019;10:524. CrossRef
2. Khassawneh AH, Al-Mistarehi AH, Zein Alaabdin AM, et al. Prevalence and predictors of thyroid dysfunction among type 2 diabetic patients: a case-control study. Int J Gen Med. 2020;13:803-816. CrossRef
3. Yang N, Zhang H, Gao X, et al. Role of irisin in Chinese patients with hypothyroidism: an interventional study. *J Int Med Res*. 2019;47(4):1592-1601. CrossRef PubMed
4. Yosaee S, Basirat R, Hamidi A, et al. Serum irisin levels in metabolically healthy versus metabolically unhealthy obesity: a case-control study. *Med J Islam Repub Iran*. 2020;34:46. CrossRef
5. Mai S, Grugni G, Mele C, et al. Irisin levels in genetic and essential obesity: clues for a potential dual role. Sci Rep. 2020;10(1):1020. CrossRef
6. Martinez Munoz IY, Camarillo Romero EDS, et al. Irisin a novel metabolic biomarker: present knowledge and future directions. Int J Endocrinol. 2018;2018:7816806. CrossRef
7. Shao L, Li H, Chen J, et al. Irisin promotes the browning of white adipose tissue via AMPKα1 activation. Steroids. 2022;183:109031. CrossRef
8. Qiu S, Bosnyák E, Mutch DM. Exercise-mediated browning of white adipose tissue: a review. Int J Mol Sci. 2021; 22(23):13094. CrossRef
9. Li M, Yang M, Zhou X, et al. Elevated circulating levels of irisin and the effect of metformin treatment in women with polycystic ovary syndrome [published correction appears in J Clin Endocrinol Metab. 2015 Aug;100(8):3219. J Clin Endocrinol Metab. 2015;100(4):1485-1493. CrossRef
10. Gesing A, Lewiński A, Karbownik-Lewińska M. The thyroid gland and the process of aging; what is new? Thyroid Res. 2012;5(1):16. CrossRef
11. Galofré JC, Pujante P, Abreu C, et al. Relationship between thyroid-stimulating hormone and insulin in euthyroid obese men. Ann Nutr Metab. 2008;53(3-4):188-194. CrossRef PubMed

JCB
J Circ Biomark 2025; 14: 5-11
ISSN 1849-4544 | DOI: 10.33393/jcb.2025.3175
ORIGINAL RESEARCH ARTICLE

Soluble interleukin-33 receptor (sST-2): a novel marker for assessing cardiovascular risk in rheumatoid arthritis

Inga Claus[1,2], Meike Hoffmeister[3,4], Constantin Remus[1,2], Werner Dammermann[4,5], Ourania Gioti[1], Oliver Ritter[2,4], Daniel Patschan[2,4], Susann Patschan[1,2]

[1]Health Center of the Brandenburg University Hospital, Brandenburg Medical School (Theodor Fontane), Brandenburg an der Havel - Germany
[2]Department of Internal Medicine I - Cardiology, Nephrology and Internal Intensive Medicine, Brandenburg University Hospital, Brandenburg Medical School (Theodor Fontane), Brandenburg an der Havel - Germany
[3]Institute of Biochemistry, Brandenburg Medical School (Theodor Fontane), Brandenburg an der Havel - Germany
[4]Faculty of Health Sciences (FGW), joint faculty of the University of Potsdam, the Brandenburg Medical School Theodor Fontane and the Brandenburg Technical University Cottbus-Senftenberg, Cottbus - Germany
[5]Department of Internal Medicine II Gastroenterology, Hepatology, Endocrinology, Brandenburg University Hospital, Brandenburg Medical School (Theodor Fontane), Brandenburg an der Havel - Germany

ABSTRACT

Background: Rheumatoid arthritis (RA) is the most common inflammatory rheumatic disease, and it significantly increases the risk of cardiovascular disease and death. The evaluation of cardiovascular risk (CVR) is crucial in these patients, but it may be underestimated using the current criteria, as they do not include nontraditional CVR factors. Soluble ST-2, which is the circulating form of the IL-33 receptor, has been identified as a biomarker for cardiovascular and rheumatic diseases. In this study, we examined the role of sST-2 in assessing CVR in RA.
Methods: Monocentric, retrospective, observational trial. Inclusion of RA patients on variable DMARD therapy. Analysis of RA disease using established scores (DAS 28, VAS, HFQ), clinical findings (number of swollen and painful joints), and laboratory investigation. Documentation of numerous CVR variables. Quantification of soluble sST-2 by ELISA.
Results: In total, 129 individuals were included. Soluble sST-2 did neither correlate nor was associated with any variable of RA disease activity. In contrast, significant associations were identified between sST-2 and a number of established CVR markers.
Conclusions: The data indicates a novel role for sST-2 in CVR prediction in RA.

Keywords: RA, sST-2, Cardiovascular risk, Prediction

Introduction

Rheumatoid arthritis (RA) is the most common entity within inflammatory rheumatic diseases, with a prevalence of approximately 1% in Central Europe and the United States (1,2). It is characterized by chronic synovial inflammation of autoimmune origin, leading to recurrent joint inflammation with a typical pattern of involvement. If left untreated, RA typically causes irreversible joint and bone damage, potentially resulting in disability for those affected.

In addition to its detrimental effects on joints, tendons, and bones, RA has also been identified as substantial risk factor for cardiovascular morbidity and mortality (3). The risk increases significantly due to the proatherogenic effects of systemic inflammation (4), as well as the hemodynamic and metabolic effects of medications used to control disease activity and progression (5). The influence of drug therapy should not be underestimated. NSAIDs and glucocorticoids have potentially strong proatherogenic effects (6,7). The observation of an increased risk of atherosclerosis in systemic inflammatory conditions was not only made in the case of RA; rather, it is likely to be an almost unspecific phenomenon of chronic inflammatory conditions of autoimmune origin. The development of an EULAR guideline addressing cardiovascular risk (CVR) management in not only RA but also other inflammatory joint disorders is not without rationale (8). Finally, traditional CVR factors accumulate in RA in the same way as in individuals without RA. In general, assessing CVR requires considering various variables, including the severity of arterial hypertension, glucose metabolism, end-organ damage, and cardiovascular sequelae. The ”2018 ESC/ESH Guidelines for the management of arterial hypertension“ (9), for example, provides a summary of relevant recommendations. However, these and other strategies used for evaluating CVR may not effectively identify the risk in patients with RA or other immune-mediated inflammatory disorders. The incorporation of CVR biomarkers has been suggested as a promising strategy in this regard (10–12).

Received: June 21, 2024
Accepted: July 7, 2025
Published online: July 28, 2025

Corresponding author:
Susann Patschan
email: spatschan@gmail.com

The cytokine Interleukin-33 (IL-33) belongs to the Interleukin-1 family (13). In RA and other autoimmune diseases, it is believed to play a crucial role in facilitating interactions between macrophages, mast cells, and other cell types (14). Its receptor, ST-2 has been identified on cell membranes and in the extracellular fluid, the latter being defined as soluble ST-2 (sST-2) (15). The circulating IL-33 receptor isoform has been evaluated as a biomarker in rheumatic (16,17) and cardiovascular diseases (18–20). In a 2022 published study by Erfurt and colleagues (21), sST-2 was identified as a predictor of in-hospital survival in patients with acute kidney injury.

The aim of this study was to analyze the role of soluble ST-2 (sST-2) in assessing CVR and disease activity in patients with RA.

Methods

Design

Monocentric, retrospective, observational trial. The study was formally approved by the ethics committee of the Brandenburg Medical School (E-01-20200316). All participants provided written consent by signing a consent form.

Patients

All patients were recruited from the rheumatology outpatient clinic of the Health Center of the Brandenburg University Hospital (Brandenburg Medical School). Inclusion criteria were: diagnosis of RA according to the 'ACR/EULAR 2010 rheumatoid arthritis classification criteria' (22). Additional inclusion criteria were as follows: individuals aged between 18 and 90 years, of any gender, with newly initiated or established disease receiving treatment with one or more conventional or biologic disease-modifying anti-rheumatic drugs, and variable daily prednisolone doses adjusted based on disease activity. Exclusion criteria consisted of uncontrolled psychiatric disorders, presence of additional autoimmune-mediated diseases, uncontrolled infectious diseases such as HIV, hepatitis B or C, and tuberculosis, uncontrolled drug or alcohol addiction, and pregnancy. The following patient characteristics were collected: nationality, height, weight, concurrent diseases, medications, smoking status, and family history of rheumatoid arthritis. Disease activity was assessed using the DAS28-CRP score. Remission, low, moderate, and high disease activity were defined by scores of <2.6, 2.6 to 3.2, 3.2 to 5.1, and >5.1, respectively. Additional tools for measuring disease activity included the visual analog scale (VAS), which ranges from 0 (no pain) to 10 (maximum pain imaginable), as well as the assessment of swollen and painful joints, and the Hannover Functional Questionnaire (HFQ) (23). The following therapy-related data were collected: current DMARD therapy (active substance and dosage), NSAID intake (active substance, dosage, and frequency of intake), and daily prednisolone dosage in mg. The assessment of CVR was conducted by capturing the following morbidities and laboratory parameters: arterial hypertension, diabetes mellitus including HbA1C (%), past and current smoking, total cholesterol (mmol/l), LDL (mmol/l), HDL (mmol/l), and Lp(a) (nmol/l). Various additional laboratory parameters were measured, including rheumatoid factor (RF) and anti-citrullinated protein antibodies (ACPA) titers, CRP levels (mg/l), complete blood count, serum creatinine (micromol/l), sodium, potassium, AST (U/l), ALT (U/l), (U/l), and proteinuria (defined as Urine Proteine Creatinine-Ratio – UPCR – of >0.3 g/g in Spot Urine).

Quantification of serum soluble Interleukin-33 receptor

Quantification of serum soluble Interleukin-33 receptor (sST-2) was performed using an ELISA method as described in detail by Erfurt and colleagues (21). The commercially available kit used was the Human ST2/IL-33R Quantikine ELISA Kit (DST 200, R&D).

Statistics

Initially, categorical data were analyzed by the Chi-Squared test. Non-categorical data were assessed for normality using the Kolmogorov-Smirnov test. Normally distributed data were compared using the t-test for two groups or the Mann-Whitney test for more than two groups. Non-normally distributed data were compared using ANOVA for two groups or the Kruskal-Wallis test for more than two groups. Correlation analyses were conducted using the Pearson correlation coefficient. Statistical significance was defined as a p-value below 0.05. Results were reported as percentages or as median with interquartile range (IQR), or as mean with standard error of the mean (SEM). All statistical analyses were conducted using the WIZARD application for the MacOS (version 2.0.14, developed by Evan Miller).

Results

Patients

A total of 129 patients were included in the study, with 87 (67.4%) being females and 42 (32.6%) being males. The average age of all individuals was 62.3 ± 12 years. The average height was 1.67 ± 0.09 meters, and the mean weight was 81.4 ± 17.2 kilograms. Rheumatoid factor (RF) and/or ACPA were detected in 73.6% of the patients. The mean DAS 28 at inclusion was 3.6 ± 1.5. The following disease-modifying anti-rheumatic drugs (DMARDs) were used: methotrexate (MTX) alone in 27.1% of cases, MTX in combination with either leflunomide, sulfasalazine, or biologics in 27.1% of cases, a MTX-free regimen in 16.3% of cases, and no DMARD at all in 29.5% of cases. In 26.4% of cases, patients were included before initiating any DMARD therapy. Table 1 summarizes all baseline characteristics, including morbidities, medication, and the results of CVR assessment.

sST-2 and RA disease activity and management

The serum levels of sST-2 did not show a significant correlation with the DAS 28 (p = 0.63). Additionally, there was no significant correlation observed between sST-2 levels and the HFQ (p = 0.19). The ratings on the visual analog scale were assigned to one of six categories (VAS 0≤ and <1, 1≤ and <3, 3≤ and <4, 4≤ and <5, 5≤ and <7, 7≤ and <10). Similar sST-2 concentrations were found in all categories (p = 0.067). Also, there were no correlations between sST-2 and the numbers of swollen or painful small or large joints, respectively (p-values: swollen small – 0.31, painful small – 0.66, swollen

TABLE 1 - Baseline characteristics of all included patients (abbreviations: SD – standard deviation; m – metres; kg – kilograms; DMARD – Disease Modifying Anti-Rheumatic Drugs; VAS – Visual Analogue Scale; HFQ – Hannover Functional Questionnaire; NSAID – Non-Steroidal Anti-Inflammatory Drugs)

Variable	Result
gender	females 87, males 42
age (years ± SD)	62.3 ± 12
height (mean m ± SD)	1.76 ± 0.09
weight (mean kg ± SD)	81.4 ± 17.2
DAS 28 (mean ± SD)	3.6 ± 1.5
VAS (mean ± SD)	4.1 ± 2.5
HFQ (mean % ± SD)	73.6 ± 23.2
DMARD therapy (substance in n)	
no DMARD	4
early disease, untreated	34
MTX alone	35
MTX + other	21
other	
seropositivity (%)	73.6
C-reactive protein (mean mg/l ± SD)	5.7 ± 9.7
Erythrocyte Sedimentation Rate (ESR) in hour 1 (mean mm ± SD)	20.5 ± 15.5
serum creatinine (mean micromol/l ± SD)	72.4 ±1 6.5
total cholesterol (mean mmol/l ± SD)	5.4 ± 1.1
LDL (mean mmol/l ± SD)	3.1 ± 0.9
HbA1C (mean % ± SD)	5.7 ± 0.7
NT-proBNP (mean pg/mL ± SD)	188.7 ± 410
proteinuria (n)	57
regular NSAID intake (n)	33
arterial hypertension (%)	65.9
diabetes mellitus (%)	15.5
coronary artery disease (CAD) (%)	9.3
family history of CAD (%)	26.4
smoking (%)	32
stress (%)	34.9
regular exercise (%)	41.1
regular alcohol consumption (%)	40.5
pulmonary disease (%)	12.4
osteoporosis (%)	16.3
history of neoplasia (%)	6.2
ESR (mean mm in hour 1 ± SD)	19.3 ± 15.9
Framingham score (mean ± SD)	9.4 ± 8.1

large – 0.45, painful large – 0.26). No significant differences were found between the 5 DMARD treatment groups (p = 0.4). If systemic glucocorticoids were used (n = 118), patients were assigned to one of three dosage categories: 0≤ and <2.5 mg daily, 2.5≤ and <5 mg daily, and 5≤ and <20 mg daily. There was once again no significant difference observed in serum sST-2 levels between these categories (p = 0.35). Patients regularly taking NSAIDs did not show different sST-2 concentrations compared to individuals without regular use of NSAIDs (p = 0.28). RF and/or ACPA positive patients did not differ in sST-2 levels compared to seronegative subjects (p = 0.47). Finally, serum sST-2 did not correlate with either C-reactive protein (p = 0.21) or the erythrocyte sedimentation rate in hour 1 (p = 0.13). Table 2 shows all variables and the p-values in detail.

TABLE 2 - sST-2 and RA disease activity (abbreviations: DMARD – Disease Modifying Anti-Rheumatic Drugs; VAS – Visual Analogue Scale; HFQ – Hannover Functional Questionnaire; NSAID – Non-Steroidal Anti-Inflammatory Drugs)

Correlation analysis		
Variable	**p-value**	
DAS 28	0.63	
HFQ	0.19	
number of swollen small joints	0.31	
number of painful small joints	0.66	
number of swollen large joints	0.45	
number of painful large joints	0.26	
C-reactive protein	0.21	
ESR (hour 1)	0.13	
Categorical analysis		
Variable	**Results**	**p-value**
VAS		
0≤ and <1	20,920 ± 2,745 pg/mL	
1≤ and <3	17,816 ± 1,433 pg/mL	
3≤ and <4	14,154 ± 2,191 pg/mL	0.067
4≤ and <5	15,347 ± 3,449 pg/mL	
5≤ and <7	16,560 ± 1,128 pg/mL	
7≤ and <10	18,637 ± 2,065 pg/mL	
DMARD therapy		
no DMARD	12,933 ± 3,981 pg/mL	
early disease, untreated	18,835 ± 1,591 pg/mL	0.4
MTX alone	15,937 ± 915 pg/mL	
MTX + other	15,706 ± 1,274 pg/mL	
other	19,531 ± 2,788 pg/mL	
systemic glucocorticoid therapy		
0≤ and <2.5 mg daily	15,522 ± 1,216 pg/mL	0.35
2.5≤ and <5 mg daily	16,423 ± 1,675 pg/mL	
5≤ and <20 mg daily	18,227 ± 1,136 pg/mL	
regular NSAID intake	yes: 15,939 ± 1,510 pg/mL; no: 17,206 ± 841 pg/mL	0.28
Seropositivity	positive: 16,802 ± 876 pg/mL; negative: 18,045 ± 1,562 pg/mL	0.47

sST-2 and CVR in RA

The analysis of serum sST-2 in relation to various surrogate markers of increased CVR (CVR) revealed numerous significant findings in RA patients. Initially, significantly lower serum levels were observed in individuals with low CVR compared to those with moderate or high CVR according to the Framingham score (low: 14,837 ± 846 pg/mL; moderate: 19,034 ± 1,303 pg/mL; high: 21,685 ± 3,106 pg/mL; p = 0.009). Soluble ST-2 was also found to have a positive correlation with the Framingham score (p < 0.001). It was higher in males than females (19,550 ± 1,308 pg/mL versus 15,961 ± 919 pg/mL; p=0.007) and positively correlated with age (p = 0.004). Patients who reported regular stress showed lower concentrations compared to those without stress (14,908 ± 1,055 pg/mL versus 18,558 ± 1,023 pg/mL; p = 0.02). Regular physical activity was also associated with lower levels (14,578 ± 945 pg/mL versus 18,909 ± 1,075 pg/mL; p = 0.005). A negative family history of CAD and the presence of CAD in the patients themselves were associated with higher sST-2 (18,432 ± 973 pg/mL versus 13,625 ± 1,005 pg/mL; p = 0.004 and 22,824 ± 2,367 pg/mL versus 16,546 ± 790 pg/mL; p = 0.006). The intake of statins (20,067 ± 1,616 pg/mL versus 16,278 ± 852 pg/mL; p = 0.009), aspirin (20,328 ± 1,925 pg/mL versus 16,508 ± 823 pg/mL; p = 0.02), and antidiabetic medications (24,982 ± 3,712 pg/mL versus 16,250 ± 703 pg/mL; p = 0.01) were all associated with higher levels of sST-2, respectively. Diabetic individuals also showed higher sST-2 than non-diabetics (24,551 ± 2,493 pg/mL versus 15,768 ± 712 pg/mL; p < 0.001). Positive correlations were identified between sST-2 and NT-proBNP (p < 0.001), serum creatinine (p < 0.001), HbA1C (p < 0.001), ALT (p = 0.02), and gGT (p = 0.001). Finally, negative correlations were found between the marker and total cholesterol (p = 0.009) and LDL (p = 0.005). Table 3 and Figure 1 show all analyzed variables and the significant findings in detail.

TABLE 3 - sST-2 and CVR variables in RA – significant findings (LDL – low density lipoproteins; ALT – alanine aminotransferase; gGT – gamma glutamyltransferase)

Correlation analysis		
Variable	**p-value**	
Age	0.004, r = 0.24	
Framingham score	<0.001, r = 0.31	
serum creatinine	<0.001, r = 0.35	
HbA1C	<0.001, r = 0.34	
NT-proBNP	<0.001, r = 0.37	
total cholesterol	0.009, r = -0.22	
LDL	0.005, r = -0.24	
ALT	0.02, r = 0.19	
gGT	<0.001, r = 0.28	
Categorical analysis		
Variable	**Results**	**p-value**
gender	females: 15,961 ± 919 pg/mL; males: 19,550 ± 1,308 pg/mL	0.007
CVR		
low	14,837 ± 846 pg/mL	0.009
moderate	19,034 ± 1,303 pg/mL	
high	21,685 ± 3,106 pg/mL	
stress	stress: 14,908 ± 1,055 pg/mL; no stress: 18,558 ± 1,023 pg/mL	0.02
regular physical activity	physical activity: 14,578 ± 945 pg/mL; no physical activity: 18,909 ± 1,075 pg/mL	0.005
family history of CAD	family history: 13,625 ± 1,005 pg/mL; no family history: 18,432 ± 973 pg/mL	0.004
CAD	CAD: 22,824 ± 2,367 pg/mL; no CAD: 16,546 ± 790 pg/mL	0.006
aspirin	aspirin: 20,328 ± 1,925 pg/mL; no aspirin: 16,508 ± 823 pg/mL	0.02
statins	statins: 20,067 ± 1,616 pg/mL; no statins: 16,278 ± 852 pg/mL	0.009
antidiabetic medication	antidiabetic medication: 24,982 ± 3,712 pg/mL; no antidiabetic medication: 16,250 ± 703 pg/mL	0.01
diabetes mellitus	diabetes mellitus: 24,551 ± 2,493 pg/mL; no diabetes mellitus: 15,768 ± 712 pg/mL	<0.001

Discussion

Our study reveals numerous associations between sST-2 and anamnestic, clinical, and laboratory surrogate markers of increased CVR in individuals with seropositive and seronegative rheumatoid arthritis under DMARD therapy. Most variables that were characterized by differences in sST-2 concentration indicate higher levels in the presence of a proatherogenic surrogate marker: male gender, older age, lack of physical activity, diabetes mellitus, including HbA1C, NT-proBNP, coronary heart disease, and finally the Framingham score itself. However, the intake of aspirin, statins, or antidiabetic drugs were also associated with higher sST-2 levels. It is important to consider that direct pharmacological impacts on sST-2 homeostasis cannot be definitively excluded. Finally, the marker correlated inversely with a positive family history of cardiovascular diseases, specifically coronary heart disease, and with total cholesterol and LDL. The latter could be explained by the fact that despite the increased CVR, patients with active Rheumatoid Arthritis (RA) have paradoxically reduced lipid levels (24-26). In the past 10-15 years, it has become increasingly evident how much rheumatoid arthritis (RA) contributes to both cardiovascular morbidity and the associated risk of death (3,7,27). The increase in risk is the combined result of the inflammatory activity of the underlying disease itself, as well as the almost routine proatherogenic substance groups such as glucocorticoids and NSAIDs (5,10). The quantification of CVR is of utmost clinical and prognostic significance in rheumatoid arthritis (RA). According to the 2015/2016 updated EULAR recommendations for CVR management in patients with RA and other inflammatory joint disorders, CVR assessment should be performed at least every 5 years based on national guidelines (8). Considering the possibility of underestimating

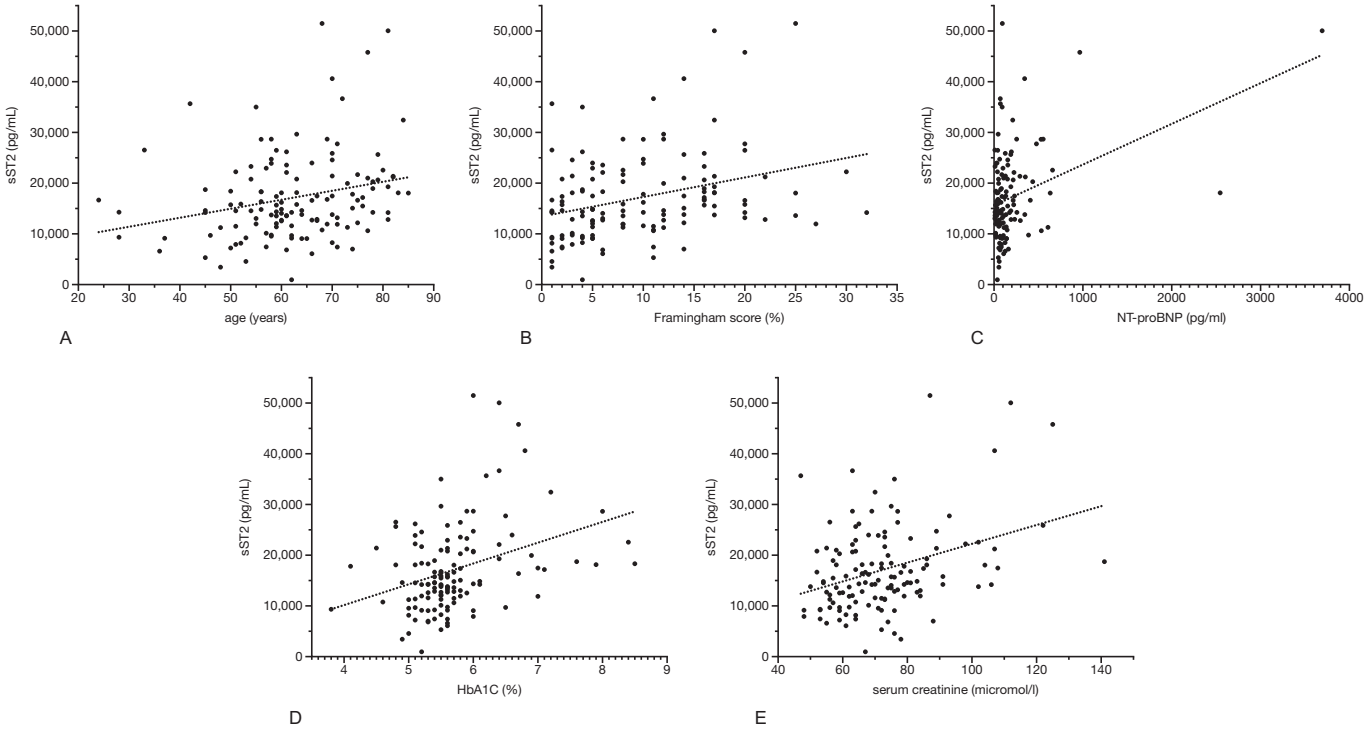

FIGURE 1 - Positive correlations between sST-2 and selected CVR variables (for p-values see text and Table 3).

the CVR in RA patients using prediction models for the general population, they concluded to an adaptation by adding a 1.5 multiplication factor for the calculated CVR. The same approach is recommended by the 2021 ESC guidelines on cardiovascular disease prevention in clinical practice (28).

In this regard, according to the guidelines of the European Society of Cardiology (ESC) (9), CVR stratification must take into account five categories: the severity of potential arterial hypertension, the presence of a diabetic metabolic condition, additional CVR factors, end-organ damage, and cardiovascular sequelae or comorbidities. The specifications do not take into account the potential additive increase in risk due to the presence of a proatherogenic inflammatory disorder or the regular use of substances such as glucocorticoids or leflunomide (29). They also do not consider the influence of antiatherogenic agents like methotrexate (30). It has been shown that chronic inflammatory diseases increase the risk of vascular calcification, not only in the case of RA. Individuals with Spondyloarthritis are also affected by this issue (31). Patients with chronic inflammatory rheumatic diseases may evade the CVR stratification system published by the ESC. This potential gap in the detection of a higher CVR could potentially be reduced in the future through the addition of biomarkers, such as sST-2.

Popsecu et al. (10) recently summarized relevant studies on this topic. They also discussed markers whose activities correlate with CVR in RA, such as anti-β2GPI IgA (positive) or miR-425-5p (negative). Curtis and colleagues (11) published a promising approach for biomarker-based CVR prediction in rheumatoid arthritis (RA). Since 2010, the determination of a so-called MBDA score has been offered in the USA, and health insurance companies cover the costs when indicated correctly. The MBDA score, primarily established for assessing RA activity, is calculated based on the quantification of 12 RA-associated biomarkers (such as IL-6, TNF-R1, EGF, and others). In the cited study, the CVR predictive potential of the score was analyzed using a Cox proportional hazards regression model. The model tested the predictive probability of different risk constellations, such as “age and gender” or “age, gender, and smoking.” The MBDA score itself was also considered as a constellation. In total, 30,751 RA patients with a cumulative count of 904 cardiovascular events were included. Ultimately, the MBDA score showed a hazard ratio of 2.89 for cardiovascular events in the following three years. With the increasing prevalence of artificial intelligence algorithms, diagnostic and therapeutic approaches in medicine are expected to undergo fundamental changes also. Al-Maini et al. (12) recently discussed the incorporation of genomic-based biomarkers (GBBM) and non-invasive radiomic-based biomarkers (RBBM) into CVR assessment in RA. They proposed the integration of GBBM and RBBM into the “AtheroEdge model” (AtheroPoint, CA, USA), a deep learning algorithm for CVR risk prediction in RA.

Without doubt, additive biomarkers are gaining recognition in determining which RA patients are particularly at high CVR. sST-2 is the circulating isoform of the IL-33 receptor. In 2011, Hong and colleagues (17) published data on sST-2 in RA, which revealed elevated serum levels of this marker in patients compared to healthy controls. Two additional studies have measured sST-2 levels in adult Still’s disease (32) and Sjögren syndrome (33), both of which found elevated levels of the marker in affected patients. In addition

to inflammatory rheumatic diseases, serum sST-2 has also been studied in cardiovascular disorders, including coronary artery disease, arterial hypertension, arrhythmias, and other conditions (18). A study conducted by our group has identified sST-2 as a novel predictor of survival in patients experiencing newly onset acute kidney injury (21). Therefore, sST-2 is suitable for identifying uncontrolled inflammatory and non-inflammatory disorders. However, it cannot be used as a universal "danger signal" in rheumatic diseases, as it does not provide a comprehensive assessment of RA disease activity on its own.

Limitations

One limitation is the low prevalence of coronary artery disease (CAD) (9.3%) or known CAD risk factors such as diabetes mellitus (15.5%) in the study cohort. Therefore, we cannot conclusively decide whether sST-2 is an even more potent CVR predictor in RA than in individuals without RA. To further enhance the understanding of sST-2 in assessing CVR, it would be beneficial to include larger numbers of RA patients with and without CAD. Another limitation is the lack of comprehensive follow-up data. On one hand, the marker was not found to correlate or be associated with variables of RA disease activity. However, analyzing the serum dynamics of sST-2 over time could potentially provide valuable information for assessing RA activity and for predicting DMARD response.

Conclusions

In RA, sST-2 may be proposed as promising marker of increased CVR and additional studies must clarify its exact role in the identification of those individuals that potentially escape traditional CVR risk profiling but may benefit from additional sST-2 analysis.

Declarations

Author contributions

Inga Claus collected blood samples and clinical data from all included patients. Meike Hoffmeister conducted ELISA analyses. Constantin Remus assisted in patient recruitment and data collection. Werner Dammermann aided in data analysis. Ourania Gioti prepared tables. Oliver Ritter aided in data analysis and figure preparation. Daniel Patschan analyzed data, prepared figures, and assisted in writing. Susann Patschan designed the study, analyzed data, and wrote the article. All authors approved the final version of the article.

Disclosures

Conflict of interest: The authors declare that they have no conflicts of interest.

Financial support: Funded by the Brandenburg Medical School publication fund supported by the Ministry of Science, Research and Cultural Affairs of the State of Brandenburg.

Data availability statement: All data will be provided by the corresponding author upon reasonable request.

References

1. Myasoedova E, Crowson CS, Kremers HM, et al. Is the incidence of rheumatoid arthritis rising? Results from Olmsted County, Minnesota, 1955-2007. Arthritis Rheum. 2010;62(6):1576-1582. CrossRef PubMed
2. Hunter TM, Boytsov NN, Zhang X, et al. Prevalence of rheumatoid arthritis in the United States adult population in healthcare claims databases, 2004-2014. Rheumatol Int. 2017;37(9):1551-1557. CrossRef PubMed
3. Fragoulis GE, Panayotidis I, Nikiphorou E. Cardiovascular risk in rheumatoid arthritis and mechanistic links: from pathophysiology to treatment. Curr Vasc Pharmacol. 2020;18(5):431-446. CrossRef PubMed
4. Meng H, Cheng IT, Yan BPY, et al. Moderate and high disease activity levels increase the risk of subclinical atherosclerosis progression in early rheumatoid arthritis: a 5-year prospective study. RMD Open. 10. Januar 2024;10(1):e003488. CrossRef
5. Choy E, Ganeshalingam K, Semb AG, et al. Cardiovascular risk in rheumatoid arthritis: recent advances in the understanding of the pivotal role of inflammation, risk predictors and the impact of treatment. Rheumatology (Oxford). 2014;53(12):2143-2154. CrossRef PubMed
6. Atchison JW, Herndon CM, Rusie E. NSAIDs for musculoskeletal pain management:current perspectives and novel strategies to improve safety. J Manag Care Pharm. 2013;19(9)(suppl A):S3-S19. PubMed
7. Atzeni F, Rodríguez-Carrio J, Popa CD, et al. Cardiovascular effects of approved drugs for rheumatoid arthritis. Nat Rev Rheumatol. 2021;17(5):270-290. CrossRef PubMed
8. Agca R, Heslinga SC, Rollefstad S, et al. EULAR recommendations for cardiovascular disease risk management in patients with rheumatoid arthritis and other forms of inflammatory joint disorders: 2015/2016 update. Ann Rheum Dis. 2017;76(1):17-28. CrossRef PubMed
9. Williams B, Mancia G, Spiering W, et al. 2018 ESC/ESH Guidelines for the management of arterial hypertension. Eur Heart J. 2018;39(33):3021–104. CrossRef
10. Popescu D, Rezus E, Badescu MC, et al. Cardiovascular risk assessment in rheumatoid arthritis: accelerated atherosclerosis, new biomarkers, and the effects of biological therapy. Life Basel Switz. 2023;13(2):319. CrossRef
11. Curtis JR, Xie F, Crowson CS, et al. Derivation and internal validation of a multi-biomarker-based cardiovascular disease risk prediction score for rheumatoid arthritis patients. Arthritis Res Ther. 4. 2020;22(1):282. CrossRef
12. Al-Maini M, Maindarkar M, Kitas GD, et al. Artificial intelligence-based preventive, personalized and precision medicine for cardiovascular disease/stroke risk assessment in rheumatoid arthritis patients: a narrative review. Rheumatol Int. 2023;43(11):1965-1982. CrossRef PubMed
13. Fields JK, Günther S, Sundberg EJ. Structural basis of IL-1 family cytokine signaling. Front Immunol. 2019;10:1412. CrossRef PubMed
14. Ouyang T, Song L, Fang H, et al. Potential mechanistic roles of Interleukin-33 in rheumatoid arthritis. Int Immunopharmacol. 2023;123:110770. CrossRef PubMed
15. Bao YS, Na SP, Zhang P, et al. Characterization of interleukin-33 and soluble ST2 in serum and their association with disease severity in patients with chronic kidney disease. J Clin Immunol. 2012;32(3):587-594. CrossRef PubMed
16. Shakerian L, Kolahdooz H, Garousi M, et al. IL-33/ST2 axis in autoimmune disease. Cytokine. 2022;158:156015. CrossRef PubMed

17. Hong YS, Moon SJ, Joo YB, et al. Measurement of interleukin-33 (IL-33) and IL-33 receptors (sST2 and ST2L) in patients with rheumatoid arthritis. J Korean Med Sci. 2011;26(9):1132-1139. CrossRef PubMed
18. Dudek M, Kałużna-Oleksy M, Migaj J, et al. Clinical value of soluble ST2 in cardiology. Adv Clin Exp Med. 2020;29(10): 1205-1210. CrossRef PubMed
19. Zagidullin N, Motloch LJ, Gareeva D, et al. Combining novel biomarkers for risk stratification of two-year cardiovascular mortality in patients with ST-elevation myocardial infarction. J Clin Med. 18. 2020;9(2):550. CrossRef
20. Bayes-Genis A, Richards AM, Maisel AS, et al. Multimarker testing with ST2 in chronic heart failure. Am J Cardiol. 2015;115(7)(suppl):76B-80B. CrossRef PubMed
21. Erfurt S, Hoffmeister M, Oess S, et al. Soluble IL-33 receptor predicts survival in acute kidney injury. J Circ Biomark. 2022;11:28-35. CrossRef PubMed
22. Kay J, Upchurch KS. ACR/EULAR 2010 rheumatoid arthritis classification criteria. Rheumatology (Oxford). 2012;51(suppl 6): vi5-vi9. CrossRef PubMed
23. Lautenschläger J, Mau W, Kohlmann T, et al. [Comparative evaluation of a German version of the Health Assessment Questionnaire and the Hannover Functional Capacity Questionnaire]. Z Rheumatol. 1997;56(3):144-155. PubMed
24. Myasoedova E, Crowson CS, Kremers HM, et al. Lipid paradox in rheumatoid arthritis: the impact of serum lipid measures and systemic inflammation on the risk of cardiovascular disease. Ann Rheum Dis. 2011;70(3):482-487. CrossRef PubMed
25. Toms TE, Panoulas VF, Douglas KMJ, et al. Are lipid ratios less susceptible to change with systemic inflammation than individual lipid components in patients with rheumatoid arthritis? Angiology. 2011;62(2):167-175. CrossRef PubMed
26. Liao KP, Cai T, Gainer VS, et al. Lipid and lipoprotein levels and trend in rheumatoid arthritis compared to the general population. Arthritis Care Res (Hoboken). 2013;65(12):2046-2050. CrossRef PubMed
27. England BR, Thiele GM, Anderson DR, et al. Increased cardiovascular risk in rheumatoid arthritis: mechanisms and implications. BMJ. 23. 2018;361:k1036. CrossRef
28. Visseren FLJ, Mach F, Smulders YM, et al. 2021 ESC Guidelines on cardiovascular disease prevention in clinical practice. Eur Heart J. 7. 2021;42(34):3227–337. CrossRef
29. Kellner H, Bornholdt K, Hein G. Leflunomide in the treatment of patients with early rheumatoid arthritis--results of a prospective non-interventional study. Clin Rheumatol. 2010;29(8): 913-920. CrossRef PubMed
30. Roubille C, Richer V, Starnino T, et al. The effects of tumour necrosis factor inhibitors, methotrexate, non-steroidal anti-inflammatory drugs and corticosteroids on cardiovascular events in rheumatoid arthritis, psoriasis and psoriatic arthritis: a systematic review and meta-analysis. Ann Rheum Dis. 2015;74(3):480-489. CrossRef PubMed
31. Bodur H. Cardiovascular comorbidities in spondyloarthritis. Clin Rheumatol. 2023;42(10):2611-2620. CrossRef PubMed
32. Han JH, Suh CH, Jung JY, et al. Serum levels of interleukin 33 and soluble ST2 are associated with the extent of disease activity and cutaneous manifestations in patients with active adult-onset Still's disease. J Rheumatol. 2017;44(6):740-747. CrossRef PubMed
33. Jung SM, Lee J, Baek SY, et al. The Interleukin 33/ST2 axis in patients with primary Sjögren syndrome: expression in serum and salivary glands, and the clinical association. J Rheumatol. 2015;42(2):264-271. CrossRef PubMed

JCB
J Circ Biomark 2025; 14: 12-20
ISSN 1849-4544 | DOI: 10.33393/jcb.2025.3510
ORIGINAL RESEARCH ARTICLE
Open Access

A comparison of inflammatory markers' potential to predict weight loss in advanced cancer: a prospective observational study

Ola Magne Vagnildhaug[1,2], Ragnhild H. Habberstad[1,2], Øyvind Salvesen[3], Trude R. Balstad[1,4], Asta Bye[5-7], Olav Dajani[5,6], Stein Kaasa[5,6], Pål Klepstad[8,9], Tora S. Solheim[1,2]

[1]Department of Clinical and Molecular Medicine, NTNU – Norwegian University of Science and Technology, Trondheim - Norway
[2]Cancer Clinic, St. Olavs Hospital – Trondheim University Hospital, Trondheim - Norway
[3]Department of Public Health and Nursing, NTNU – Norwegian University of Science and Technology, Trondheim - Norway
[4]Department of Clinical Medicine, Clinical Nutrition Research Group, UiT The Arctic University of Norway, Tromsø - Norway
[5]Regional Advisory Unit for Palliative Care, Department of Oncology, Oslo University Hospital, University of Oslo, Oslo - Norway
[6]European Palliative Care Research Centre (PRC), Department of Oncology, Oslo University Hospital and Institute of Clinical Medicine, University of Oslo, Oslo - Norway
[7]Department of Nursing and Health Promotion, Faculty of Health Sciences, OsloMet-Oslo Metropolitan University, Oslo - Norway
[8]Department of Circulation and Medical Imaging, NTNU – Norwegian University of Science and Technology, Trondheim - Norway
[9]Department of Anesthesiology and Intensive Care Medicine, St Olavs Hospital, Trondheim University Hospital, Trondheim - Norway

ABSTRACT

Background: Systemic inflammation is crucial in cancer cachexia, but the optimal measurement method remains unclear. This study compares markers of systemic inflammation (MoSI) in predicting weight loss in patients with metastatic cancer.

Methods: This prospective, observational multi-center study involved patients undergoing radiotherapy for bone metastases. Baseline assessments included demographics, clinical characteristics, previous weight loss, and appetite loss. MoSI included: C-reactive protein (CRP), albumin, white blood cells, neutrophil-to-lymphocyte ratio, monocyte-to-lymphocyte ratio, interleukin-6 (IL-6), modified Glasgow Prognostic Score (mGPS), and Prognostic Nutritional Index. Body weight was recorded at baseline, 3, and 8 weeks post-radiotherapy. Multiple linear regression assessed MoSI's predictive ability for weight loss, adjusting for previous weight loss, appetite loss, and primary tumour type. Goodness-of-fit was assessed using adjusted R^2.

Results: Out of 574 recruited patients, 540 and 470 were analyzed at 3 and 8 weeks, respectively. The median age (IQR) was 67 (15), 330 (61%) were male, and 397 (74%) had a Karnofsky performance status ≥70. In a base model without MoSI, significant predictors of weight loss at 3 weeks were appetite loss and urological, lung, and gastrointestinal cancer (adjusted R^2 of 0.064), while at 8 weeks, urological and lung cancer were significant (adjusted R^2 of 0.035). At 3 weeks, all MoSI significantly improved the base model, with adjusted R^2 between 0.078 and 0.091. At 8 weeks: CRP, mGPS, albumin and IL-6 improved the model; however only CRP and mGPS retained an adjusted R^2 of ~0.09.

Conclusions: All MoSI predicted weight loss, but CRP and mGPS were the most optimal.

Keywords: Cancer, Cachexia, Biomarkers, Inflammation

Introduction

Cachexia is particularly prevalent in patients with advanced cancer, but also occurs in earlier stages of the disease (1). The condition results from altered metabolism and is characterized by loss of muscle, with or without loss of fat mass. Appetite loss, systemic inflammation, insulin resistance, and increased muscle protein breakdown are frequently associated with cachexia, and unlike undernutrition, cachexia cannot be reversed by nutritional support alone (2).

While cachexia is a major cause of weight loss in patients with cancer, there are also other etiologies of cancer-associated weight loss, such as bowel obstruction, treatment-related nausea or other side effects, and psychosocial factors. Differentiating between etiologies of weight loss or assessing their relative impact remains challenging. This is particularly challenging in clinical studies, where a lack of reliable biomarkers for cancer cachexia can result in

Received: February 27, 2025
Accepted: July 8, 2025
Published online: July 28, 2025

Corresponding author:
Ola Magne Vagnildhaug
email: ola.m.vagnildhaug@ntnu.no

heterogenous study samples. To address this, study selection criteria often include a range of cachexia-associated parameters, such as weight loss, appetite loss, fatigue, various laboratory tests, and primary tumor types highly associated with cachexia (3-5).

Systemic inflammation is integral to the pathophysiology of cachexia (6,7), and this is recognized in the 2011 international consensus paper on the definition of cachexia, but not implemented in the proposed diagnostic criteria, which are based on weight loss and body composition (2). To differentiate between changes in weight and body composition due to either cachexia or undernutrition, the Global Leadership Initiative on Malnutrition (GLIM) has suggested that the presence of systemic inflammation is necessary to diagnose cachexia (8). However, the optimal method to measure systemic inflammation in cancer cachexia is not established.

For a marker of systemic inflammation to be of value in clinical assessment of cachexia, it needs to be easily accessible, reliable, discriminate against other conditions, and have the potential to predict cachexia development. While several inflammatory biomarkers have been associated with cachexia and proposed as potential diagnostic markers (9), their predictive strength has not been directly compared, leaving the choice of biomarker unclear.

Although optimal treatment strategies remain to be established, identifying biomarkers of cachexia is important to identify patients at risk and in need of special follow-up, nutritional advice, and treatment. Additionally, patients with cachexia have a poor prognosis and may have reduced tolerance to anti-cancer treatment (10,11) and identifying the condition can therefore affect cancer treatment decisions. Knowledge of biomarkers may also lead to improved patient selection in cachexia clinical trials and to greater insight into the pathophysiology of cancer cachexia (2,6,7). Moreover, markers of systemic inflammation are increasingly being used as targets for new treatment (12,13).

Our group has previously proposed a model that predicts cachexia development in patients with incurable cancer, identifying primary tumor type, appetite loss, and early weight loss (<5%) as significant predictors (14). A weakness of this model is that it lacks a marker of systemic inflammation.

In order to enable early detection and consequently facilitate prompt management of cachexia, the objective of this study is to evaluate and compare the ability of different markers of systemic inflammation (MoSI) to predict weight loss in a cohort of patients with metastatic cancer.

Material and methods

Patients

This study was a preplanned part of the Palliative Radiotherapy and Inflammation study (PRAIS) (15). Patients were recruited from seven European oncological centers (Norway, Italy, Spain and UK) between December 2013 and December 2017. Key eligibility criteria were age > 18, a verified cancer diagnosis, and about to undergo palliative radiotherapy for painful bone metastases. Other details are published previously (15). The reporting is guided by the STROBE checklist for cohort studies (16).

Assessments

Patients were assessed at baseline and at study visits 3 and 8 weeks after the end of radiotherapy. Age, sex, primary tumor type, and Charlson Comorbidity Index were recorded at baseline. The Patient-Generated Subjective Global Assessment Short Form (PG-SGA SF) was used to assess weight loss in the 6 months prior to baseline (17) and European Organization for Research and Treatment of Cancer Quality of Life Questionnaire (EORTC QLQ) C15 PAL was used to assess appetite loss (18). Appetite loss is scored on a single-item 4-point Likert scale and linearly transformed to a score between 0 and 100, where a higher score indicates worse appetite. Height was recorded at baseline and weight was measured with light clothing at each study visit. In case of missing weight measurements, the patient reported weight was accepted. Weight loss was chosen as the endpoint in this study in favor of cachexia to maximize the use of data. Choosing cachexia as the endpoint in this longitudinal study would necessitate discarding all observations related to patients already suffering from cachexia at baseline. The current definition of cachexia is based on weight loss and body composition, and a change in body composition over time would almost certainly be reflected by weight loss (2).

C-reactive protein (CRP) (mg/L), albumin (g/L), white blood cell count (WBC) (10^9/L), neutrophil to lymphocyte ratio (NLR), monocyte to lymphocyte ratio (MLR), Interleukin-6 (IL-6) (pg/mL), modified Glasgow Prognostic Score (mGPS) and Prognostic Nutritional Index (PNI) were used to assess systemic inflammation at baseline. Clinical chemistry analyses were performed at local laboratory facilities at each study site. IL-6 was included in the analysis because it is a central mediator of cancer cachexia (6) and because we wanted to evaluate the predictive effect of a cytokine alongside more easily accessible MoSI. IL-6 analyses were performed with Bio-Plex Pro™ Human Cytokine Plex-27 Assay (Bio-Rad Laboratories, Hercules, CA, USA) at Nordland Hospital Trust (Bodø, Norway). The mGPS is based on CRP and albumin levels, and patients are scored 0 (CRP ≤ 10 mg/L, any albumin), 1 (CRP > 10 mg/L, albumin ≥ 35 g/L) or 2 (CRP > 10 mg/L, albumin < 35 g/L). PNI is calculated as albumin (g/L) + 5 × lymphocytes (10^9/L). The mGPS and PNI were included in the analyses in addition to CRP, albumin, NLR and MLR because they are well validated, accessible and frequently used scores to assess systemic inflammation and cancer prognosis (19,20). Further details on the analytical methods are published previously (15).

Ethical considerations

This study was approved by The Regional Committee for Medical and Health Research Ethics in Central Norway (2013/1126) as well as medical research ethics committees in each participating country. The study was conducted in keeping with the 1964 Declaration of Helsinki and its later amendments. All patients gave written informed consent prior to the inclusion in the study.

Statistical analysis

Sample size was estimated based on the primary outcome of the PRAIS-study, and not on the outcome used in

this secondary analysis. A detailed justification for the sample size is provided in the protocol paper (21). Descriptive statistics were used to analyze baseline characteristics. To evaluate ability to predict weight loss after 3 and 8 weeks, linear regression was used with percentage weight loss from baseline to 3 and 8 weeks after end of radiotherapy, respectively, as dependent variables. Two base models, one for 3 weeks' weight loss and one for 8 weeks' weight loss, were created with primary tumor type and appetite loss as independent variables, based on a previously published model (14). Both models were adjusted for reported weight loss prior to baseline. The different MoSI were added to the two base models one by one, and adjusted R^2 were used to compare goodness-of-fit between models. CRP, NLR, MLR and IL6 were logarithmically transformed after a sensitivity analysis conducted to determine which inflammatory markers would benefit from such transformation. To aid clinical decision-making, an analysis was performed to find the optimal cutoffs of the best-performing inflammatory marker(s). To accomplish this, regression analyses were performed multiple times with the inflammatory marker dichotomized with consecutive cutoffs, and the optimal cutoff was determined based on which regression model resulted in the highest explained variance in terms of adjusted R^2.

To maximize use of collected data and address bias due to missing data, multiple imputations with chained equations were applied, using all variables included in the regression analyses, as well as Charlson comorbidity index and survival time as auxiliary variables. Ninety imputations were performed. Estimates and variances were combined using Rubin's rules (22). Stata MP ver. 18.0 (College Station, TX, USA) was used for the statistical analysis.

Results

Figure 1 shows the selection of patients for the final analysis. A total of 574 patients were recruited. Two patients were excluded for not meeting inclusion/exclusion criteria, two withdrew before completing the baseline case report form (CRF), and for one patient, the baseline CRF was lost. Additionally, 29 patients died before the first follow-up and 99 patients died before the second follow-up. Consequently, the analysis 3 and 8 weeks after end of radiotherapy included 540 and 470 patients, respectively. Regarding missing data, 210 (38%) at 3 weeks and 189 (40%) at 8 weeks had at least one missing variable. The variable most frequently missing at both 3 and 8 weeks was weight loss with 106 (20%) and 90 (19%) missing observations, respectively. Table 1 shows the baseline characteristics. For the full sample of 540 patients, the median age (IQR) was 67 (15), 210 (39%) were female and 397 (74%) had a Karnofsky performance status of 70 or higher. The mean (SD) patient-reported weight loss prior to baseline was 3.1% (7.8) (2.7 kg [6.1]). The subsample of 470 patients had a slightly longer time since diagnosis, but had otherwise similar baseline characteristics, which are shown in Table 1.

The mean (SD) weight loss from baseline to 3 weeks was 1.5% (4.2) (1.1 kg [3.2]) and the mean (SD) weight loss after 8 weeks was 1.9% (5.6) (1.5 kg [4.1]). Tables 2a and 2b shows the results of the regression analysis. Lung cancer and urological cancer were predictive of weight loss in both 3 and 8 weeks. GI-cancer and appetite loss were predictive of weight loss in 3 weeks, but not in 8 weeks. Adjusted R^2 for the base model was 0.064 in 3 weeks and 0.035 in 8 weeks. All MoSI significantly improved prediction of weight loss in 3 weeks. CRP, Albumin, mGPS, and IL6 improved prediction of weight loss in 8 weeks, of which CRP and mGPS yielded the highest explained variance. Adjusted R^2 for all models using MoSI to predict weight loss in 3 weeks ranged from 0.076 to 0.091. Only the two models using CRP and mGPS maintained this level of goodness-of-fit after 8 weeks, with adjusted R^2 of 0.096 and 0.093, respectively.

As CRP, which proved to be one of the more robust and predictive markers, is a continuous variable, an exploratory analysis was performed to establish the optimal cutoff for predicting weight loss. Figure 2 shows the explained variance of weight loss after 3 and 8 weeks using consecutive cutoffs of CRP from 5 to 100 in increments of 5. A cutoff of 25 yielded

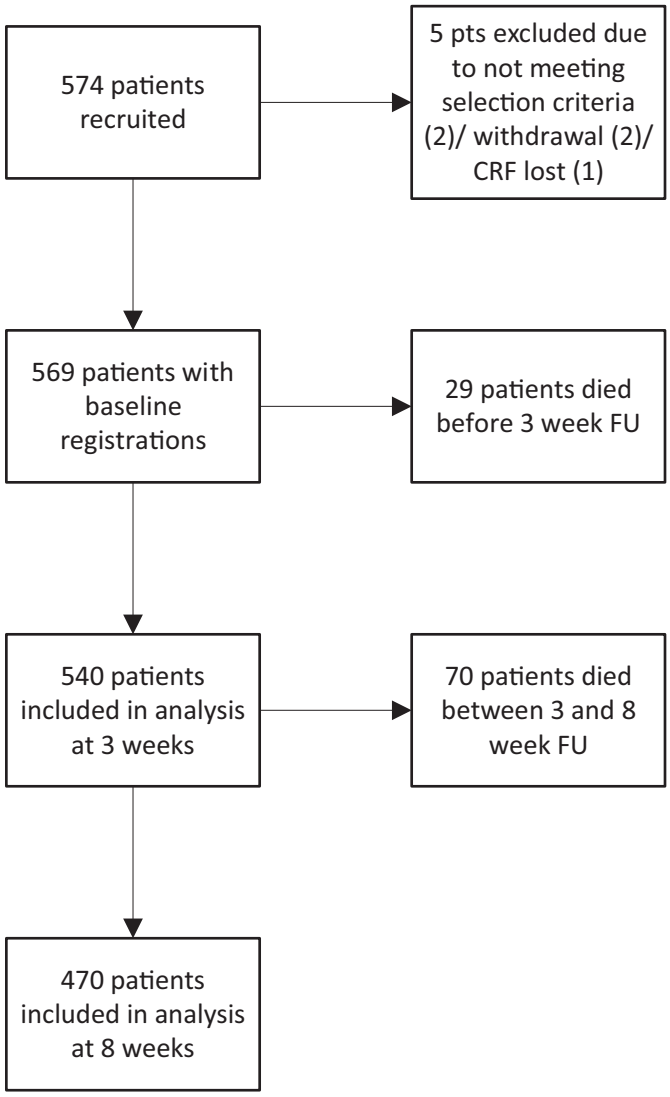

FIGURE 1 - Patient selection.

TABLE 1 - Baseline characteristics

	3 wk. cohort		8 wk. cohort	
N	540		470	
Age (years) median (IQR)	67	(15)	67	(14)
Sex f (%)				
Male	330	(61)	283	(60)
Female	210	(39)	187	(40)
Primary tumor type f (%)				
Breast cancer	110	(20)	104	(22)
Prostate cancer	140	(26)	131	(28)
Lung cancer	95	(18)	82	(17)
Gastrointestinal cancer	87	(16)	67	(14)
Urological cancer	59	(11)	47	(10)
Other	49	(9)	39	(8)
Location of metastases outside bone f (%)				
Lung	156	(29)	129	(27)
Liver	139	(26)	111	(24)
CNS	34	(6)	26	(6)
Other	219	(41)	184	(39)
None	207	(38)	194	(41)
Time since diagnosis (wks.) median (IQR)	82	(230)	96	(246)
KPS f (%)				
0-60	143	(26)	103	(22)
70-100	397	(74)	367	(78)
WL (%) at baseline mean (SD)	3.1	(7.8)	2,6	(7.5)
BMI (kg/m^2) mean (SD)	25.9	(4.6)	26	(4.6)
Lack of appetite at baseline f (%)				
Not at all	228	(43)	207	(44)
A little	158	(29)	139	(30)
Quite a bit	89	(17)	76	(16)
Very much	61	(11)	44	(9)
Skeletal region of radiation f (%)				
Vertebral column	277	(51)	231	(49)
Pelvis	206	(38)	183	(39)
Extremities	60	(11)	53	(11)
Thorax (excl. vertebral column)	58	(11)	53	(11)
Other	12	(2)	12	(2)
Radiation dose[a)] f (%)				
8 Gy x 1	189	(35)	167	(36)
4 Gy x 5	155	(29)	132	(28)
3 Gy x 10	144	(27)	125	(27)
Other	52	(10)	46	(10)
Concurrent systemic anti-cancer treatment (within 6 wks.) f (%)				
Yes	353	(72)	319	(74)
No	139	(28)	111	(26)

Abbreviations: Wk, week; IQR, Interquartile Range; f, frequency; KPS, Karnofsky performance status; WL, weight loss; SD, standard deviation; BMI, body mass index.
a) for the 119 patients that received two parallel treatments, the highest total dose is reported.

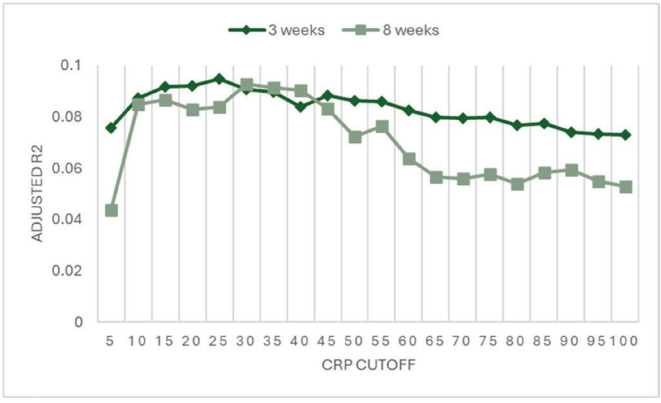

FIGURE 2 - Explained variance in weight loss after 3 and 8 weeks according to CRP cutoff. Cutoffs of CRP between 10 and 60 or 10-45 yields an explained variance of weight loss (adjusted R2) > 0.08 after 3 and 8 weeks, respectively.

the highest explained variance at 3 weeks, with adjusted R^2 of 0.095, while a cutoff of 30 yielded the highest explained variance at 8 weeks, with adjusted R^2 of 0.093. However, cutoffs between 10 and 60 or 10 and 45, all yielded comparable explained variance for the 3- and 8-week cohorts, respectively.

Discussion

In this study, we demonstrate that MoSI improve prediction of weight loss compared to other clinical markers. Specifically, CRP and the partly CRP-derived mGPS predict weight loss with higher accuracy and reliability than other MoSI included in this analysis.

In a previous longitudinal observation study, we identified early weight loss (<5%), primary tumor type and appetite loss as predictors for future development of cachexia (14). Building on this model, our aim was to evaluate whether MoSI would improve the ability to predict future weight loss in a similar patient population. In the current study we confirm that both primary tumor type and appetite loss predict weight loss in the short term. Although gastrointestinal cancer was not statistically significant in predicting weight loss after 8 weeks, urological and lung cancer remained highly significant in this time frame. The association between cachexia and certain primary tumor types has been shown in several cross-sectional studies (1,10,23). In the present study, we show that effect of tumor type remains significant even when contrasted by MoSI. This suggests that the association between weight loss and specific tumor types cannot be solely attributed to the tumor's ability to trigger systemic inflammation.

Contrary to the effect of systemic inflammation, effect of appetite loss seemed to dissipate over time as appetite loss was not significant in predicting weight loss after 8 weeks. This may indicate that weight loss associated with non-inflammatory appetite loss may have a greater potential for recovery. This is supported by a finding in a small retrospective study evaluating predictors of the appetite stimulant anamorelin, where MoSI negatively predicted the effect of

TABLE 2a - Clinical factors and MoSI predicting weight loss in 3 weeks post-radiotherapy

	Base model			Base model + WBC			Base model + NLR (log)			Base model + MLR (log)			Base model + CRP (log)			Base model + Albumin			Base model + mGPS			Base model + IL-6 (log)			Base model + PNI		
	β	**SE**	**p**	**β**	**SE**	**p**	**β**	**SE**	**p**	**β**	**SE**	**p**	**β**	**SE**	**p**	**β**	**SE**	**p**	**β**	**SE**	**p**	**β**	**SE**	**p**	**β**	**SE**	**p**
Appetite loss (0-100)	.62	.22	.006	.66	.22	.003	.60	.22	.006	.60	.22		.44	.22	.05	.55	.22	.01	.46	.23	.04	.56	.22	.01	.54	.22	.01
Primary tumour type																											
Breast cancer	0			0			0			0			0			0			0			0			0		
Prostate cancer	.71	.54	.19	.67	.54	.21	.66	.54	.22	.65	.54	.23	.48	.54	.38	.55	.54	.31	.38	.54	.48	.59	.54	.28	.62	.54	.25
Lung cancer	1.8	.61	.003	1.5	.61	.01	1.6	.61	.009	1.6	.61	.009	1.4	.61	.03	1.7	.60	.005	1.3	.62	.04	1.6	.61	.009	1.7	.60	.004
GI cancer	2.0	.64	.002	1.9	.63	.003	1.7	.63	.006	1.6	.64	.01	1.7	.63	.01	1.9	.63	.002	1.7	.64	.009	1.9	.63	.003	1.9	.63	.003
Urological cancer	2.6	.74	<.001	2.5	.73	<.001	2.4	.73	<.001	2.4	.73	.001	2.0	.74	.008	2.5	.73	<.001	2.0	.74	.006	2.4	.74	.002	2.4	.73	<.001
Other	1.1	.76	.16	.84	.76	.27	.88	.76	.25	.82	.76	.28	.90	.76	.23	.86	.76	.26	.86	.76	.25	1.1	.76	.15	.89	.76	.24
WL (%) at baseline	.013	.030	.66	.008	.029	.79	.006	.029	.84	.011	.030	.71	.007	.030	.78	.005	.030	.87	.002	.030	.93	.003	.030	.91	.006	.030	.85
WBC				.15	.049	.002																					
NLR (log)							.76	.27	.005																		
MLR (log)										.85	.31	.007															
CRP (log)													.54	.16	<.001												
Albumin																-.11	.045	.02									
mGPS																											
0																			0								
1																			1.1	.44	.02						
2																			2.3	.76	.003						
IL-6 (log)																						.34	.14	.02			
PNI																									-.084	.033	.01
Goodness-of-fit (adjusted R^2)	.064			.083			.085			.084			.090			.078			.091			.076			.080		

TABLE 2b - Clinical factors and MoSI predicting weight loss in 8 weeks post-radiotherapy

	Base model			Base model + WBC			Base model + NLR (log)			Base model + MLR (log)			Base model + CRP (log)			Base model + Albumin			Base model + mGPS			Base model + IL-6 (log)			Base model + PNI		
	β	SE	p	β	SE	p	β	SE	p	β	SE	p	β	SE	p	β	SE	p	β	SE	p	β	SE	p	β	SE	p
Appetite loss (0-100)	.26	.31	.40	.29	.31	.34	.27	.31	.38	.24	.31	.45	-.083	.31	.79	.14	.31	.66	-.066	.31	.83	.20	.31	.52	.18	.31	.57
Primary tumour type																											
Breast cancer	0			0			0			0			0			0			0			0			0		
Prostate cancer	1.3	.77	.10	1.3	.77	.10	1.3	.77	.10	1.2	.77	.12	.82	.75	.27	1.1	.77	.17	.64	.75	.40	1.1	.76	.14	1.2	.77	.12
Lung cancer	3.2	.87	<.001	3.0	.88	<.001	3.1	.88	<.001	3.0	.88	<.001	2.2	.87	.01	3.0	.87	<.001	2.0	.88	.02	2.9	.87	.001	3.1	.87	<.001
GI cancer	1.7	.93	.07	1.6	.92	.08	1.6	.93	.09	1.4	.93	.12	1.1	.90	.22	1.6	.92	.08	.96	.91	.29	1.6	.92	.09	1.6	.92	.09
Urological cancer	3.3	1.0	.002	3.3	1.0	.002	3.3	1.1	.002	3.2	1.1	.002	2.1	1.0	.05	3.2	1.0	.002	2.3	1.0	.03	3.0	1.0	.004	3.2	1.0	.002
Other	1.8	1.1	.11	1.7	1.1	.13	1.7	1.1	.12	1.6	1.1	.14	1.6	1.1	.14	1.5	1.1	.18	1.6	1.1	.15	1.8	1.1	.10	1.6	1.1	.14
WL (%) at baseline	-.018	.044	.69	-.020	.044	.65	-.020	.044	.66	-.017	.044	.70	-.026	.043	.55	-.028	.045	.54	-.031	.043	.48	-.031	.044	.49	-.022	.044	.62
WBC				.12	.075	.12																					
NLR (log)							.27	.38	.48																		
MLR (log)										.56	.42	.18															
CRP (log)													1.1	.25	<.001												
Albumin																-.16	.069	.018									
mGPS																											
0																			0								
1																			2.6	.67	<.001						
2																			3.9	1.0	<.001						
IL-6 (log)																						.45	.19	.02			
PNI																									-.076	.047	.11
Goodness-of-fit (adjusted R^2)	.035			.039			.035			.038			.096			.053			.093			.047			.041		

Abbreviations: WBC, white blood cell count; NLR, neutrophil to lymphocyte ratio; MLR, monocyte to lymphocyte ratio; CRP, C-reactive protein; mGPS, modified Glasgow prognostic score; IL-6, interleukin-6; PNI, Prognostic Nutritional Index; WL, weight loss.

the treatment (24). Thus, weight loss associated with systemic inflammation seems more refractory, aligning with the treatment resilience seen in cancer cachexia.

Patient-reported weight loss at baseline did not have any effect on future weight loss. This might seem surprising as one would believe that patients with a history of weight loss would be at risk of further weight loss. Lack of effect could possibly be attributed to the uncertainty of patient reporting; however, it also should be noted that the time frame for assessment of baseline weight loss is six months prior to baseline. Thus, the lack of observed effect of prior weight loss could mean that many have experienced weight loss some time ago, but that body weight is now stabilized (but not regained) due to anti-cancer treatment or other interventions. If weight loss closer to baseline had been assessed, the results might have been different.

Systemic inflammation occurs when pro-inflammatory cytokines are released from immune cells and chronically activates the innate immune system. Systemic inflammation can lead to development or progression of several diseases such as cardiovascular disease, diabetes mellitus, chronic kidney disease or cancer (25). MoSI have known prognostic value in cancer (19,26,27), and have been shown to be associated with weight loss and cachexia in cross-sectional studies (28,29). Recently, also a longitudinal analysis was published, showing that activation of several pro-inflammatory pathways and circulating growth differentiation factor 15 (GDF15) was predictive of cachexia in lung cancer (30). In the present longitudinal study, we now show that readily available MoSI predict weight loss independent of tumor type, appetite loss and previous weight loss, and may therefore serve as markers of cachexia development or progression.

Although all evaluated MoSI significantly improved prediction of weight loss at three weeks, CRP and mGPS demonstrated the highest levels of explained variance. Notably, these two markers were the only ones retaining the same level of explained variance at 8 weeks. This suggests that CRP and mGPS are the most robust predictors of weight loss, indicating a stronger and more sustained relationship with weight loss than the other MoSI in this study. mGPS scores systemic inflammation from 0-2 based on serum elevation of CRP and/or albumin (19). CRP and albumin are acute phase proteins synthesized in the liver. While CRP is upregulated in response to pro-inflammatory cytokines, albumin is downregulated, thus they are termed positive and negative acute phase proteins, respectively. Neither CRP nor albumin has a known direct role in the pathophysiology of cachexia (31). However, the regulation of both CRP and albumin depends on pro-inflammatory cytokines such as Interleukin-1 (IL-1), Tumor Necrosis Factor alpha (TNFα), Transforming Growth Factor beta (TGFβ), and IL6 (32), which are all implicated in cachexia pathophysiology (6). CRP and albumin, which are more readily available in clinical practice, may therefore serve as surrogate markers of cytokine activation and cachexia. Notably, both CRP and albumin more accurately predicted weight loss than IL-6 in this study.

According to our model, predicted weight loss increased with increasing CRP. In order to find the cutoff most accurately predicting weight loss, we explored several consecutive cutoffs of CRP and found that an optimal compromise for both short- and long-term prediction is a CRP cutoff in the lower end of the scale (between 10 and 45). The mGPS uses a CRP cutoff of 10 and with the addition of low albumin (mGPS 2), the predicted weight loss increased considerably compared to patients with elevated CRP only (mGPS 1). However, the explained variance was similar between CRP and mGPS. This means that although addition of low albumin increases the amount of predicted weight loss, it did not explain more of the variation in future weight loss. Thus, combining low albumin and elevated CRP as a required criterion for cachexia probably means that many patients with relevant weight loss will not be detected. Consequently, a slightly elevated CRP seems like the most optimal inflammatory marker to diagnose cachexia. However, mGPS is useful to grade severity of cachexia.

In this study, weight loss in patients with metastatic cancer was chosen as the outcome. The rationale behind this decision is that the cachexia diagnostic criteria are mainly based on weight loss. A 5% weight loss in the last 6 months in patients with normal or obese body composition, or 2% in patients with lean body composition is diagnostic of cachexia, and while the definition additionally states that the weight loss is caused by metabolic alterations and cannot be reversed by nutritional intervention alone, this is not integrated in the diagnostic criteria (2). Weight loss in cancer may have several different causes, many of which may not be related to cachexia, according to the definition. Typical examples are weight loss related to dysphagia or other types of malignant bowel obstruction, in which weight loss often can be significantly improved by nutritional intervention. Using weight loss as the only diagnostic criterion is thus not sufficiently specific. An obvious pitfall is that patients with weight loss not related to cachexia might be recruited to cachexia intervention studies, potentially obscuring the actual effect of the intervention on the outcome. Consequently, many intervention studies in the later years have used additional ad hoc criteria to diagnose cachexia, such as appetite loss, fatigue, or laboratory markers, including various MoSI (4,33,34). In the GLIM criteria for malnutrition, it is advocated that systemic inflammation is a necessary criterion for cachexia; however, no specific marker for systemic inflammation was named (8). Our results show that MoSI are indeed predictive of weight loss in cancer and may serve as biomarkers of cachexia development. Furthermore, we identify CRP and mGPS as the most robust and predictive markers among several other MoSI, and they should be considered implemented in the diagnostic criteria of cachexia and used in future clinical trials as selection criteria to identify patients with cachexia.

Limitations

This is a preplanned secondary analysis of a study, whose primary objective was to identify predictors of response to palliative radiotherapy for painful bone metastases (21). The strengths of this study include the availability of MoSI in a longitudinal dataset of patients with metastases from various primary tumor types and with a considerable spread in weight loss. A limitation is that all patients have bone metastases, thus the sample is not representative of the total population of patients with metastatic cancer. However, bone

metastases are common in advanced cancer and found in 85% of patients dying from prostate, breast, and lung cancer (35). Furthermore, animal models of cancer-induced bone pain have been shown to be a useful platform to study cancer cachexia (35). Additionally, all patients in this study received palliative radiotherapy after baseline observations, and although this treatment is generally very well tolerated, this may have affected development of symptoms such as appetite loss. It is difficult to deduce the significance of these two limitations, and the results should be interpreted with caution. Adjusted R^2 of the investigated models can be perceived as low with a value around 0.09 for the best models (CRP and mGPS), meaning that 9% of the variance in weight loss is explained by the predictors in the model. This may be owed to the multifactorial nature of weight loss, meaning that other factors not included in the models are important to the prediction of weight loss. The aim of this study was not to identify all relevant predictors, but to compare predictive ability of several MoSI. With respect to that, we chose to rely on a previously published model when selecting prior weight loss, primary tumor type, and appetite loss as covariates for the base model (14). The observed increase in R^2 following the addition of MoSI indicates that these markers significantly enhance the predictive accuracy for weight loss. The measurements of IL6 were not standardized to a specific time of day. As IL6 is known to have some diurnal variation (36), this may have introduced variance in the measurements, weakening a possible association with weight loss. As is common in studies with patients with advanced cancer, the attrition was high. To compensate for the bias that might arise from this, we have performed multiple imputations of missing values at baseline, and for patients still alive, but with missing data at follow-up. The results of this study are not validated in another patient cohort and should be considered exploratory. The results must therefore be seen in conjunction with previous publications, and future multi-center studies on the subject are necessary.

Conclusion

Systemic inflammation is an important biomarker for cachexia/cancer associated weight loss, and several specific MoSI are applicable. However, CRP and mGPS seem the most accurate and robust in predicting weight loss both short- and long-term. Smaller elevations in CRP serum levels seem to optimally stratify risk of future weight loss, while mGPS is useful for grading severity of future weight loss.

Acknowledgments

The authors would like to thank the patients participating in this study, without whom this study would not be possible.

Disclosures

Conflict of interest: The authors have no conflicts of interests to declare.

Financial support: This work was supported by non-restricted grants from the Norwegian Cancer Society and the Liaison Committee for Education, Research and Innovation in Central Norway.

Authors' contributions: *Conceptualization*: RHH, PK, TSS and SK. *Data curation: RHH, OMV. Formal analysis*: OMV, ØS. *Funding acquisition*: SK, RHH, OMV. *Investigation:* RHH, PK, OD and AB. *Methodology:* RHH, PK, TSS, TRB, OMV, ØS. *Project administration*: RHH, PK. *Resources:* RHH, AB, OD. *Supervision*: PK, TSS. *Visualization*: OMV. *Writing – original draft*: OMV, TSS, RHH, TRB. *Writing – review & editing*: All authors.

Availability of data and materials: The data that support the findings of this study are not openly available due to reasons of sensitivity and are available from the corresponding author upon reasonable request.

Trial registration: ClinicalTrials.gov NCT02107664, date of registration April 8, 2014 (retrospectively registered).

References

1. Vagnildhaug OM, Balstad TR, Almberg SS, et al. A cross-sectional study examining the prevalence of cachexia and areas of unmet need in patients with cancer. Support Care Cancer. 2018;26(6):1871-1880. CrossRef PubMed
2. Fearon K, Strasser F, Anker SD, et al. Definition and classification of cancer cachexia: an international consensus. Lancet Oncol. 2011;12(5):489-495. CrossRef PubMed
3. Solheim TS, Laird BJA, Balstad TR, et al. A randomized phase II feasibility trial of a multimodal intervention for the management of cachexia in lung and pancreatic cancer. J Cachexia Sarcopenia Muscle. 2017;8(5):778-788. CrossRef PubMed
4. Takayama K, Katakami N, Yokoyama T, et al. Anamorelin (ONO-7643) in Japanese patients with non-small cell lung cancer and cachexia: results of a randomized phase 2 trial. Support Care Cancer. 2016;24(8):3495-3505. CrossRef PubMed
5. Temel JS, Abernethy AP, Currow DC, et al. Anamorelin in patients with non-small-cell lung cancer and cachexia (ROMANA 1 and ROMANA 2): results from two randomised, double-blind, phase 3 trials. Lancet Oncol. 2016;17(4):519-531. CrossRef PubMed
6. Fearon KC, Glass DJ, Guttridge DC. Cancer cachexia: mediators, signaling, and metabolic pathways. Cell Metab. 2012;16(2):153-166. CrossRef PubMed
7. Rohm M, Zeigerer A, Machado J, et al. Energy metabolism in cachexia. EMBO Rep. 2019;20(4):e47258. CrossRef PubMed
8. Cederholm T, Jensen GL, Correia M, et al. GLIM criteria for the diagnosis of malnutrition – a consensus report from the global clinical nutrition community. Clinical nutrition (Edinburgh, Scotland). 2018. CrossRef
9. Yule MS, Thompson J, Leesahatsawat K, et al. Cancer Cachexia Endpoints Working Group. Biomarker endpoints in cancer cachexia clinical trials: systematic Review 5 of the cachexia endpoint series. J Cachexia Sarcopenia Muscle. 2024;15(3):853-867. CrossRef PubMed
10. Dewys WD, Begg C, Lavin PT, et al. Eastern Cooperative Oncology Group. Prognostic effect of weight loss prior to chemotherapy in cancer patients. Am J Med. 1980;69(4):491-497. CrossRef PubMed
11. Ross PJ, Ashley S, Norton A, et al. Do patients with weight loss have a worse outcome when undergoing chemotherapy for lung cancers? Br J Cancer. 2004;90(10):1905-1911. CrossRef PubMed
12. Chen IM, Johansen JS, Theile S, et al. Randomized phase II study of Nab-paclitaxel and gemcitabine with or without tocilizumab as first-line treatment in advanced pancreatic cancer: survival and cachexia. Journal of Clinical Oncology. 2025;0(0):JCO.23.01965. CrossRef

13. Groarke JD, Crawford J, Collins SM, et al. Phase 2 study of the efficacy and safety of ponsegromab in patients with cancer cachexia: PROACC-1 study design. J Cachexia Sarcopenia Muscle. 2024;15(3):1054-1061. CrossRef PubMed
14. Vagnildhaug OM, Brunelli C, Hjermstad MJ, et al. A prospective study examining cachexia predictors in patients with incurable cancer. BMC Palliat Care. 2019;18(1):46. CrossRef PubMed
15. Habberstad R, Aass N, Mollnes TE, et al. Inflammatory markers and radiotherapy response in patients with painful bone metastases. J Pain Symptom Manage. 2022;64(4):330-339. CrossRef PubMed
16. von Elm E, Altman DG, Egger M, et al. STROBE Initiative. The Strengthening the Reporting of Observational Studies in Epidemiology (STROBE) statement: guidelines for reporting observational studies. Lancet. 2007;370(9596):1453-1457. CrossRef PubMed
17. Vigano AL, di Tomasso J, Kilgour RD, et al. The abridged patient-generated subjective global assessment is a useful tool for early detection and characterization of cancer cachexia. J Acad Nutr Diet. 2014;114(7):1088-1098. CrossRef PubMed
18. Groenvold M, Petersen MA, Aaronson NK, et al. The development of the EORTC QLQ-C15-PAL: a shortened questionnaire for cancer patients in palliative care. European journal of cancer (Oxford, England: 1990). 2006;42(1):55-64. CrossRef
19. Dolan RD, Daly L, Sim WMJ, et al. Comparison of the prognostic value of ECOG-PS, mGPS and BMI/WL: Implications for a clinically important framework in the assessment and treatment of advanced cancer. Clinical nutrition (Edinburgh, Scotland). 2019. CrossRef
20. Yamamoto T, Kawada K, Obama K. Inflammation-Related Biomarkers for the Prediction of Prognosis in Colorectal Cancer Patients. Int J Mol Sci. 2021;22(15):8002. CrossRef PubMed
21. Habberstad R, Frøseth TCS, Aass N, et al. The Palliative Radiotherapy and Inflammation Study (PRAIS) – protocol for a longitudinal observational multicenter study on patients with cancer induced bone pain. BMC Palliat Care. 2018;17(1):110. CrossRef PubMed
22. White IR, Royston P, Wood AM. Multiple imputation using chained equations: issues and guidance for practice. Stat Med. 2011;30(4):377-399. CrossRef PubMed
23. Sun L, Quan XQ, Yu S. An epidemiological survey of cachexia in advanced cancer patients and analysis on its diagnostic and treatment status. Nutr Cancer. 2015;67(7):1056-1062. CrossRef PubMed
24. Iwai N, Sakai H, Oka K, et al. Predictors of response to anamorelin in gastrointestinal cancer patients with cachexia: a retrospective study. Support Care Cancer. 2023;31(2):115. CrossRef PubMed
25. Furman D, Campisi J, Verdin E, et al. Chronic inflammation in the etiology of disease across the life span. Nat Med. 2019;25(12):1822-1832. CrossRef PubMed
26. Ruan GT, Xie HL, Yuan KT, et al. Prognostic value of systemic inflammation and for patients with colorectal cancer cachexia. J Cachexia Sarcopenia Muscle. 2023;14(6):2813-2823. CrossRef PubMed
27. Shibutani M, Maeda K, Nagahara H, et al. The prognostic value of the systemic inflammatory score in patients with unresectable metastatic colorectal cancer. Oncol Lett. 2018;16(1):666-672. CrossRef PubMed
28. Blum D, Stene GB, Solheim TS, et al. Validation of the consensus-definition for cancer cachexia and evaluation of a classification model–a study based on data from an international multicentre project (EPCRC-CSA). Annals of Oncology : Official Journal of the European Society for Medical Oncology/ESMO. 2014;25(8):1635-42. CrossRef
29. Richards CH, Roxburgh CS, MacMillan MT, et al. The relationships between body composition and the systemic inflammatory response in patients with primary operable colorectal cancer. PLoS One. 2012;7(8):e41883. CrossRef PubMed
30. Al-Sawaf O, Weiss J, Skrzypski M, et al. TRACERx Consortium. Body composition and lung cancer-associated cachexia in TRACERx. Nat Med. 2023;29(4):846-858. CrossRef PubMed
31. Robinson TP, Hamidi T, Counts B, et al. The impact of inflammation and acute phase activation in cancer cachexia. Front Immunol. 2023;14:1207746. CrossRef PubMed
32. Aguilar-Cazares D, Chavez-Dominguez R, Marroquin-Muciño M, et al. The systemic-level repercussions of cancer-associated inflammation mediators produced in the tumor microenvironment. Front Endocrinol (Lausanne). 2022;13:929572. CrossRef PubMed
33. Katakami N, Uchino J, Yokoyama T, et al. Anamorelin (ONO-7643) for the treatment of patients with non-small cell lung cancer and cachexia: results from a randomized, double-blind, placebo-controlled, multicenter study of Japanese patients (ONO-7643-04). Cancer. 2018;124(3):606-616. CrossRef PubMed
34. Stewart Coats AJ, Ho GF, Prabhash K, et al. ACT-ONE study group. Espindolol for the treatment and prevention of cachexia in patients with stage III/IV non-small cell lung cancer or colorectal cancer: a randomized, double-blind, placebo-controlled, international multicentre phase II study (the ACT-ONE trial). J Cachexia Sarcopenia Muscle. 2016;7(3):355-365. CrossRef PubMed
35. Hasegawa T, Kawahara K, Sato K, et al. Characterization of a cancer-induced bone pain model for use as a model of cancer cachexia. Curr Issues Mol Biol. 2024;46(12):13364-82 CrossRef
36. Nilsonne G, Lekander M, Åkerstedt T, et al. Diurnal variation of circulating interleukin-6 in humans: a meta-analysis. PLoS One. 2016;11(11):e0165799. CrossRef PubMed

JCB
J Circ Biomark 2025; 14: 21-29
ISSN 1849-4544 | DOI: 10.33393/jcb.2025.3486
ORIGINAL RESEARCH ARTICLE

Monocyte Distribution Width (MDW) as a useful and cost-effective biomarker for sepsis prediction

Dimitrios Theodoridis[1], Angeliki Tsifi[2], Emmanouil Magiorkinis[3], Riris Ioannis[4], Vatistas Ioannis[5], Evgenia Moustaferi[1], Kanakaris Christos[1], Tsiligianni Ekaterini[1], Anastasios Ioannidis[6], Efstathios Chronopoulos[4], Stylianos Chatzipanagiotou[7]

[1]Hematology Laboratory, Konstantopoulio General Hospital, Nea Ionia - Greece
[2]Intensive Care Unit, General Hospital of Athens EVANGELISMOS, Athens - Greece
[3]Hematology Laboratory, Metaxa Cancer Hospital, Pireas - Greece
[4]School of Medicine, School of Health Sciences, National and Kapodistrian University of Athens, Athens - Greece
[5] Internal medicine resident at Konstantopoulio General Hospital, Nea Ionia - Greece
[6]Laboratory of Basic Health Sciences, Department of Nursing, Faculty of Health Sciences, University of Peloponnese, Tripoli - Greece
[7]Department of Biopathology and Clinical Microbiology, Aeginition Hospital, Medical School, National and Kapodistrian University of Athens, Athens - Greece

ABSTRACT

Background: Sepsis is a life-threatening condition and a major cause of hospital mortality worldwide. This study investigated the diagnostic utility of monocyte mean volume (MONO MEAN-V), monocyte distribution width (MDW), monocyte mean conductivity (MONO MEAN-C), and monocyte standard deviation conductivity (MONO Sd-C) for sepsis, compared to conventional markers.
Methods: A prospective cohort study was conducted in two centers, enrolling adult patients classified into three groups: sepsis, septic shock, and febrile. Blood was drawn from septic patients on days 1, 3, and 5 of admission. MDW and other inflammatory parameters were measured in all patients.
Results: Patients with sepsis or septic shock exhibited significantly elevated MONO MEAN-V, MDW, and MONO MEAN-C and lower MONO Sd-C compared to febrile patients. Among the biomarkers evaluated, MDW emerged as a reliable predictor of sepsis. A cut-off MDW value of 25.1 on day 1 demonstrated optimal diagnostic performance, with an area under the ROC curve of 0.84 (95% CI: 0.77-0.91), sensitivity of 75%, and specificity of 91.2%.
Conclusions: MDW appears to be a cost-effective, rapid marker for sepsis detection, performing at least as effectively as existing biomarkers. Our findings corroborate other published studies, highlighting MDW's potential to enhance early sepsis recognition.

Keywords: Biomarker, Diagnosis, MDW, Sepsis

Introduction

Sepsis, according to the Sepsis-3 conference, is a life-threatening condition characterized by the dysregulation of the host immune reaction as a response to an infection, which leads to systemic inflammation and multiple organ failure (1). The importance of organ dysfunction has been stressed during the last decade by the creation of the sequential organ failure assessment (SOFA) score in 1994, which was employed to describe the sequence of complications of severe disease and acute patient mortality under different circumstances (2,3). Septic shock is a serious complication of sepsis involving metabolic, cellular, and circulatory anomalies, which leads to an increased risk of mortality compared with sepsis alone (1). It constitutes a global health problem and indicates a steady increase in incidence, with 49 million cases and 11 million sepsis-related deaths worldwide in 2017 (4). Cases of sepsis due to fungi have increased in recent years, and the MDW is more efficient than biomarkers like C-reactive protein (CRP) and procalcitonin (PCT) (8).

Diagnosis and early detection of sepsis are crucial for improving patient survival and reducing healthcare costs (5). The use of biomarkers is vital in the early diagnosis, recognition of organ dysfunction, prognosis, and stratification of patients, leading to individualization of medical intervention. It also contributes to the avoidance of the overconsumption

Received: February 3, 2025
Accepted: June 17, 2025
Published online: August 14, 2025

Corresponding author:
Dimitrios Theodoridis
email: dimdrteo@gmail.com

of antibiotics, which otherwise may lead to an increase in antimicrobial resistance. According to the National Institutes of Health (NIH) Biomarkers Definitions Working Group, a biomarker is objectively measured and evaluated as an indicator of normal biological processes, pathogenic processes, or pharmacological responses to a therapeutic intervention"(6).In 2001, a series of biomarkers, such as CRP and PCT, were included in the diagnosis of sepsis, and there has been an exponential growth of studies analyzing various biomarkers (5,7,8). A series of various biomarkers have been employed in the diagnosis and monitoring of sepsis; these include acute phase proteins such as high sensitivity CRP (hsCRP), complement proteins such as complement component 5amonocyte chemo (C5a) and Pentatrexin (PTX-3), cytokines such as interleukin-10(IL-10), monocyte chemoattractant protein-1 (MCP-1), tumor necrosis factor-a (TNF-a), interleukin-1b (IL-1b) and interleukin-6 (IL-6), damage-associated molecular patterns (DAMPs) such as calprotectin and high mobility group box-1 protein (HMGB-1), endothelial cell and blood-brain barrier (BBB) markers such as syndecan-1, very late antigen-3 (VLA-3), angiopoietin-1 (Ang-1), angiopoietin-2 (Ang-2), claudin-5 (CLDN-5), occludin (OCLN), plasminogen activator inhibitor-1 (PAI-1), soluble intercellular adhesion molecule-1 (sICAM-1), calcium-binding protein B (S100B) and E-selectin (5).

Several other biomarkers have been explored, focusing on the parameters included in complete blood count (CBC). CBC is a simple examination and has several advantages: it is a first-line test, can be easily performed, is inexpensive, quick, and available in all medical facilities. The CBC parameters that have been studied include the absolute number of neutrophils, lymphopenia (9, 10), monocytosis or monocytopenia (11,12), eosinopenia (13), basocytopenia (14), anemia (as defined by hemoglobin (Hb) <12 g/dl) (15), an increased red cell distribution width (RDW) (>15%) (13,16,17), a low platelet (PLT) count (PC) (18), neutrophil-to-lymphocyte ratio (NLR) (19-22), monocyte-to-lymphocyte ratio (MLR)and PC-to-mean PLT volume (MPV) ratio (PC/MPV) (23-25). Novel indicators produced by modern hematology analyzers have also been employed, such as delta neutrophil index (26-28), immature PLT fraction (IPF) (29), mean neutrophils volume (NEUTRO MEAN-V), and mean monocytes volume (MONO MEAN-V) (30-31).

Monocytes play a central role in sepsis and in the mechanisms of natural and acquired immunity. A new CBC parameter provided by a modern analyzer with new-generation volume-conductivity-scatter (VSC) technology is the MDW, which depicts the anisocytosis of circulating monocytes, represents the standard deviation (SD) of a set of monocyte cell volumes and seems to be an important diagnostic and prognostic tool for the development and progression of sepsis (49). COULTER VCS established white blood cell (WBC) leukocyte-type technology using three measurements: single-cell volume, high-frequency conductivity, and laser light scattering. The combination of low-frequency current, high-frequency current, and light scattering technology provides information about each cell that can be expressed in data plots (two- and three-dimensional nephelograms), as well as surface plots).

In 2019, the Food and Drug Administration (FDA) authorized the clinical application of MDW for the detection of sepsis in adult patients in the emergency room (ER). This biomarker has also been tested in other clinical settings, such as the intensive care unit (ICU) and infectious disease units, as well as in vitro stability tests (8,32-41). The role of MDW and other monocyte parameters in sepsis prognosis has been the focus of much research in recent years.

The aim of our study was to investigate the role of MDW and other monocyte parameters in sepsis prognosis and to compare these parameters with other biomarkers widely used to predict sepsis.

Materials and Methods

Patients and identification of high-risk patients

A comparative, prospective study was carried out with 136 patients (68 patients with sepsis and 68 non-septic patients) from the Emergency Department of the General Hospital of New Ionia Konstantopouleio-Patision and Eginitio. Sepsis was defined based on the guidelines of the third international consensus on sepsis and septic shock (1). The Sepsis-3 definitions suggest that patients with at least two of the three clinical variables mentioned below may be prone to poor outcomes typical of sepsis: (1) low systolic blood pressure (SBP ≤ 100 mmHg), (2) high respiratory rate (≥22 breaths per min), or (3) altered mental status (Glasgow Coma Scale < 15). Quick SOFA(qSOFA) score includes one point for each of the above three criteria. A qSOFA score ≥ 2 with suspected infection was suggestive of sepsis or septic shock. Originally, 136 patients were screened for sepsis and were divided into two groups, with 68 patients each: those with possible infection and worse prognosis and a qSOFA score ≥2 and those without a possible infection and a qSOFA score < 2. This is how the "septic" patients came about. Patients with hematological malignancies or those undergoing recent chemotherapy or taking medications affecting the monocyte population, such as injectable growth factors, were excluded from our study. Also, pediatric cases were excluded due to the non-availability of pediatric clinics in the two survey hospitals. Patients who scored qSOFA ≥2 either came directly to the emergency department of the General Hospital of New Ionia Konstantopouleio-Patision or were already hospitalized in one of the two hospitals, and their clinical profile changed, resulting in them also having a qSOFA score ≥2. Septic patients were classified into two categories based on sepsis-3 classifications, "sepsis"and "septic shock." So, according to the aforementioned parameters, three categories of patients emerged, "febrile," "patients with sepsis," and "patients with septic shock."

Measurement of sepsis biomarkers

Several sepsis indicators have been studied (PCT, IL-6, and CRP), including The following tests were performed for all patients: CBC, prothrombin time (*PT*/INR), PT-INR-activated partial thromboplastin time (*aPTT* or *APTT*), aPTT- fibrinogen-d-dimers, serum PCT, CRP, arterial blood gas (*ABG*), lactate (LAC), serum ferritin (FER), serum TNF-α, and *IL-6*. For CBC and MDW calculation, blood samples were collected in K2

EDTA vials using the Coulter DXH900 hematology analyzer (Beckman Coulter Diagnostics SA, California, US), and PT-INR-aPTT-FIB and d-dimers were measured in sodium citrate vials using a BCS-XP Siemens analyzer (Siemens Healthcare Diagnostics, Illinois, US). For FER, CRP, PCT, TNF-a, and IL-6 serum was isolated from gel clot activator blood tubes; FER was measured by chemiluminescence immunoassay at the UniCel DxI 800 Access Immunoassay System (Beckman Coulter Diagnostics SA, California, US), CRP by immunoturbidimetric method at the Roche cobas c501 system (Roche Diagnostics, Indianapolis, USA), PCT by chemiluminescence at the Abbott Alinity C system (Abbott Diagnostics, Illinois, USA), and TNF-a and IL-6 by ELISA at the Brio 2 (Diachel). The LAC and ABGs were measured using an ABL 800 FLEX(RADIO METER) ABG analyzer. Below, the statistical analysis presents some of the biomarkers measured in the patients.

For each patient with sepsis before the initiation of antimicrobial therapy, 10 ml of blood was drawn in Bactec culture vials (one pair for each patient) and incubated for a total of 5 days in the BD Bactec™ FX Blood system (Becton Dickinson, New Jersey, US). One blood culture set was collected from patients, except for those for whom endocarditis was suspected, for whom three sets were collected. Biological samples were cultured and incubated in common culture media and were evaluated. Microbial isolates were identified using the Vitek 2 Compact system (Biomerieux SA, Craponne, France), and antibiograms were obtained using the MIC and the E-test method using the standard criteria EUCAST.

In all patients with sepsis, the hematological markers were measured from morning samples one hour after sampling on the 1st, 3rd, and 5th day to check their prognostic value for the patient's outcome. In febrile patients, the hematological markers were measured in the same way only on the 1st day. Blood cultures were taken from all patients, as well as other biological samples such as urine, sputum, bronchoalveolar lavage, and CSF, in order to identify the possible source of infection before the initiation of empirical antibiotic therapy. We evaluated the clinical history of each patient, including various comorbidities or any factors contributing to immunosuppression, co-administration of other drugs, family history of dementia, and the status of the patient.

Statistical analysis

Quantitative variables are represented by mean values (standard deviation) and median (interquartile range), while categorical variables are represented by absolute and relative frequencies. Chi-square tests were used to compare the proportions. Students' t-tests were used to compare the ages of septic patients and febrile. The Mann–Whitney test was used to compare data between the two groups. ROC curves were used to estimate the predictive ability of MONO MEAN-V, MONO MEAN-C, monocyte volume standard deviation (MONO Sd-V), and monocyte standard deviation conductivity (MONO Sd-C). The sensitivity and specificity were calculated for the optimal cut-off values. The area under the curve (AUC) was also calculated. All the reported p-values were two-tailed. Statistical significance was set at $p < 0.05$, and analyses were conducted using the SPSS statistical software (version 26.0).

Results

TABLE 1 - Sample characteristics in the total sample and by outcome

		Group				P
		Sepsis and septic shock (n = 68, 50%)		Febrile (n = 68, 50%)		
		n	%	n	%	
Gender	Women	37	54.4	35	51.5	0.731+
	Men	31	45.6	33	48.5	
Age (years), mean (SD)		73,4 (16,1)		58,1 (19,1)		**<0.001++**

+ Pearson's chi-square test; ++Student's test

One hundred thirty-six patients were included in the study. Half of them (n = 68; 50%) had sepsis or septic shock, and the other half were febrile (n = 68; 50%). The mean age of septic patients was 73.4 years (SD = 16.1 years), and the mean age of febriles was 58.1 years (SD = 19.1 years) .The majority of both groups were women, 54.4% of septic patients and 51.5% of febriles. Their characteristics are presented in Table 1 for the total sample and by outcome. A significant difference was found between septic patients and febriles, as far as age is concerned.

The comorbidities of patients with sepsis are described in Table 2. 36.8% of the patients suffered from arterial hypertension and 33.8% from heart failure.

TABLE 2 - Comorbidities

Comorbidities	n	%
Diabetes mellitus	14	20.6
Arterial hypertension	25	36.8
Heart failure	23	33.8
COPD	10	14.7
Immunosuppression	11	16.2
Other disease	53	77.9

MONO MEAN-V, MDW, MONO MEAN-C, and MONO-SdC values by a group of "septic," "septic shock," and "febrile" patients are presented in Table 3.

On the 1st day, there were significant differences in MONO MEAN-V, MDW, MONO MEAN-C, and MONO-SdC among the three groups. More specifically, after Bonferroni correction, it was found that febrile cases had significantly lower MONO MEAN-V and MDW compared to the sepsis group ($p = 0.001$ and $p < 0.001$, respectively) and significantly greater MONO MEAN-C compared to the sepsis group ($p < 0.001$). In addition, febrile patients had significantly lower MONO-SdC and MDW than the sepsis group ($p < 0.001$ for both groups) and significantly greater MONO MEAN-C than the septic shock group ($p = 0.002$). No significant differences were found between the sepsis and septic shock groups after Bonferroni correction for measurements on the 1st day. In

TABLE 3 - MONO MEAN-V, MONO MEAN-C, MDW, MONO Sd-C values by outcome. Values of p < 0.05 are marked in bold

	Group						P
	Sepsis (n = 22; 16.2%)		Septic shock (n = 46; 33.8%)		Febriles (n = 68; 50%)		
	Mean (SD)	Median (IQR)	Mean (SD)	Median (IQR)	Mean (SD)	Median (IQR)	
MONO MEAN-V							
1st day	189.2 (11,2)	191.5 (186-195)	186.9 (12.8)	184 (178-195)	18.2 (10.3)	182 (174-188)	**0.003+**
3rd day	186.9 (11,8)	187 (181-191)	183 (9.8)	181 (179-193.5)	–	–	0.586++
5th day	182.4 (10.3)	181 (177-185)	179.9 (10.2)	182 (172.185)	–	–	0.820++
MONO MEAN-C							
1st day	119.5 (4,9)	120.5 (117-123)	120.2 (8.4)	121 (118-125)	123.9 (3.8)	123 (121.5-125.5)	**<0,001+**
3rd day	120.9 (3,1)	123 (119-123)	122.3 (5.2)	124 (120.5-125.5)	–	–	**0.030++**
5th day	122.6 (3.3)	123 (120.5-124.5)	114.7 (17.2)	121 (116-125)	–	–	0.526++
MDW							
1st day	26.3 (2.9)	26.1 (25.1-28,8)	28.8 (5.4)	29.6 (24.8-32.4)	22.6 (2.3)	22.2 (21.2-24.2)	**<0.001+**
3rd day	25.7 (3.3)	25 (23.5-27.3)	27.8 (4.8)	28.4 (23.5-31,1)	–	–	0.213++
5th day	23.3 (2.3)	23.5 (21.6-24.5)	29.1 (6.6)	29.2 (24.6-32.1)	–	–	**0.003++**
MONO Sd-C							
1st day	12.6 (11.7)	6.9 (4.8-14.6)	15.1 (12.3)	9.4 (5.4-20.3)	7.3 (4.9)	5.4 (4.8-6.3)	**<0.001+**
3rd day	25 (41.7)	6.6 (4.6-21)	13.8 (9.6)	11.1 (8.3-16,4)	–	–	0.153++
5th day	6.8 (6.3)	5.3 (4.9-5.5)	17.4 (18.1)	7 (5.1-24.1)	–	–	0.104++

+Kruskal–Wallis test; ++Mann–Whitney test

contrast, MONO MEAN-C on day 3 and MDW on day 5 were significantly greater in the septic shock group.

Some other indicators that are currently used to predict sepsis have been measured, and the results are shown in Table 4.

LAC, PCT, TNF-a, IL-6, and CRP values were significantly lower in febrile patients compared to septic patients (sepsis and septic shock).

In febrile cases, no significant correlation was found between MONO MEAN-V, MDW, MONO MEAN-C, MONO Sd-C and LAC, PCT, TNFa, IL-6, CRP, and NLR values on the 1st day (results are shown in Table 5).

In contrast, in sepsis cases, it was found that greater LAC, PCT, and CRP values were significantly associated with greater MONO MEAN-V and greater TNFa values with lower MONO MEAN-V.In addition, greater TNFa and lower NLR were significantly associated with greater MONO Sd. Furthermore, greater PCT, CRP, and NLR, as well as lower TNFa and IL-6 levels, were significantly associated with greater MDW. Lower TNFa and greater NLR were significantly associated with greater MONO-SdC.

In septic shock cases, greater TNFa values were significantly associated with lower MONO MEAN-V and higher MDW and MONO Sd-C. Also, greater IL-6 values were significantly associated with lower MONO MEAN-V and higher MDW.

The predictive ability of MONO MEAN-V, MONO MEAN-C, MDW, and MONO Sd-C between febrile and septic events during the first day was examined via ROC curves, the results of which are presented in Table 6. All factors had a significant predictive ability. More specifically, for MEAN–V, the optimal cut-off was set at 180.5, with 72.1% sensitivity and 48.5% specificity. For MEAN-C, the optimal cut-off was set at 120.5, with 48.5% sensitivity and 88.2% specificity. For MDW, the optimal point was 25.1, with 75.0% sensitivity and 91.2% specificity, and for MONO Sd-C, the optimal point was 6.9, with 58.8% sensitivity and 80.9% specificity.

Discussion

Our results indicated that MDW, a biomarker that can be easily measured using a common CBC test, can be used

TABLE 4 - LAC, CRP, PCT, TNFa, IL-6, and NLR values by outcome. Values of p < 0.05 are marked in bold

	Outcome						P
	Febriles (n = 68, 50%)			Sepsis and septic shock (n = 68; 50%)			
	n	Mean (SD)	Median (IQR)	n	Mean (SD)	Median (IQR)	
LAC (mmol/L)							
Day 1	68	1.34 (0.51)	1.35 (1-1,8)	68	5.26 (3.29)	4.45 (3.1-6,8)	**<0.001**
Day 3	0	–	–	49	3.6 (3)	2.8 (2.2-4.1)	–
Day 5	0	–	–	49	2.78 (2.55)	1.8 (1.2-3.2)	–
CRP (mg/L)							
Day 1	68	151.28 (108.61)	135.5 (67-248.84)	68	202.18 (121.98)	169 (106-259.5)	**0.017**
Day 3	0	–	–	51	170.22 (97.01)	149 (90-234)	–
Day 5	0	–	–	50	144.42 (105.89)	123 (66-188)	–
PCT (ng/L)							
Day 1	68	0.47 (0.57)	0.28 (0.07-0.8)	68	22.19 (29.08)	4.7 (1.12-43.5)	**<0.001**
Day 3	0	–	–	51	11.38 (16.77)	4.62 (0.89-15.76)	–
Day 5	0	–	–	48	7.98 (18.84)	2.44 (0.51-6.01)	–
TNFa (pg/mL)							
Day 1	67	69.16 (20.57)	62.9 (54.4-84.4)	68	104.86 (31.43)	101 (76.15-135.5)	**<0.001**
Day 3	0	–	–	46	48.37 (55.02)	16.5 (15.2-129)	–
Day 5	0	–	–	43	33.84 (57.67)	5.2 (3.7-5.9)	–
IL-6 (pg/mL)							
Day 1	67	20.16 (10.12)	17.9 (12.9-26.1)	68	63.53 (46.34)	51.25 (4.1-108.4)	**<0.001**
Day 3	0	–	–	46	42.65 (44.58)	40.15 (3-103.2)	–
Day 5	0	–	–	44	80.01 (27.37)	80.85 (58.45-100.7)	–

for the detection of sepsis. The MDW and other correlated parameters, such as MONO MEAN-V and MONO MEAN-C mono, can be easily calculated from the CBC (42). This could be of crucial importance since the management of patients with sepsis remains a major problem in clinical practice.

Studies have shown the importance of MDW in detecting sepsis as a reliable diagnostic marker for the early detection of sepsis compared to classic biomarkers, such as PCT and CRP, in various patient populations (13,32-34,36,38,44-60) published a score incorporating the modified early warning score (MEWS), neutrophil-to-lymphocyte ratio (NLR), MDW, and CRP, and showed that MEWS ≥3 with white blood cell (WBC) count ≥11 × 109/L, NLR ≥8, and MDW ≥20 demonstrated the highest diagnostic accuracy in all age subgroups in detecting sepsis in an early stage (61) suggested the incorporation of MDW along with NLR and PLR to improve sepsis scores. Early detection of sepsis is crucial because it is associated with the early initiation of broad-spectrum antibiotics, which can be lifesaving for patients with sepsis (43). In conclusion, the value, mainly, of MDW as a biomarker for sepsis prediction in comparison with existing sepsis biomarkers was confirmed in this study as well as in other similar studies (43).

In our study, MDW, MONO MEAN-V, MONO Sd-C, and MONO MEAN-C acted as biomarkers for the diagnosis of sepsis since septic patients had significantly higher values of MDW, MONO MEAN-V, MONO Sd-C, and significantly lower MONO MEAN-C, on the first day. In addition, our study did not find significant differences in the abovementioned biomarkers between septic and septic shock patients on the first day. The above indicates that these biomarkers could be very useful tools for the early diagnosis of sepsis. Furthermore, significant differences were found between septic and septic shock patients for MONO MEAN-C on day 3 and MDW on day 5, indicating that some monocyte parameters could also be useful tools for the diagnosis of septic shock. These findings are in line with those of other studies that suggest the use of MDW in combination with WBC for the diagnosis of sepsis (58,63). Furthermore, our findings are in agreement with other studies that have found that increased monocyte parameters, such as MDW or MONO MEAN-V, contribute to the early diagnosis of sepsis (33,64,65). The same applies to MONO MEAN-C, as other studies have found what we have found, that septic patients have significantly lower values of MONO MEAN-C.

TABLE 5 - LAC, CRP, PCT, TNFa, IL-6, and NLR values by outcome. Values of p < 0.05 are marked in bold

			MONO MEAN-V	MONO MEAN-C	MDW	MONO Sd-C
Febriles	**LAC (mmol/L)**	rho	−0,13	0.05	−0.03	0.16
		P	0.305	0.714	0.839	0.182
	PCT (ng/L)	rho	−0.08	−0.08	−0.04	0.00
		P	0.503	0.500	0.729	0.971
	TNFa (pg/mL)	rho	−0.10	−0.02	0.06	0.08
		P	0.413	0.867	0.616	0.540
	IL-6 (pg/mL)	rho	−0.12	−0.04	0.03	0.08
		P	0.324	0,743	0.835	0.518
	CRP (mg/L)	rho	−0.18	0.00	0.06	0.11
		P	0.137	0.990	0.655	0.379
	NLR	rho	−0.16	−0.17	−0.04	0.07
		P	0.202	0.166	0.748	0.557
Sepsis	**LAC (mmol/L)**	rho	0.57	0.05	0.42	0.24
		P	**0.006**	0.841	0.053	0.276
	PCT (ng/L)	rho	0.63	−0.07	0.52	0.06
		P	**0.002**	0.760	**0.014**	0.792
	TNFa (pg/mL)	rho	−0.45	0.42	−0.61	−0.43
		P	**0.037**	**0.050**	**0.003**	**0.046**
	IL-6 (pg/mL)	rho	−0.26	0.37	−0.48	−0.35
		P	0.243	0.087	**0.023**	0.106
	CRP (mg/L)	rho	0.50	−0.16	0.48	0.22
		P	**0.017**	0.485	**0.023**	0.334
	NLR	rho	0.26	−0.53	0.69	0.51
		P	0.233	**0.011**	**<0.001**	**0.015**
Septic shock	**LAC (mmol/L)**	rho	0.10	0.04	0.39	0.27
		P	0.528	0.777	**0.007**	0.075
	PCT (ng/L)	rho	0.09	−0.07	0.19	0.22
		P	0.535	0.660	0.204	0.146
	TNFa (pg/mL)	rho	−0.34	−0.23	0.34	0.30
		P	**0.019**	0.121	**0.020**	**0.045**
	IL-6 (pg/mL)	rho	−0.31	−0.17	0.37	0.28
		P	**0.038**	0.262	**0.012**	0.064
	CRP (mg/L)	rho	0.20	−0.18	0.21	0.11
		P	0.183	0.233	0.152	0.469
	NLR	rho	−0.09	0.08	−0.22	−0.02
		P	0.540	0.605	0.138	0.903

In our study, the significant predictive ability of MONO MEAN-V, MONO MEAN-C, MDW, and MONO Sd-C was found via ROC analysis. For MONO MEAN-V, the optimal cut-off was found to be 180.5, with a sensitivity of 72.1% and specificity of 48.5%. For MONO MEAN-C, it was found to be 120.5, with a sensitivity of 48.5 % and specificity of 88.2 %. For MDW, the optimal cut-off was found to be 25.1, with a sensitivity of 75.0% and specificity of 91.2%, and for MONO Sd-C was found to be 6.9, with a sensitivity of 58.8 % and specificity of 80.9%. The cut-off of MDW is in line with other studies that find cut-offs of 20-25 units for the detection of sepsis, with values >25 generally indicating higher severity (49). Overall,

TABLE 6 - ROC analysis results

	AUC (95% ΔE)+	P	Optimal cut-off	Sensitivity (%)	Specificity (%)
MONO MEAN-V (1st day)	0.65 (0.56-0.74)	**0.002**	>180.5	72.1	48.5
MONO MEAN-C (1st day)	0.7 (0.61-0.79)	**<0.001**	<120.5	48.5	88.2
MDW (1st day)	0.84 (0.77-0.91)	**<0.001**	>25.1	75.0	91.2
MONO SD-C (1st day)	0.7 (0.61-0.78)	**<0.001**	>6.9	58.8	80.9

+Area Under the Curve (95% CI)

our results point out that MDW is an independent predictor of outcomes in septic patients administered in the ICU. The predictive value of MDW in the diagnosis of sepsis has been confirmed, and it is demonstrated why researchers are now focusing on this particular marker, as it is a monocyte parameter that can provide a low-cost, rapid, and reliable solution for the diagnosis of sepsis.

As mentioned above, patients with hematological malignancies or those undergoing recent chemotherapy or taking medications affecting the monocyte population, such as injectable growth factors, were excluded from our study. Also, pediatric cases were excluded due to the non-availability of pediatric clinics in the two survey hospitals. Moreover, the sample could have been bigger, but due to the limitations of COVID-19, this was not possible. More research should be carried out in the future. For example, the diagnostic ability of the MDW in pediatric cases and the correlation of the diagnostic ability of the MDW with various pathogenic factors should be clarified. Also, it would be useful to compare the results of our research with those of studies where the sample is larger.

Disclosures

Conflicts of interest: The authors declare no conflicts of interest.

Financial support: This research received no external funding

Data availability statement: The original contributions presented in the study are included in the article. Further inquiries can be directed to the corresponding authors.

Author contributions: Conceptualization, D.T.; Data Curation, S.T.; Investigation, A.T., D.T., X.T., A.V., E.M., N.S.; Writing—Original Draft Preparation, D.T. and E.M.; Writing—Review and Editing, E.C., S.C. and A.I. All authors have read and agreed to the published version of the manuscript.

References

1. Singer M, Deutschman CS, Seymour CW, et al. The Third International Consensus Definitions for Sepsis and Septic Shock (Sepsis-3). JAMA. 2016;315(8):801-810. CrossRef PubMed
2. Vincent JL, Moreno R, Takala J, et al. The SOFA (Sepsis-related Organ Failure Assessment) score to describe organ dysfunction/failure. On behalf of the Working Group on Sepsis-Related Problems of the European Society of Intensive Care Medicine. Intensive Care Med. 1996;22(7):707-710. CrossRef PubMed
3. Lambden S, Laterre PF, Levy MM, et al. The SOFA score-development, utility and challenges of accurate assessment in clinical trials. Crit Care. 2019;23(1):374. CrossRef PubMed
4. Rudd KE, Johnson SC, Agesa KM, et al. Global, regional, and national sepsis incidence and mortality, 1990-2017: analysis for the Global Burden of Disease Study. Lancet. 2020;395(10219):200-211. CrossRef PubMed
5. Barichello T, Generoso JS, Singer M, et al. Biomarkers for sepsis: more than just fever and leukocytosis-a narrative review. Crit Care. 2022;26(1):14. CrossRef PubMed
6. Biomarkers Definitions Working Group. Biomarkers and surrogate endpoints: preferred definitions and conceptual framework. Clin Pharmacol Ther. 2001;69(3):89-95. CrossRef PubMed
7. Su W, Fan M, Shen W, et al. Advances in pediatric sepsis biomarkers - what have we learnt so far? Expert Rev Mol Diagn. 2025;25(5):183-198. CrossRef
8. Agnello L, Bivona G, Vidali M, et al. Monocyte distribution width (MDW) as a screening tool for sepsis in the Emergency Department. Clin Chem Lab Med. 2020;58(11):1951-1957. CrossRef PubMed
9. Drewry AM, Samra N, Skrupky LP, et al. Persistent lymphopenia after diagnosis of sepsis predicts mortality. Shock. 2014;42(5):383-391. CrossRef PubMed
10. Chung KP, Chang HT, Lo SC, et al. Severe lymphopenia is associated with elevated plasma interleukin-15 levels and increased mortality during severe sepsis. Shock. 2015;43(6):569-575. CrossRef PubMed
11. Radzyukevich YV, Kosyakova NI, Prokhorenko IR. Participation of monocyte subpopulations in progression of experimental endotoxemia (EE) and systemic inflammation. J Immunol Res. 2021;2021:1762584. CrossRef PubMed
12. Chung H, Lee JH, Jo YH, et al. Circulating monocyte counts and its impact on outcomes in patients with severe sepsis including septic shock. Shock. 2019;51(4):423-429. CrossRef PubMed
13. Lin Y, Rong J, Zhang Z. Silent existence of eosinopenia in sepsis: a systematic review and meta-analysis. BMC Infect Dis. 2021;21(1):471. CrossRef PubMed
14. Piliponsky AM, Shubin NJ, Lahiri AK, et al. Basophil-derived tumor necrosis factor can enhance survival in a sepsis model in mice. Nat Immunol. 2019;20(2):129-140. CrossRef PubMed
15. Docherty AB, Turgeon AF, Walsh TS. Best practice in critical care: anaemia in acute and critical illness. Transfus Med. 2018;28(2):181-189. CrossRef PubMed
16. Fan YW, Liu D, Chen JM, et al. Fluctuation in red cell distribution width predicts disseminated intravascular coagulation morbidity and mortality in sepsis: a retrospective single-center study. Minerva Anestesiol. 2021;87(1):52-64. CrossRef PubMed
17. Han YQ, Zhang L, Yan L, et al. Red blood cell distribution width predicts long-term outcomes in sepsis patients admitted to the intensive care unit. Clin Chim Acta. 2018;487:112-116. CrossRef PubMed

18. Assinger A, Schrottmaier WC, Salzmann M, et al. Platelets in sepsis: an update on experimental models and clinical data. Front Immunol. 2019;10:1687. CrossRef PubMed
19. Meshaal MS, Nagi A, Eldamaty A, et al. Neutrophil-to-lymphocyte ratio (NLR) and platelet-to-lymphocyte ratio (PLR) as independent predictors of outcome in infective endocarditis (IE). Egypt Heart J. 2019;71(1):13. CrossRef PubMed
20. Rehman FU, Khan A, Aziz A, et al. Neutrophils to lymphocyte ratio: earliest and efficacious markers of sepsis. Cureus. 2020;12(10):e10851. CrossRef PubMed
21. Velissaris D, Pantzaris ND, Bountouris P, et al. Correlation between neutrophil-to-lymphocyte ratio and severity scores in septic patients upon hospital admission. A series of 50 patients. Rom J Intern Med. 2018;56(3):153-157. CrossRef PubMed
22. Huang Z, Fu Z, Huang W, et al. Prognostic value of neutrophil-to-lymphocyte ratio in sepsis: a meta-analysis. Am J Emerg Med. 2020;38(3):641-647. CrossRef PubMed
23. Djordjevic D, Rondovic G, Surbatovic M, et al. Neutrophil-to-lymphocyte ratio, monocyte-to-lymphocyte ratio, platelet-to-lymphocyte ratio, and mean platelet volume-to-platelet count ratio as biomarkers in critically ill and injured patients: which ratio to choose to predict outcome and nature of bacteremia? Mediators Inflamm. 2018;2018:3758068. CrossRef PubMed
24. Oh GH, Chung SP, Park YS, et al. Mean platelet volume to platelet count ratio as a promising predictor of early mortality in severe sepsis. Shock. 2017;47(3):323-330. CrossRef PubMed
25. Shen Y, Huang X, Zhang W. Platelet-to-lymphocyte ratio as a prognostic predictor of mortality for sepsis: interaction effect with disease severity-a retrospective study. BMJ Open. 2019;9(1):e022896. CrossRef PubMed
26. Ahn C, Kim W, Lim TH, et al. The delta neutrophil index (DNI) as a prognostic marker for mortality in adults with sepsis: a systematic review and meta-analysis. Sci Rep. 2018;8(1):6621. CrossRef PubMed
27. Kim HW, Yoon JH, Jin SJ, et al. Delta neutrophil index as a prognostic marker of early mortality in gram negative bacteremia. Infect Chemother. 2014;46(2):94-102. CrossRef PubMed
28. Celik IH, Arifoglu I, Arslan Z, et al. The value of delta neutrophil index in neonatal sepsis diagnosis, follow-up and mortality prediction. Early Hum Dev. 2019;131:6-9. CrossRef PubMed
29. Tauseef A, Zafar M, Arshad W, et al. Role of immature platelet fraction (IPF) in sepsis patients: a systematic review. J Family Med Prim Care. 2021;10(6):2148-2152. CrossRef PubMed
30. Arora P, Gupta PK, Lingaiah R, et al. Volume, conductivity, and scatter parameters of leukocytes as early markers of sepsis and treatment response. J Lab Physicians. 2019;11(1):29-33. CrossRef PubMed
31. Mammen J, Choudhuri J, Paul J, et al. Cytomorphometric neutrophil and monocyte markers may strengthen the diagnosis of sepsis. J Intensive Care Med. 2018;33(12):656-662. CrossRef PubMed
32. Agnello L, Vidali M, Lo Sasso B, et al. Monocyte distribution width (MDW) as a screening tool for early detecting sepsis: a systematic review and meta-analysis. Clin Chem Lab Med. 2022;60(5):786-792. CrossRef PubMed
33. Agnello L, Sasso BL, Giglio RV, et al. Monocyte distribution width as a biomarker of sepsis in the intensive care unit: A pilot study. Ann Clin Biochem. 2021;58(1):70-73. CrossRef PubMed
34. Agnello L, Iacona A, Lo Sasso B, et al. A new tool for sepsis screening in the emergency department. Clin Chem Lab Med. 2021;59(9):1600-1605. CrossRef PubMed
35. Agnello L, Lo Sasso B, Vidali M, et al. Validation of monocyte distribution width decisional cut-off for sepsis detection in the acute setting. Int J Lab Hematol. 2021;43(4):O183-O185. CrossRef PubMed
36. Piva E, Zuin J, Pelloso M, et al. Monocyte distribution width (MDW) parameter as a sepsis indicator in intensive care units. Clin Chem Lab Med. 2021;59(7):1307-1314. CrossRef PubMed
37. Marcos-Morales A, Barea-Mendoza JA, García-Fuentes C, et al. Elevated monocyte distribution width in trauma: an early cellular biomarker of organ dysfunction. Injury. 2022;53(3):959-965. CrossRef PubMed
38. Polilli E, Frattari A, Esposito JE, et al. Monocyte distribution width (MDW) as a new tool for the prediction of sepsis in critically ill patients: a preliminary investigation in an intensive care unit. BMC Emerg Med. 2021;21(1):147. CrossRef PubMed
39. Agnello L, Lo Sasso B, Bivona G, et al. Reference interval of monocyte distribution width (MDW) in healthy blood donors. Clin Chim Acta. 2020;510:272-277. CrossRef PubMed
40. Agnello L, Giglio RV, Gambino CM, et al. Time-dependent stability of monocyte distribution width (MDW). Clin Chim Acta. 2022;533:40-41. CrossRef PubMed
41. Bordignon JC, Bueno Gardona RG, Vasconcellos LS, et al. Thermal and chronological stability of monocyte distribution width (MDW), the new biomarker for sepsis. Clin Chem Lab Med. 2022;60(10):e232-e234. CrossRef PubMed
42. Ahmed Bentahar MD. What is monocyte distribution width (MDW) and what role does it play in the early detection of sepsis? Online (Accessed February 2025)
43. Kim HI, Park S. Sepsis: early recognition and optimized treatment. Tuberc Respir Dis (Seoul). 2019;82(1):6-14. CrossRef PubMed
44. Huang YH, Chen CJ, Shao SC, et al. Comparison of the diagnostic accuracies of monocyte distribution width, procalcitonin, and c-reactive protein for sepsis: a systematic review and meta-analysis. Crit Care Med. 2023;51(5):e106-e114. CrossRef PubMed
45. Frugoli A, Ong J, Meyer B, et al. Monocyte distribution width predicts sepsis, respiratory failure, and death in COVID-19. Cureus. 2023;15(12):e50525. CrossRef PubMed
46. Mubaraki MA, Faqihi A, AlQhtani F, et al. Blood biomarkers of neonatal sepsis with special emphasis on the monocyte distribution width value as an early sepsis index. Medicina (Kaunas). 2023;59(8):1425. CrossRef PubMed
47. Mateescu V, Lankachandra K. Novel hematological biomarker adopted for early sepsis detection emerges as predictor of severity for COVID infection. Mo Med. 2023;120(3):196-200. PubMed
48. Encabo M, Hernández-Álvarez E, Oteo D, et al. Monocyte distribution width (MDW) as an infection indicator in severe patients attending in the emergency department: a pilot study. Rev Esp Quimioter. 2023;36(3):267-274. CrossRef PubMed
49. Jo SJ, Kim SW, Choi JH, et al. Monocyte distribution width (MDW) as a useful indicator for early screening of sepsis and discriminating false positive blood cultures. PLoS One. 2022;17(12):e0279374. CrossRef PubMed
50. Singla N, Jandial A, Sharma N, et al. Monocyte Distribution Width (MDW) as an early investigational marker for the diagnosis of sepsis in an emergency department of a tertiary care hospital in North India. Cureus. 2022;14(10):e30302. CrossRef PubMed
51. Cusinato M, Sivayoham N, Planche T. Sensitivity and specificity of monocyte distribution width (MDW) in detecting patients with infection and sepsis in patients on sepsis pathway in the emergency department. Infection. 2023;51(3):715-727. CrossRef PubMed
52. Polilli E, Di Iorio G, Silveri C, et al. Monocyte Distribution Width as a predictor of community acquired sepsis in patients prospectively enrolled at the Emergency Department. BMC Infect Dis. 2022;22(1):849. CrossRef PubMed

53. Ognibene A, Lorubbio M, Montemerani S, et al. Monocyte distribution width and the fighting action to neutralize sepsis (FANS) score for sepsis prediction in emergency department. Clin Chim Acta. 2022;534:65-70. CrossRef PubMed
54. Hou SK, Lin HA, Tsai HW, et al. Monocyte Distribution Width in children with systemic inflammatory response: retrospective cohort examining association with early sepsis. Pediatr Crit Care Med. 2022;23(9):698-707. CrossRef PubMed
55. Malinovska A, Hinson JS, Badaki-Makun O, et al. Monocyte distribution width as part of a broad pragmatic sepsis screen in the emergency department. J Am Coll Emerg Physicians Open. 2022;3(2):e12679. CrossRef PubMed
56. Poz D, Crobu D, Sukhacheva E, et al. Monocyte distribution width (MDW): a useful biomarker to improve sepsis management in emergency department. Clin Chem Lab Med. 2022;60(3):433-440. CrossRef PubMed
57. Li Y, She Y, Fu L, et al. Association between red cell distribution width and hospital mortality in patients with sepsis. J Int Med Res. 2021;49(4):3000605211004221. CrossRef PubMed
58. Hausfater P, Robert Boter N, Morales Indiano C, et al. Monocyte distribution width (MDW) performance as an early sepsis indicator in the emergency department: comparison with CRP and procalcitonin in a multicenter international European prospective study. Crit Care. 2021;25(1):227. CrossRef PubMed
59. Woo A, Oh DK, Park CJ, et al. Monocyte distribution width compared with C-reactive protein and procalcitonin for early sepsis detection in the emergency department. PLoS One. 2021;16(4):e0250101. CrossRef PubMed
60. Crouser ED, Parrillo JE, Martin GS, et al. Monocyte distribution width enhances early sepsis detection in the emergency department beyond SIRS and qSOFA. J Intensive Care. 2020;8(1):33. CrossRef PubMed
61. Hou SK, Lin HA, Chen SC, et al. Monocyte Distribution Width, neutrophil-to-lymphocyte ratio, and platelet-to-lymphocyte ratio improves early prediction for sepsis at the emergency. J Pers Med. 2021;11(8):732. CrossRef PubMed
62. Agnello L, Ciaccio AM, Del Ben F, et al. Monocyte distribution width (MDW) kinetic for monitoring sepsis in intensive care unit. Diagn Berl Ger. 22 April 2024. CrossRef
63. Crouser ED, Parrillo JE, Seymour C, et al. Improved early detection of sepsis in the ED with a novel monocyte distribution width biomarker. Chest. 2017;152(3):518-526. CrossRef PubMed
64. Kumar D, Sudha M, Tarai B, et al. Evaluation of mean monocyte volume in septicemia caused by Salmonella species. J Lab Physicians. 2018;10(4):397-400. CrossRef PubMed
65. Khandal AR, Khanduri S, Ahmad S, et al. Analysis of changes in variation of neutrophil and monocyte parameters, including volume, conductivity and scatter in sepsis patients and healthy controls: a cross-sectional study. J Clin Diagn Res. 2024;18(5):EC17-EC23. CrossRef

JCB
J Circ Biomark 2025; 14: 30-38
ISSN 1849-4544 | DOI: 10.33393/jcb.2025.3564
ORIGINAL RESEARCH ARTICLE

Diagnostic value of carcinoembryonic antigen, cancer antigen 15-3, and cell-free DNA as blood biomarkers in early detection of canine mammary tumor

Diksha Singh[1], Prashant P Rokade[1], Neeraj K Gangwar[1], Mukul G Gabhane[1], Sunil Malik[1], Kavisha Gangwar[1], Shyama N Prabhu[1], Renu Singh[1], DD Singh[1], Sonam Kumari[2], Soumen Chaudhary[2], Jitendra K Choudhary[3]

[1]Department of Veterinary Pathology, College of Veterinary Science & Animal Husbandry, Veterinary University, Mathura, Uttar Pradesh - India
[2]Department of Veterinary Pharmacology and Toxicology, College of Veterinary Science & Animal Husbandry, Veterinary University, Mathura, Uttar Pradesh - India
[3]Animal Genetics and Breeding, College of Veterinary Science & Animal Husbandry, Veterinary University, Mathura, Uttar Pradesh - India

ABSTRACT

Introduction: Blood biomarkers play a crucial role in the diagnosis and prognosis of tumor. The present research was designed to study the diagnostic effect of serum biomarkers, namely carcino-embryonic antigen (CEA), cancer antigen 15-3 (CA15-3), and plasma biomarker *viz.,* circulating cell-free DNA (cfDNA); and their correlation with cytological and histopathological results.

Methods: A total of 60 blood samples were collected. Out of which 36 samples were from the dogs affected with canine mammary tumors, and 24 samples were from the apparently healthy dogs. CEA and CA15-3 were estimated using Sandwich ELISA, and cfDNA was estimated by the ccfDNA kit. A significant Positive correlation was observed between tumor blood biomarker levels, cytology and histopathological grades of the tumors.

Results: We found that CA15-3 can be a more effective serum tumour biomarker than CEA for diagnosing canine mammary gland tumours. This finding showed a positive correlation with the clinical grade of the disease. The concentration of serum markers and cfDNA in animals affected with malignant mammary gland tumours was higher compared to the benign entity of tumours and healthy control groups. The ROC curve analysis revealed that the sensitivity (Se) and specificity (Sp) of CEA and CA15-3 biomarkers improved when used together. IN comparison to healthy controls, canines with both benign and malignant neoplasia showed significantly higher ($p < 0.05$) cfDNA concentrations.

Conclusion: This study highlights the role of blood tumor biomarkers for routine screening of animals in early diagnosis of tumors, further treatment, and prognosis.

Keywords: CA15-3, CEA, cfDNA, Cytology, Histopathology, Mammary gland tumors

Introduction

Cancer is the most common ailment and the leading cause of death in aged canines and humans despite advances in cancer therapies (1). According to the World Health Organization, cancer was responsible for nearly one in six deaths globally in 2020, underscoring its status as a major health burden for both humans and animals. Among the various types of cancer, breast cancer is one of the most commonly diagnosed malignancies in women, with its incidence continuing to rise due to a combination of genetic predispositions and environmental influences (2). Similarly, in female dogs, canine mammary gland tumours (CMTs) represent the second most common cause of tumour-related mortality, with fatality rates ranging from 50% to 75%, depending on the tumour type, stage of disease, and the treatment regimen employed (3). Notably, Canine mammary gland tumours (CMTs) exhibit significant morphological, behavioural, and genetic similarities to human breast cancer, making dogs a valuable comparative model for studying the disease in terms of diagnosis, prognosis, and therapeutic intervention (4). Early detection of cancer is critical for improving survival outcomes. Tumour markers have emerged as vital tools in the early screening, prognostication, and monitoring of therapeutic responses in malignancies (5). These biomarkers may be produced directly by tumour cells or elicited in the host as a response to tumour presence. An ideal tumour marker is characterized by high sensitivity and specificity, enabling the accurate detection of malignancy at an early stage to facilitate timely clinical intervention and enhance

Received: April 20, 2025
Accepted: July 21, 2025
Published online: August 21, 2025

Corresponding author:
Neeraj Kumar Gangwar
email: neerajgangwarvet@gmail.com

screening efficacy (6). Carcino-embryonic antigen (CEA) is a glycoprotein expressed in the gastrointestinal mucosa and in low concentrations in epithelial cell membranes. It is markedly overexpressed in various malignancies, including those of the colon, breast, and lung (7). CEA contributes to intercellular adhesion and is clinically valuable in cancer diagnosis, staging, recurrence detection, and the monitoring of therapeutic responses, particularly during chemotherapy (8). Cancer antigen 15-3 (CA15-3) is a mucinous glycoprotein that belongs to the MUC1 family. During malignant transformation, CA15-3 is overexpressed on the cell membrane and in the cytoplasm. In this state, MUC1 can function as an anti-adhesive molecule, promoting tumour cell detachment, invasion, and metastasis (9). Additionally, circulating cell-free DNA (cf-DNA), which consists of extracellular nucleic acid fragments released by tumour cells through apoptosis, necrosis, or active secretion, holds promise as a minimally invasive biomarker for early cancer detection. Under physiological conditions, cf-DNA levels remain low, but they increase significantly in various pathological states, including inflammation, diabetes, and cancer (10). The aim of this study is to evaluate the diagnostic and prognostic potential of the combined detection of blood-based biomarkers—CEA, CA15-3, and cf-DNA—in canine mammary gland tumours. This combinatorial approach is expected to enhance sensitivity and specificity in early diagnosis and case prognosis.

Materials and Methods

Sample Collection

Samples for this prospective study were collected during the period from January 2024 to October 2024 from the animals presented at the Veterinary Clinical Complex, Pandit Deen Dayal Upadhyaya Pashu Chikitsa Vigyan Vishwavidyalaya Evam Go-Anusandhan Sansthan, Mathura (DUVASU), Mathura, UP, India. A total of sixty blood samples of dogs were collected with the owner's consent. Out of these, thirty-six are from dogs affected with canine mammary tumours, and twenty-four were from healthy dogs. The study was approved by the Institutional Animal Ethics Committee, DUVASU, Mathura, India, with certification No. IAEC/22/2/4 and letter No. 145/IAEC/24/1/27, dated 05-03-2024. All selected cases subjected to a thorough clinical examination and owner's contact information; age, sex; breed and body weight of animals; location of the lesion(s); number of mammary glands involved; size of the affected gland; colour, texture, and consistency of the neoplastic growth; duration of the illness; history of prior inflammation or injury; history of parity and spaying were recorded. Ultrasonographic and/or radiographic examinations carried out to determine the spread of tumour to distance lymph nodes and visceral organs. Out of 36 selected neoplastic cases, 31 cytology, 36 serum, 36 plasma, and 21 tissue samples were obtained for examinations (Table 1).

TABLE 1 - Clinical history of cases showing occurrence of canine mammary tumor (n = 36)

Case No.	Breed	Age	Body wt.	No. of glands affected	Gland effected	Size (cm)	Consistency
1.	Labrador	11 yrs.	41 Kg	2	Right inguinal & right caudal abdominal	5–6 cm	Hard
2.	Rottweiler	4 yrs.	36 Kg	4	Left & right Inguinal	4–5 cm	Soft
					Left & right caudal abdominal	2–3 cm	
3.	Beagle	8 yrs.	11 Kg	2	Left & right Inguinal	6–7 cm	Soft
4.	German Shepherd	9 yrs.	39 Kg	1	Left caudal abdominal	4–5 cm	Semi-hard
5.	German Shepherd	12 yrs.	42 Kg	2	Left & right caudal thoracic	12–13 cm	Semi-hard
6.	Rottweiler	9 yrs.	45 Kg	1	Left inguinal	4–5 cm	Semi-hard
7.	Indian Spitz	11 yrs.	10 Kg	1	Left inguinal	7–8 cm	Semi-hard
8.	Pomeranian	9 yrs.	6 Kg	1	Right inguinal	9–10 cm	Soft
9.	Indian Spitz	11 yrs.	9 Kg	1	Left inguinal	5–6 cm	Soft
10.	German Shepherd	3 yrs.	38 Kg	1	Left cranial abdominal	4–5 cm.	Semi-hard
11.	Indian Spitz	10 yrs.	8 Kg	1	Right inguinal	5–6 cm.	Hard
12.	Labrador	2.5 yrs.	41 Kg	1	Left inguinal	7–8 cm.	Semi-hard
13.	German Shepherd	3 yrs.	41 Kg	1	Left caudal abdominal	5–7 cm.	Semi-hard
14.	Labrador	4 yrs.	46 Kg	1	Left inguinal	7–8 cm.	Hard
15.	Non-descript	12 yrs.	36 Kg	1	Left inguinal	2–3 cm.	Semi-hard
16.	German Shepherd	6 yrs.	47 Kg	2	Right inguinal & caudal abdominal	15–18 cm.	Semi-hard to hard

Case No.	Breed	Age	Body wt.	No. of glands affected	Gland effected	Size (cm)	Consistency
17.	German Shepherd	9 yrs.	38 Kg	2	Left & right inguinal	9–10 cm.	Soft
18.	German shepherd	10 yrs.	43 Kg	1	left inguinal	8–9 cm.	Semi-hard
19.	Indian Spitz	8 yrs.	10 Kg	1	Right cranial abdominal	2–3 cm.	Soft
20.	German shepherd	6 yrs.	44 Kg	2	Left cranial abdominal	7–8 cm.	Semi-hard
21.	Pomeranian	5 yrs.	8 Kg	1	Right inguinal	5–6 cm.	Hard
22.	Pomeranian	8 yrs.	9 Kg	1	Left inguinal	8–9cm.	Semi-hard
23.	Non-descript	8 yrs.	42 Kg	2	Left inguinal & caudal abdominal	6–7 cm.	Semi-hard
24.	Non-descript	7 yrs.	21 Kg	2	Right inguinal & caudal abdominal	10–11 cm.	Semi-hard
25.	German shepherd	9 yrs.	40 Kg	1	Right caudal abdominal	3–4 cm.	Soft
26.	Rottweiler	4 yrs.	32 Kg	1	Left inguinal	6–7 cm.	Soft
27.	Non-descript	8 yrs.	19 Kg	1	Right cranial thoracic	5–6 cm.	Hard
28.	Non-descript	13 yrs.	39 Kg	1	Right caudal thoracic	4–5 cm.	Semi-hard
29.	Great dane	1.5 yrs.	34 Kg	1	Right cranial thoracic	7–8 cm.	Soft
30.	Rottweiler	8 yrs.	42 Kg	1	Left cranial thoracic	5–7 cm	Soft to semi-hard
31.	Non-descript	8 yrs.	37 Kg	1	Left cranial abdominal	3–4 cm	Soft
32.	Rottweiler	8 yrs.	41 Kg	2	Left & right caudal abdominal	8–9 cm	Semi-hard
33.	Labrador	10 yrs.	46 Kg	1	Right cranial abdominal	3–4 cm	Semi-hard
34.	Non-descript	7 yrs.	17 Kg	4	Right & left caudal thoracic	7–8 cm	Semi-hard
					Left cranial & caudal abdominal	2–3 cm	
35.	Pomeranian	7 yrs.	9 Kg	1	Left inguinal	4–5 cm	Soft to semi-hard
36.	German shepherd	9 yrs.	65 Kg	2	Right inguinal & caudal abdominal	13–15 cm	Semi-hard

Blood collection

Peripheral blood samples were aseptically collected from the cephalic or saphenous vein of dogs using sterile, single-use 5 mL vacutainer tubes. A total of 4 mL of blood was collected from each subject, divided equally between two vacutainers depending on the intended analysis. For cfDNA quantification, 2 mL of blood was drawn into an EDTA-coated vacutainer to prevent clotting. The sample was gently inverted several times to ensure proper mixing with the anticoagulant. These samples were processed immediately. Plasma was separated by centrifugation at 3500 × g for 10 minutes at room temperature. The supernatant (plasma) was carefully aspirated and transferred into a sterile, labelled plain 2 mL micro-centrifuge tube. Plasma samples were stored at −80°C until cfDNA extraction. cfDNA was isolated using the QIAamp MinElute ccfDNA Mini Kit (QIAGEN, Germany; Catalogue No. 55204). For estimation of serum tumour biomarkers— CEA and CA15-3, an additional 2 mL of blood was collected into plain vacutainer tubes without anticoagulant. These samples were allowed to clot at room temperature, and the serum was separated out after clotting of the blood. The resulting serum was transferred to labelled sterile 2 mL micro-centrifuge tubes and stored at −80°C until further analysis. CEA concentrations were measured using a canine-specific Carcinoembryonic Antigen ELISA Kit (Bioassay Technology Laboratory, Shanghai, China; Catalogue No. E0157Ca), while CA15-3 levels were determined using a Canine Carbohydrate Antigen 15-3 ELISA Kit (Bioassay Technology Laboratory, Shanghai, China; Catalog No. E0156Ca). All plasma and serum samples were appropriately labelled with animal identification, date of collection, and sample type, and stored at −80°C until further use.

Fine needle aspiration cytology (FNAC)

Prior to sampling, strict aseptic protocols were followed. The overlying skin of the affected mammary gland region was clipped and cleansed thoroughly using sterile gauze swabs soaked in 70% isopropyl alcohol. The area was allowed to air-dry to ensure complete disinfection and reduce the risk of contamination during aspiration. Fine needle aspiration (FNA) was performed using a 22-gauge sterile needle attached to a 5 mL disposable syringe. The needle was carefully inserted percutaneously into the mammary gland mass, targeting the central region of the growth. Multiple passes (2-3) were made in

different directions within the same insertion site to ensure representative sampling of the lesion. Negative pressure was applied gently to aspirate cellular material into the syringe. Care was taken to minimize blood contamination and ensure adequate cellularity. Upon obtaining the aspirate, the needle was detached from the syringe, and a small volume of air was drawn into the syringe. The needle was then re-attached, and the aspirated material was expelled onto a clean, dry, grease-free glass microscope slide. Using another slide, a thin smear was prepared. The prepared smears were stained with Giemsa stain following standard cytological staining protocols. Stained slides were then examined under a light microscope for cytomorphological evaluation of the neoplastic cells. Parameters such as cellularity, nuclear pleomorphism, chromatin pattern, nucleolar prominence, mitotic activity, and cytoplasmic features were assessed. Cytological grading of the mammary tumor was conducted based on the criteria outlined in Robinson's grading system, which provides a standardized method for classifying canine mammary tumours according to cytological features indicative of tumour aggressiveness and malignancy (11).

Histopathology

This technique is considered a gold standard for determining the changes in tissue and identification of tumour types, and the grade of malignancy. Tissue samples obtained from the mammary gland masses were immediately fixed in 10% neutral buffered formalin (NBF) for a minimum of 24 to 48 hours to ensure optimal preservation of cellular and tissue morphology. Following fixation, tissues were subjected to standard histological processing, which involved dehydration through a graded series of ethanol (70%, 80%, 95%, and absolute), clearing in xylene, and embedding in paraffin wax. Paraffin-embedded tissue blocks were sectioned at a thickness of 4-5 µm using a rotary microtome. Sections were mounted onto clean, albumin-coated glass slides and allowed to dry, followed by deparaffinization in xylene and rehydration through a descending alcohol series (absolute, 95%, 70%) to distilled water. The slides were then stained with Harris's Hematoxylin for 5-10 minutes to visualize nuclear detail, followed by rinsing in running tap water. Differentiation was performed using 1% acid alcohol. Subsequently, slides were counterstained with Eosin Y for 1-2 minutes to stain the cytoplasm and extracellular matrix. Finally, the stained sections were dehydrated through ascending grades of alcohol, cleared in xylene, and mounted with a coverslip using a resinous mounting medium. The prepared slides were then examined under a light microscope for histopathological evaluation of tumor architecture and cellular characteristics (12). The histopathological sections were then analyzed and classified based on the criteria established by Goldschmidt et al. (13), classification criteria, and histopathological grading of CMTs based on the Elston and Ellis system of classification (14).

Statistical Analysis

Statistical analysis was performed using SPSS 27.0 software. A general linear model of one-way ANOVA based on Fisher's Least Significant Difference method was used, and significant values were further analyzed using Duncan's Multiple Range Test. Results are expressed as mean ± standard error (SE). Statistical significance was set at $p < 0.05$, while $p < 0.01$ was considered highly significant.

The sensitivity, specificity, and accuracy of tumour markers in the diagnosis of canine mammary gland tumours are as follows:

Sensitivity = (True positive/True positive + False negative)
Specificity = (True negative/True negative + False positive)
Accuracy = (True positive + True negative)/(True positive + True negative + False positive + False negative)

The boundary value of the tumour markers is defined by the method of the receiver operating characteristic curve of the subject, or ROC curve. The higher the area under the curve (AUC), the higher the diagnostic value. Accuracy reaches its highest when AUC > 0.9. Specificity and sensitivity of tumour markers in canine mammary gland tumours evaluated using the ROC curve. The area under the curve (AUC) 1.0 is considered the ideal index. There is no diagnostic value if AUC < 0.5.

Results

Epidemiological characteristics of mammary gland tumours in dogs

A total of eight dog breeds with mammary gland tumours were included, and the results showed that German Shepherds had the highest incidence of canine mammary tumours (27.77%), with pure breeds being the most affected. Animals older than seven years of age were frequently affected. The 7-12 years age group had the highest incidence of tumours (19/36 – 52.7%). In comparison to the anterior pairs of mammary glands, the posterior pairs had a higher frequency of tumors, inguinal (47.06%), caudal abdominal (25.49%), cranial abdominal (11.76%), caudal thoracic (9.80%), and cranial thoracic (5.89%) glands were involved in decreasing order. Only four animals (11%) out of the 36 animals in the current study had undergone spaying.

Cytology

Based on cytology, tumours classified as grade 1 were deemed benign, whereas grade 2 or 3 were deemed malignant (15). The maximum sample was from the grade II category (65%) (Fig. 1b), followed by grade I (29%) (Fig. 1a) and then grade III (6%) (Fig. 1c). A total of 31 samples were graded out of which 22 are of epithelial origin and nine are of mesenchymal origin.

Histopathology

In the present study, 81% of tumours were classified as malignant, while 19% as benign on histopathology. The most common type of malignant mammary tumours was carcinoma mixed type accounted for 20% of malignant tumours (Fig. 2a), whereas the most common type of benign tumor was fibroadenoma accounted for 50% of all benign tumours (Fig. 2b). The other common tumors are shown in Figures 2c, d, and e. The normal histological structure of the canine mammary gland is shown (Fig. 2f). On the basis of grading, 80% of tumors belonged to the grade II category.

Level of CEA, CA15-3, and cfDNA biomarkers

Results showed that the serum levels of CEA and CA15-3 in the malignant group were significantly higher than the healthy controls ($p < 0.05$) (Figs 3a and b). cfDNA level in plasma of malignant mammary gland tumour group was also significantly higher than that of benign mammary gland tumour group and healthy control group ($p < 0.05$) (Fig. 3c). Univariate analysis showed that serum CA15-3, CEA, and plasma cfDNA concentrations were significantly Higher in dogs with lymph node invasion, metastasis, and histologic grading (Table 2).

Sensitivity, specificity of single and combined detections of CA15-3, CEA, and cfDNA

The individual detection sensitivity for tumour biomarkers revealed that circulating free DNA (cfDNA) had the highest sensitivity at 78.9%, followed by CA15-3 and CEA, with sensitivities of 70.3% and 65.2%, respectively (Table 3). Similarly, cfDNA demonstrated the highest specificity (72.7%), whereas CA15-3 and CEA showed lower specificities of 56.5% and 43.2%, respectively. When the three biomarkers—CA15-3, CEA, and cfDNA—were used in combination, the sensitivity and accuracy increased to 80.0% and 78.0%, respectively,

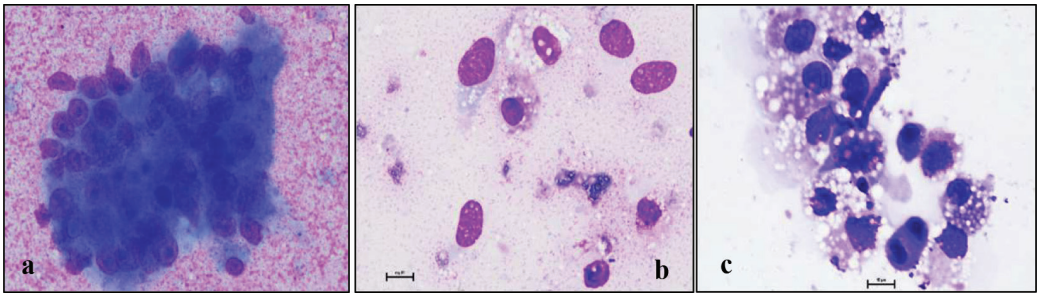

FIGURE 1 - Cytological observation of different mammary gland tumours in dogs (Geimsa Stain, 1000X). (a) Mildly pleomorphic cells arranged in clusters, Grade I; (b) singly arranged cells with vacuolated cytoplasm, Grade II; (c) Mixed population of pleomorphic cells showing karyokinesis stage, Grade III.

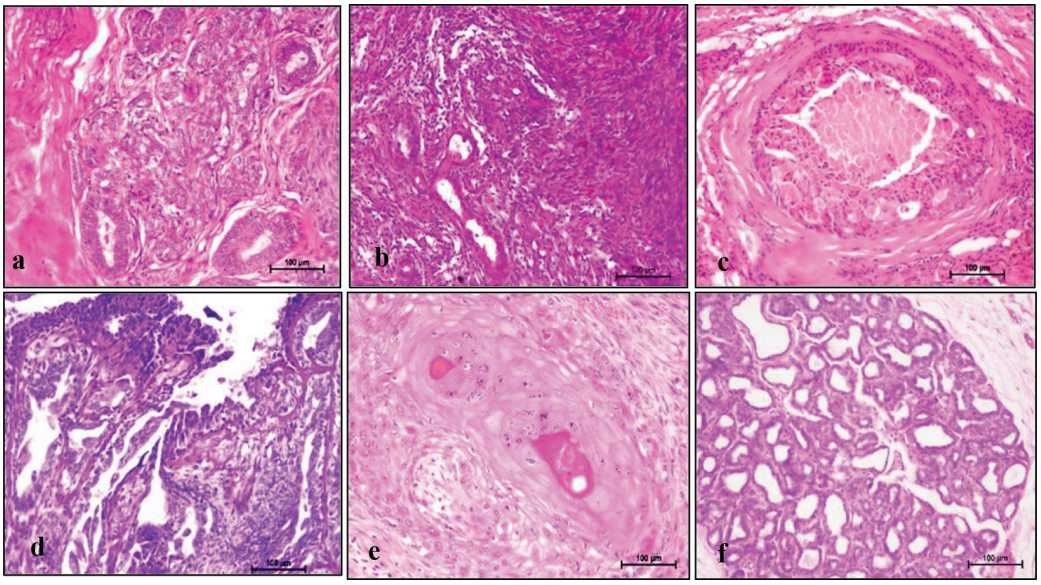

FIGURE 2 - Histopathological observation of different mammary gland tumours in dogs (HE Staining, 200X). (a) Carcinoma Mixed Type; (b) Fibroadenoma; (c) comedocarcinoma; (d)tubulo-papillary carcinoma; (e) squamous cell carcinoma; (f) Healthy mammary gland.

TABLE 2 - Serum CEA, CA15-3, and plasma cfDNA concentration of control and canine mammary gland tumor conditions

GROUPS	CEA (ng/L)		CA15-3 (kU/L)		CfDNA concentration (ng/µL)	
	Mean ± SE	95%CI	Mean ± SE	95% CI	Mean ± SE	95% CI
CONTROL	610.29±40.69^{a}	520.73-699.85	1.49 ± 0.14^{a}	1.17-1.82	4.667±0.4851^{a}	3.599-5.734
BENIGN	690.95±74.88^{ab}	518.26-863.64	2.74 ± 0.38^{b}	1.86-3.62	8.089±0.2756^{b}	7.453-8.724
MALIGNANT	899.60±70.69^{bc}	753.00-1046.20	3.85 ± 0.21^{c}	3.41-4.29	14.900±0.6040^{c}	13.647-16.153
METASTATIC	1199.64±235.64^{d}	450.03-1949.24	5.57 ± 1.13^{d}	1.95-9.19	25.775±1.914^{d}	19.682-31.868

CEA: Carcinoembryonic antigen, CA15-3 : Cancer Antigen 15-3, cfDNA: Cell free DNA.

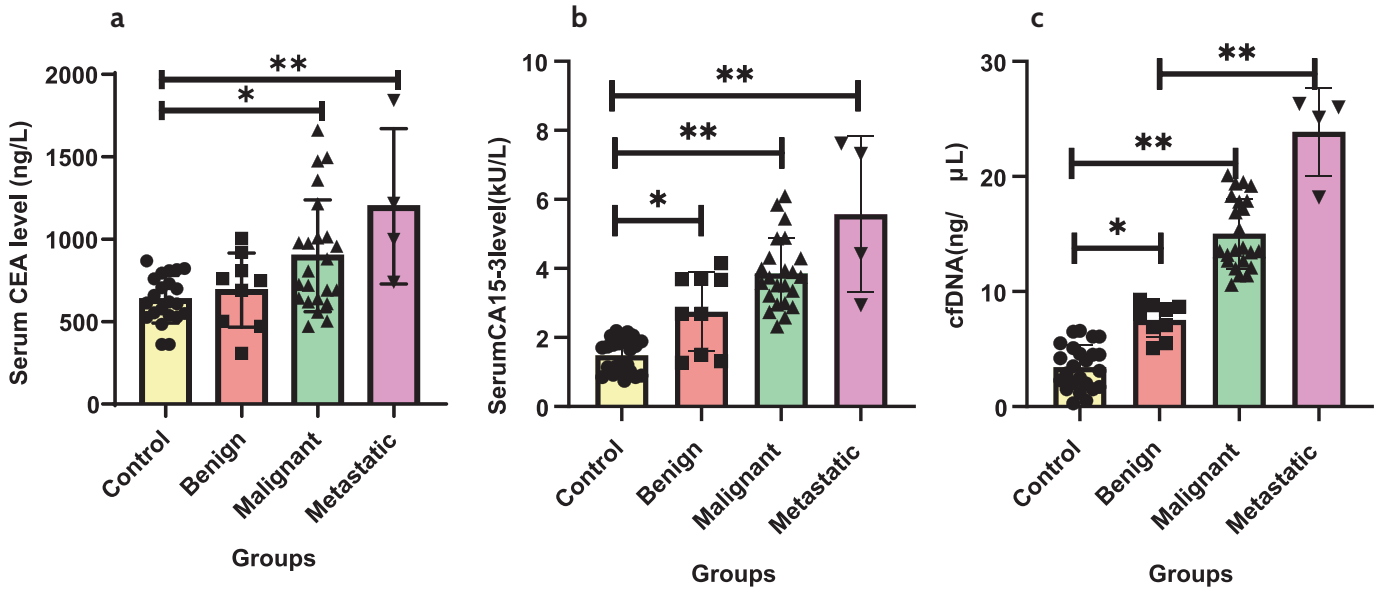

FIGURE 3 - Expression levels of CEA, CA15-3 in serum and cfDNA in plasma of canine mammary tumor. (a) Serum CEA levels of the malignant tumor group, the benign tumor group, and the healthy control group. (b) Serum CA15-3 levels of the three groups. (c) Plasma cfDNA levels of the three groups. Note: *p < 0.05 showed a significant difference, **p < 0.01 showed an extremely significant difference.

surpassing the diagnostic performance of any individual biomarker. However, the specificity of the combined detection (68.0%) was lower than that of cfDNA alone. These findings indicate that the combined detection of CA15-3, CEA, and cfDNA improves overall diagnostic performance and may serve as a more effective approach for the diagnosis of canine mammary gland tumours compared to single biomarker detection.

TABLE 3 - Sensitivity, specificity of single and combined detections of serum CA15-3, CEA, and plasma cfDNA

Tumor Markers	Sensitivity (%)	Specificity (%)	Accuracy (%)
CEA	65.2	43.2	51.6
CA15-3	70.3	56.5	65.0
cfDNA	78.9	72.7	76.6
CEA + CA15-3	79.4	65.4	73.3
CEA+ CA15-3+ cfDNA	80.0	68.0	78.0

Determination of the area under the ROC of CA15-3, CEA after single and combined detection

In order to assess the value of tumor markers in the diagnosis of canine mammary gland tumors (CMGTs), a receiver operating characteristic (ROC) curve was used and determine the area under the curve (AUC). According to Table 4 and Figures 4a to c, each tumour marker demonstrated diagnostic significance for canine mammary gland tumours, with all AUC values exceeding 0.5. Among the individual markers, CA15-3 showed the highest diagnostic accuracy (AUC = 0.823), followed by CEA (AUC = 0.756). When the two serum tumour markers were combined (CEA + CA15-3), the diagnostic performance further improved, yielding the highest AUC value (AUC = 0.875). Overall, the combined detection of biomarkers provided a significantly higher diagnostic accuracy compared to the use of individual markers.

TABLE 4 - The area under the ROC curve of CEA, CA15-3, and CEA + CA15-3

Tumor Markers	AUC	*p*-value	95% CI
CEA	0.756	<0.05	0.613-0.899
CA15-3	0.823	<0.05	0.706-0.939
CEA + CA15-3	0.875	<0.05	0.806-0.945

Discussion

Cancer remains a major cause of mortality in both humans and canines, with mammary gland tumors being the most frequently diagnosed neoplasms in female dogs. Early detection of these tumours significantly improves prognosis and survival rates. The current study focused on evaluating the diagnostic potential of serum biomarkers—carcinoembryonic antigen (CEA) and cancer antigen 15-3 (CA15-3)—and plasma cell-free DNA (cfDNA), in relation to cytological and histopathological findings in canine mammary gland tumors (CMTs).

Breed distribution in our study varied, reflecting geographical differences in breed predisposition. Purebred dogs showed a higher incidence of mammary tumours, suggesting a genetic component in tumour susceptibility (16,17). Cytological grading revealed that benign tumours were more common in dogs aged 5-7 years, while malignant tumours peaked between 8-12 years, supporting the hypothesis that age-related accumulation of tumorigenic factors may contribute to malignancy (17,18). The caudal mammary glands were more frequently affected than the cranial glands, with a higher incidence on the right side of the body. This may be due to the larger size and increased hormonal sensitivity of the caudal glands, particularly to estrogen, making them more

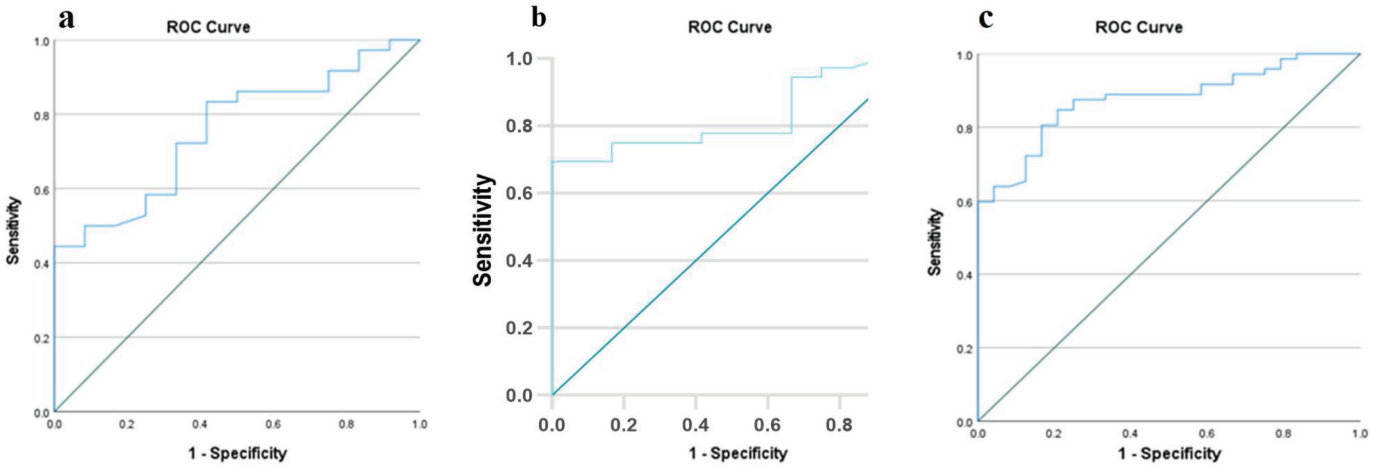

FIGURE 4 - The ROC curve of single and combined detection in the diagnosis of canine mammary gland tumor. (a) The ROC curves for the single detection of CEA. (b) The ROC curves for the single detection of CA15-3. (c) The ROC curves of the combined detection of CA15-3+CEA.

prone to proliferative changes (19). Fine needle aspiration cytology (FNAC) was used for sample collection, with most tumours (65%) falling into grade II (17,20,21). While cytology and histopathology remain gold standards for tumour classification, they require skilled personnel, invasive tissue sampling, and can be time-consuming and costly. In contrast, serum and plasma-based biomarkers such as CEA, CA15-3, and cfDNA offer a less invasive, quicker, and potentially more cost-effective alternative. CEA levels were significantly elevated in malignant tumours (22), particularly those with lymph node involvement, larger size, and distant metastasis (23,24). Conversely, no significant difference was detected between the benign and healthy control group (25). A notable decline in CEA levels post-mastectomy suggests its potential role as a marker for early detection of relapse or metastasis. However, CEA alone is not highly specific, as some malignant cases may not exhibit elevated levels, and no significant difference was noted between benign tumors and healthy controls (24). CA15-3 levels were also significantly higher in dogs with larger, metastatic tumours and higher histopathological grades (26). This marker, a member of the mucin family that detects soluble MUC-1 protein, plays a key role in tumour progression by promoting angiogenesis, immune evasion, and resistance to apoptosis (23). Like CEA, CA15-3 alone lacks high specificity, and some tumours may not express it in detectable amounts. Importantly, the combination of CEA and CA15-3 significantly improved diagnostic sensitivity and specificity compared to individual markers (25). This suggests that these biomarkers may reflect different biological characteristics or stages of tumour development. For instance, some tumours may express high levels of CEA but low CA15-3, or vice versa. By utilizing both markers, clinicians can improve the overall diagnostic accuracy and capture a broader spectrum of tumour profiles (27). Despite this, it is essential to acknowledge that even in combination, these biomarkers are not highly specific and should not be solely relied upon for definitive diagnosis (28). Furthermore, cfDNA levels were significantly higher in malignant and metastatic cases compared to benign and healthy controls (29,30). The elevated cfDNA in metastatic cases is likely due to increased cell turnover, necrosis, and release of fragmented DNA from aggressive tumour cells (31,32). In human oncology, cfDNA has emerged as a promising non-invasive biomarker for early detection, prognosis, and monitoring of treatment response. Unlike tissue-based diagnostics, which require skilled personnel and are costly and time-consuming, these serum and plasma markers can be detected using routine blood tests. Although individually not highly specific, their combined use significantly improves diagnostic sensitivity. Early detection through these markers can reduce the high costs associated with late-stage cancer treatment by enabling timely intervention. In veterinary medicine, its application as a "liquid biopsy" holds promise for reducing the reliance on invasive procedures, thereby lowering the overall cost and improving the accessibility of cancer diagnostics. Compared to cytology and histopathology, the detection of serum and plasma biomarkers is generally more accessible and less expensive, especially in settings where advanced histopathological infrastructure is limited. Blood-based testing also reduces the need for anesthesia, surgical intervention, and repeat sampling, thus minimizing patient discomfort and veterinary costs. Although these biomarkers lack the diagnostic precision of histopathology, their integration into routine screening protocols could facilitate earlier detection, guide treatment planning, and monitor disease progression more effectively. While cytology and histopathology remain indispensable for definitive tumour characterization, the use of serum CEA, CA15-3, and plasma cfDNA as adjunct diagnostic tools offers a promising, minimally invasive, and cost-effective strategy for early detection and monitoring of canine mammary tumors. Their combined application improves diagnostic sensitivity and may reduce treatment costs through early intervention and reduced reliance on invasive diagnostics. Although CEA, CA15-3, and cfDNA are not individually highly specific markers for cancer, numerous studies support their combined utility in enhancing early detection of tumours, especially in breast and gastrointestinal cancers. The rationale is based on the concept that multi-marker approaches improve diagnostic performance by compensating for the limitations of single markers.

Each marker reflects different aspects of tumour biology. CEA is a glycoprotein involved in cell adhesion and is frequently elevated in colorectal, breast, and lung cancers. CA15-3, a mucin-type glycoprotein, is predominantly associated with tumour burden in breast cancer. cfDNA consists of short DNA fragments released into the circulation from apoptotic and necrotic tumour cells and can harbour tumour-specific genetic and epigenetic alterations, including point mutations, methylation patterns, and copy number variations. When assessed in combination, these biomarkers offer complementary information: CEA and CA15-3 reflect protein-level changes related to tumour burden and inflammatory processes, while cfDNA provides molecular insights at the genomic level. This multianalyte approach has been shown to improve early detection capabilities. Therefore, despite their individual limitations in specificity, the combined use of CEA, CA15-3, and cfDNA increases diagnostic yield through the integration of diverse biological signals, supporting their utility as part of a comprehensive biomarker panel for early tumour detection.

Conclusion

CA15-3 demonstrated superior diagnostic performance compared to CEA and may be considered a more reliable tumour marker for the detection of mammary gland tumours. Its levels showed a strong positive correlation with tumour progression and clinical staging, highlighting its potential utility in both diagnosis and disease monitoring. The combined use of CA15-3 and CEA resulted in improved sensitivity and specificity compared to either marker alone, indicating that their combined assessment may facilitate earlier detection and improve prognostic evaluation. Elevated serum levels of CA15-3 and CEA, as well as increased concentrations of circulating cell-free DNA (cfDNA) in plasma, were significantly associated with decreased survival rates, suggesting their prognostic value. Fluctuations in plasma cfDNA and serum biomarker levels appear to reflect tumour burden and may indicate the presence of cancer-specific genetic alterations. Thus, these biomarkers serve as valuable tools for monitoring tumour dynamics. Given that liquid biopsy is a minimally invasive diagnostic approach, the routine evaluation of cfDNA, CA15-3, and CEA offers a promising strategy for the early detection and prognosis of canine mammary tumours. When compared with cytological findings and histopathological (HP) examination—the current gold standards in cancer diagnosis—liquid biopsy-based tumour marker assessment offers a non-invasive alternative with the potential for real-time monitoring. Incorporating serum biomarkers and cfDNA analysis into routine clinical practice could facilitate early detection, improve treatment planning, and aid in monitoring therapeutic response, thereby improving clinical outcomes.

Acknowledgment

We thank Veterinary Pathology Laboratory, Veterinary Clinical Complex, and the authority of Veterinary University, Mathura-281001, Uttar Pradesh, India, for great support in completing the research study, and all the animals and animal owners involved in the study.

This is the final version of record of this article as stated in CrossRef

Disclosures

Conflict of interest: The authors declare that they have no potential conflicts of interest.
Funding statement: This research received no specific grant from any funding agency in the public, commercial, or not-for-profit sectors.
Ethical approval: Ethical approval for this study was obtained from the Institutional Animal Ethics Committee (IAEC), having Certification No. IAEC/22/2/4 and Letter No. 145/IAEC/24/1/27.
Author's contribution: Conceptualization: DS, NKG; Data curation: DS, PPR, MGG; Formal analysis: JKC; Investigation: DS, SM, SK; Methodology: KG, SNP, RS; Project Administration: DDS, NKG, SC; Resources: DDS, NKG; Supervision: DDS; Validation: NKG; Writing—original draft: DS, KG; Writing—review & editing: NKG, SNP, RS.

References

1. Reif J. The epidemiology and incidence of cancer. In: Withrow SJ, Vail DM, Page RL, eds. *Withrow & MacEwen's Small Animal Clinical Oncology.* 5th ed. Saunders Elsevier; 2007;68-76. CrossRef
2. Bray F, McCarron P, Parkin DM. The changing global patterns of female breast cancer incidence and mortality. *Breast Cancer Res*. 2004;6(6):229-239. CrossRef PubMed
3. Matos AJ, Baptista CS, Gärtner MF, et al. Prognostic studies of canine and feline mammary tumours: the need for standardized procedures. *Vet J*. 2012;193(1):24-31. CrossRef PubMed
4. Gray M, Meehan J, Martínez-Pérez C, et al. Naturally-occurring canine mammary tumours as a translational model for human breast cancer. *Front Oncol*. 2020;10:617. CrossRef PubMed
5. Das S, Dey MK, Devireddy R, et al. Biomarkers in cancer detection, diagnosis, and prognosis. Sensors (Basel). 2024;24(1):37. CrossRef
6. Amayo AA, Kuria JG. Clinical application of tumour markers: a review. *East Afr Med J*. 2009;86(12)(suppl):S76-S83. CrossRef PubMed
7. Shao Y, Sun X, He Y, et al. Elevated levels of serum tumour markers CEA and CA15-3 are prognostic parameters for different molecular subtypes of breast cancer. *PLoS One*. 2015;10(7):e0133830. CrossRef PubMed
8. Wu SG, He ZY, Zhou J, et al. Serum levels of CEA and CA15-3 in different molecular subtypes and prognostic value in Chinese breast cancer. *Breast*. 2014;23(1):88-93. CrossRef PubMed
9. Manuali E, De Giuseppe A, Feliziani F, et al. CA15-3 cell lines and tissue expression in canine mammary cancer and the correlation between serum levels and tumour histological grade. *BMC Vet Res*. 2012;8(1):86. CrossRef PubMed
10. Heitzer E, Haque IS, Roberts CES, et al. Current and future perspectives of liquid biopsies in genomics-driven oncology. *Nat Rev Genet*. 2019;20(2):71-88. CrossRef PubMed
11. Robinson IA, McKee G, Nicholson A, et al. Prognostic value of cytological grading of fine-needle aspirates from breast carcinomas. *Lancet*. 1994;343(8903):947-949. CrossRef PubMed
12. Luna LG. *Histologic staining methods of the Armed Forces Institute of Pathology. 3rd sed.* McGraw-Hill Book Co; 1972: 12-17.
13. Goldschmidt M, Peña L, Rasotto R, Zappulli V. Classification and grading of canine mammary tumors. *Vet Pathol*. 2011; 48(1):117-131. CrossRef PubMed
14. Peña L, De Andrés PJ, Clemente M, et al. Prognostic value of histological grading in noninflammatory canine mammary carcinomas in a prospective study with two-year follow-up: relationship with clinical and histological characteristics. *Vet Pathol*. 2013;50(1):94-105. CrossRef PubMed

15. Dolka I, Czopowicz M, Gruk-Jurka A, Wojtkowska A, Sapierzyński R, Jurka P. Diagnostic efficacy of smear cytology and Robinson's cytological grading of canine mammary tumors with respect to histopathology, cytomorphometry, metastases and overall survival. *PLoS One*. 2018;13(1):e0191595. CrossRef PubMed
16. Nithya P, Vairamuthu S, Balachandran C. Factors influencing the occurrence of mammary gland tumours in dogs. *Indian J Vet Pathol*. 2018;42(4):249-253. CrossRef
17. Schwartz SM, Urfer SR, White M, et al. Lifetime prevalence of malignant and benign tumours in companion dogs: cross-sectional analysis of Dog Aging Project baseline survey. Vet Comp Oncol. 2022;20(4):797-804. CrossRef
18. Pastor N, Caballé NC, Santella M, et al. Epidemiological study of canine mammary tumours: age, breed, size and malignancy. *Austral J Vet Sci*. 2018;50(3):143-147. CrossRef
19. Salas Y, Márquez A, Diaz D, et al. Epidemiological study of mammary tumors in female dogs diagnosed during the period 2002-2012: a growing animal health problem. PLoS One. 2015;10(5):e0127381. CrossRef
20. Phukan JP, Sinha A, Deka JP. Cytological grading of breast carcinoma on fine needle aspirates and its relation with histological grading. South Asian J Cancer. 2015;4(01):032-034. CrossRef
21. Pal S, Gupta ML. Correlation between cytological and histological grading of breast cancer and its role in prognosis. *J Cytol*. 2016;33(4):182-186. CrossRef PubMed
22. Jain M, Ingole SD, Deshmukh RS, et al. CEA, CA15-3, and miRNA expression as potential biomarkers in canine mammary tumors. *Chromosome Res*. 2021;29(2):175-188. CrossRef PubMed
23. Pinheiro BQ, da Silva IN, Faustino AM, et al. The prognostic value of serum neoplastic biomarkers CA15-3 and CEA in canine mammary neoplasms: a review. *Rev Bras Reprod Anim*. 2022;46(3):290-297. CrossRef
24. Senhorello ILS, Terra EM, Sueiro FAR, et al. Clinical value of carcinoembryonic antigen in mammary neoplasms of bitches. *Vet Comp Oncol*. 2020;18(3):315-323. CrossRef PubMed
25. Fan Y, Ren X, Liu X, et al. Combined detection of CA15-3, CEA, and SF in serum and tissue of canine mammary gland tumor patients. *Sci Rep*. 2021;11(1):6651. CrossRef PubMed
26. Kaszak I, Witkowska-Piłaszewicz O, Domrazek K, et al. The novel diagnostic techniques and biomarkers of canine mammary tumors. *Vet Sci*. 2022;9(10):526. CrossRef PubMed
27. Stieber P, Nagel D, Blankenburg I, et al. Diagnostic efficacy of CA15-3 and CEA in the early detection of metastatic breast cancer—a retrospective analysis of kinetics on 743 breast cancer patients. *Clin Chim Acta*. 2015;448:228-231. CrossRef PubMed
28. Valencakova-Agyagosova A, Frischova Z, Sevcikova Z, et al. Determination of carcinoembryonic antigen and cancer antigen (CA15-3) in bitches with tumours on mammary gland: preliminary report. *Vet Comp Oncol*. 2014;12(3):205-214. CrossRef PubMed
29. Khurram I, Khan MU, Ibrahim S, et al. Efficacy of cell-free DNA as a diagnostic biomarker in breast cancer patients. *Sci Rep*. 2023;13(1):15347. CrossRef PubMed
30. Pushpanjali P, Keshari JR, Prakash P, et al. Correlation between circulating cell-free DNA levels and breast cancer subtypes: a prospective observational study. *Cureus*. 2023;15(7):e42247. CrossRef PubMed
31. Kim J, Bae H, Ahn S, et al. Cell-free DNA as a diagnostic and prognostic biomarker in dogs with tumours. *Front Vet Sci*. 2021;8:735682. CrossRef PubMed
32. Panagopoulou M, Esteller M, Chatzaki E. Circulating cell-free DNA in breast cancer: searching for hidden information towards precision medicine. *Cancers (Basel)*. 2021;13(4):728. CrossRef PubMed

JCB
J Circ Biomark 2025; 14: 39-45
ISSN 1849-4544 | DOI: 10.33393/jcb.2025.3561
ORIGINAL RESEARCH ARTICLE
Open Access

Association of hypertension and diabetes with COVID-19 severity in comparison to healthy patients

Muslima Mahmood Ismail[1], Abdulhakeem D. Hussein[2], Othman Ghazi Najeeb[1], Mohammed Hadi Ali Al-Jumaili[2]

[1]Department of Applied Chemistry, College of Applied Science, University of Anbar, Al-Anbar - Iraq
[2]Department of Applied Chemistry, College of Applied Science, University of Fallujah, Al-Anbar - Iraq

ABSTRACT

Introduction: The coronavirus is a novel pandemic disease that began in Wuhan, China, and further spread globally. Therefore, the aim of this retrospective work was to look at the clinical characteristics and outcomes of diabetic and blood pressure patients compared with a healthy patient who was infected with coronavirus disease (COVID-19).

Methods: Data and outcomes were gathered from medical records and analyzed in 150 patients. The disease is frequently diagnosed via nucleic acid-based viral identification from swabs, sputum, or bronchial alveolar lavage fluid (BALF) using diagnostic reagents such as quantitative reverse transcription-polymerase chain reaction (RT-qPCR). COVID-19 chest radiographs were obtained, and clinical characteristics and outcomes were evaluated. In this study, we analyzed and compared the severity of the disease, its outcome, any associated complications, and clinical laboratory findings in COVID-19 patients between diabetic, hypertensive, and healthy individuals.

Results and Conclusion: According to the findings, COVID-19 can cause a wide range of symptoms, which range from asymptomatic to severe respiratory problems and death. Diabetes appears to be one of the most significant comorbidities associated with a worse COVID-19 result. COVID-19 patients with diabetes (50 (33%) and hypertension (50 (33%)) had more ICU admissions compared with the non-diabetic and non-blood pressure patients (50 (33%)). During the treatment follow-up, 10 (6.6%) of the 150 patients passed away, 140 (93%) were released, 110 (73%) were discharged, and 30 (20%) kept in the hospital. Compared to non-diabetic and healthy COVID-19 patients, diabetic COVID-19 patients had a greater mortality rate.

Keywords: Blood pressure, Clinical characteristics, COVID-19, Diabetes mellitus, RT-qPCR

Introduction

By December 2019, an unsolved outbreak of extreme acute respiratory disease in Wuhan, Hubei Province, China, had been reported. The overwhelming majority of these instances were associated with a wholesale market specializing in human seafood (1). ''The Severe Acute Respiratory Syndrome – Corona Virus 2 (SARS-CoV-2)'' is constantly changing but still remains poorly understood (2) . Quickly, this coronavirus (COVID-19) spread throughout the world and caused severe lung inflammation, acute respiratory distress syndrome (ARDS), cardiac and renal injury (3,4). These viruses consist of genetic material encased in a protein shell and are microscopic pathogens responsible for common infectious diseases such as the common cold, influenza, and warts, as well as more severe illnesses like Ebola, the Spanish influenza, and COVID-19 (5).

Diabetes mellitus patients are more susceptible to viral and bacterial infections, including those of the respiratory tract (6). The lazy leukocyte syndrome, which represents impaired leukocyte phagocytosis function, is one of the mechanisms responsible for this predisposition (impaired immunity) (7). This emphasizes the possibility of a higher risk of COVID-19 infection in diabetic cohorts. Diabetes mellitus causes microangiopathy, which impairs lung compliance and thus affects gaseous exchange, especially in patients over the age of 65 and with comorbidities such as diabetes mellitus, hypertension, and heart failure (8,9). According to the epidemiological studies, people with diabetes and hypertension are more susceptible to catching some kinds of unusual diseases and are more sensitive to specific consequences when infected with pathogens (10,11).

Received: April 15, 2025
Accepted: September 1, 2025
Published online: October 7, 2025

Corresponding author:
Mohammed Hadi Ali Al-Jumaili
email: mohammedhadi@uofallujah.edu.iq

Furthermore, many diabetes medications, such as GLP-1 agonists, as well as anti-hypertension medications like Angiotensin-Converting Enzyme (ACE) inhibitors and statins, increase ACE2 expression (12). Therefore, the severity of COVID-19 may be increased in diabetes as a result of increased ACE2 receptor expression in a variety of tissues. Moreover, ACE2 has been reported in both the exocrine and endocrine pancreas (13).

The inflammatory process linked with diabetes, as well as chronically high blood glucose levels, might result in a poor immune response, which can exacerbate infections in diabetic individuals (14,15). In addition, people with high blood pressure are at a higher risk of COVID-19 infections and complications, according to growing evidence (16). Preliminary data from both China and the United States show that high blood pressure is the most frequent shared pre-existing condition among those hospitalized, affecting between 30% and 50% of patients (17).

Several COVID-19 patients possess pre-existing hypertension, and numerous medications can raise the risk of hypertension. Stroke and other heart problems are caused by high blood pressure, which can damage your arteries and reduce blood flow to your heart in patients infected with the virus, which can lead to death in aged patients (18,19). A compromised immune system is one reason why people with high blood pressure, diabetes, and other health conditions are more susceptible to coronavirus. The immune system is weakened by long-term health problems and aging, making it less effective in fighting the infection (20,21).

High blood pressure affects nearly two-thirds of people over the age of 60, resulting in greater mortality rates among patients with diabetes and high blood pressure (22). Both diseases are highly contagious, with incubation periods ranging from a few days to two weeks. Fever, tiredness, and a dry cough are common early symptoms of the disease. Some patients experience a "cytokine storm" during the advanced, more acute phase, which leads to severe consequences such as acute respiratory distress syndrome (ARDS), shock, multiorgan failure, and possibly death, which is caused by both the viral infection and the host response (23,24). Laboratory testing may reveal a low white blood cell count, lymphopenia, hypoxemia, and abnormal liver and renal function (25,26).

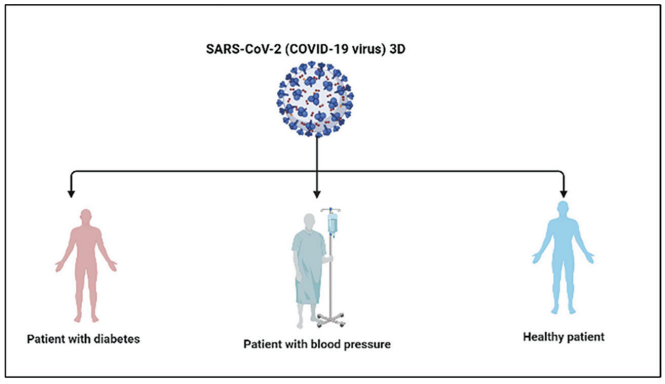

FIGURE 1 - Three separate groups were chosen to be tested in the presence of COVID-19 infection. The diagram was generated using BioRender.com.

The purpose of this study was to assess the prognosis of COVID-19 diabetic patients and high blood pressure compared with the healthy COVID-19 patients, as well as the impact of previous glycemic control. Furthermore, the effect of the generally utilized antidiabetic and antihypertensive medicines on the prognosis of diabetic patients and high blood pressure patients with COVID-19 infection. In this work, we looked at COVID-19 infection in three different groups, including diabetes patients, blood pressure patients, and healthy people, as clarified above in Figure 1.

Methodology

Study Design and Participants

This comparative effectiveness study was carried out at Al Karama Teaching Hospital, Baghdad, Iraq. One hundred and fifty COVID-19 patients with diabetes and elevated blood pressure were admitted to the hospitals. All patients enrolled were confirmed positive for SARS-CoV-2 by physicians who performed quantitative reverse transcription polymerase chain reaction on nasopharynx swab samples, and outcome data were collected prospectively. All of the patients self-reported their hypertension history, blood pressure medications, and diabetes. Cases of COVID-19 that had an epidemiological history, two clinical symptoms, and microbiological evidence were considered established.

Category for determination between severe vs. mild COVID-19 disease

Patients admitted to the intensive care unit (ICU) and given medication for more than 3 days were categorized as extreme cases, whereas other known cases were classified as moderate. Patients with COVID-19 were divided according to their medical history into three groups: patients with diabetes, patients with high blood pressure, and healthy patients. Based on age, gender, and comorbidities, patients without diabetes were compared to those with diabetes and high blood pressure (hypertension, hyperlipemia, and chronic renal diseases).

Laboratory Tests

Clinical and laboratory findings, including signs and symptoms, illness severity of COVID-19 patients were classified as mild, moderate, severe, or critical according to the novel Coronavirus Pneumonia. The Berlin definition of ARDS was used to make the diagnosis. Laboratory data, complete blood count, white blood cell count, lymphocyte count, C-reactive protein (CRP), coagulation profile, D-dimer, urea, and creatinine (Crea), renal and liver function, were retrospectively collected. Clinical symptoms were those present at the time of admission, and laboratory examinations were performed using a blood test. Figure 2 depicts the COVID-19 molecular diagnostic used in this study. The first step in the testing procedure was to collect respiratory specimens such as nasal swabs, sputum, and bronchoalveolar lavage fluid (BALF) from patients who were exhibiting symptoms, after which the specimens were sent for RNA extraction. The quantitative reverse transcription

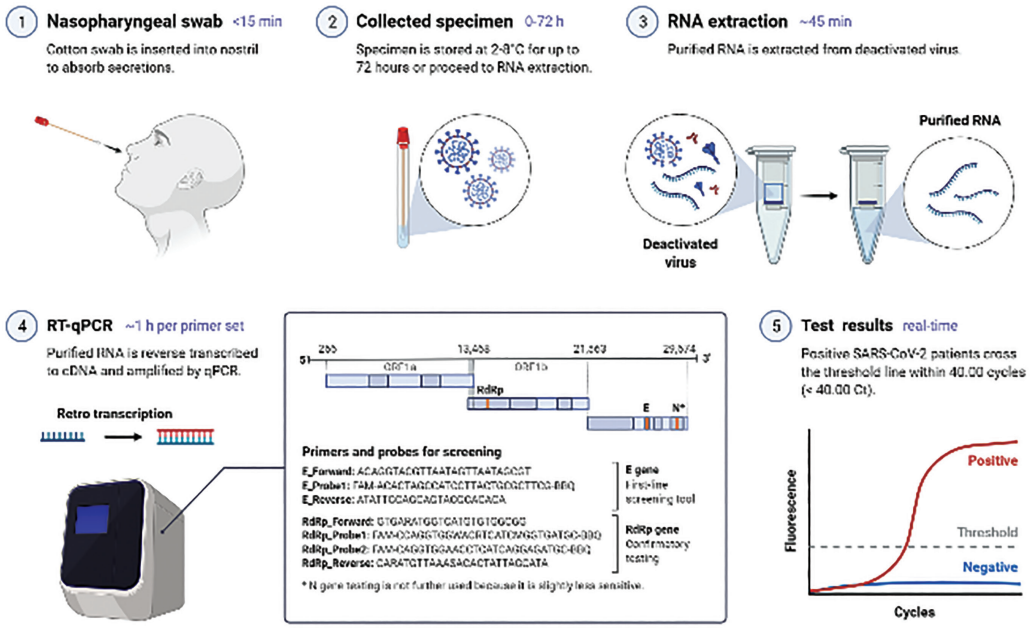

FIGURE 2 - Explaining the molecular diagnosis process for COVID-19. The diagram was created with BioRender.com.

PCR (RT-qPCR) technique was used to analyze SARS-CoV-2, because RT-qPCR can detect the novel coronavirus genetic information (RNA) even if the virus is present in very small amounts.

Results and Discussion

In this work, 150 patients with COVID-19 were included, and the reverse transcription-polymerase chain reaction (RT-PCR) test was used to confirm their infection. They were divided into three groups: 50 of them were found to be diabetics, 50 were non-diabetics, and blood pressure and COVID-19 patients, respectively. Tables 1, 4, and 5 indicate the general information of these patients and the samples collected, as well as the characteristics of the patients with diabetes and high blood pressure. The average length of hospitalization was 2 weeks. The most prevalent symptoms at the start of the infection were fever, dry cough, dyspnea, fatigue, Myalgia/arthralgia, and cold. In addition, headache, nausea or vomiting, chest pain, diarrhea, taste loss, sputum production, and smell loss were some of the less prevalent symptoms, and earache and haemoptysis were uncommon.

As shown in Table 1, a total of 50 specimens were taken, which were classified depending on their age, from mild patients to severe diabetic patients. Among them, 5% (2/40) of patients were under the age of 18, 20% (8/40) were between the ages of 19 and 40, 50% (10/40) were between the ages of 41 and 60, and 25% (20/40) were beyond the age of 60. 20% (10/50) of these patients progressed to severe COVID-19. Twenty percent (2/10) of these patients were between the ages of 19 and 40, 30% (3/10) were between the ages of 41 and 60, and 50% (5/10) were over the age of 60. There was a significant difference in the age of severe patients (age 60 years) compared to moderate patients. The diabetic group experienced more fever, shortness of breath, and fatigue than the non-diabetic group. However, the differences in other symptoms between the two groups were not significant. Diabetes and blood pressure were associated with a higher prevalence of comorbidities such as asthma, cardiovascular disease, and chronic renal disease.

TABLE 1 - Clinical characteristics of diabetic patients infected with COVID-19 (n = 50)

Characteristics	Total (n = 50)	Mild (n = 40)	Severe (n = 10)
Age groups: n (%)			
≤ 18	2	2 (5)	0 (0)
19-40	10	8 (20)	2 (20)
41-60	15	10 (50)	3 (30)
61-80	24	20 (25)	5 (50)
Female	22	16 (40)	3 (30)
male	28	24 (60)	7 (70)
Total	50	40 (80%)	10 (20%)

COVID-19 patients may undergo several hemodynamic changes during hospitalization, affecting their BP level. In case of persistently elevated/fluctuating BP values in the clinic, an ambulatory BP monitoring should be performed to evaluate the hypertension state, assess BP control, and detect other risk features of 24-hour BP, for instance, non-dripping pattern, nocturnal hypertension, and morning surge, as well as assess heart rate response. The optimization of antihypertensive treatment and close follow-up at the hypertension clinic is essential to achieve BP control and avoid hypertension-induced target organ damage in these vulnerable patients.

Also, 50 samples were taken from high blood pressure patients infected with COVID-19. Among them 10 samples were from patients with severe blood pressure as presented in Table 2. 2.5% (1/40) of these patients were under the age of 18, 12.5% (5/40) were between the ages of 19 and 40, 30% (12/40) were between the ages of 41 and 60, and 55% (22/40) were above the age of 60. 20% (10/50) progressed to severe COVID-19. Also, 40% (4/10) were aged 41–60, and 60% (6/ 10) were older than 60.

TABLE 2 - Clinical characteristics of blood pressure patients infected with COVID-19 (n = 50)

Characteristics	Total (n = 50)	Mild (n = 40)	Severe (n = 10)
Age groups: n (%)			
≤ 18	1	1 (2.5)	0
19-40	5	5 (12.5)	0
41-60	20	12 (30)	4 (40)
61-80	24	22 (55)	6 (60)
Female	24	22 (55)	6 (60)
Male	26	18 (45)	4 (40)
Total	50	40 (80%)	10 (20%)

A total of 50 samples were taken from 40 mild patients and 10 severe patients, as well as from healthy people, as can be seen in Table 3. From these patients, 5 % (2/ 40) were younger than 18, 45% (18/40) were aged 19-40, 35% (14/40) were aged 41-60, and 15% (6/ 40) were older than 60. Moreover, 20% (10/50) progressed to severe COVID-19, 30% (3/10) were aged 19-40, 40% (4/10) were aged 41-60, and 30% (3/ 10) were older than 60.

TABLE 3 - Clinical characteristics of healthy patients infected with COVID-19 (n = 50)

Characteristics	Total (n = 50)	Mild (n = 40)	Severe (n = 10)
Age groups: n (%)			
≤ 18	2	2 (5)	0
19 - 40	22	18 (45)	3 (30)
41- 60	18	14 (35)	4 (40)
61- 80	8	6 (15)	3 (30)
Female	28	24 (60)	2 (20)
Male	22	16 (40)	8 (80)
Total	50	40 (80%)	10 (20%)

Age and Gender

As presented in Table 3, the characteristics of COVID-19 patients with diabetes were classified based on disease severity at the time of admission. Patients with severe/critical COVID-19 were older and had diabetes for a longer period of time than patients with moderate disease. Men made up a higher proportion of hospitalized patients, showing that men are more sensitive to COVID-19 infection, which has been associated with a higher prevalence of smoking in men in several studies. However, current smokers made up a small percentage of COVID-19 patients and there was no significant link between smoking and COVID-19 (27,28).

Patients who had recovered had a lower chance of severe COVID-19 infection, which required ICU and hospitalization, as well as a faster recovery rate from SARS-CoV-2 infection. Diabetes prevalence rises with age in both the general population and COVID-19 patients. COVID-19 patients who also had hypertension had a high average SBP and a lot of SBP/DBP variability throughout their hospital stay, which was linked to in-hospital mortality, ICU admission, and heart failure.

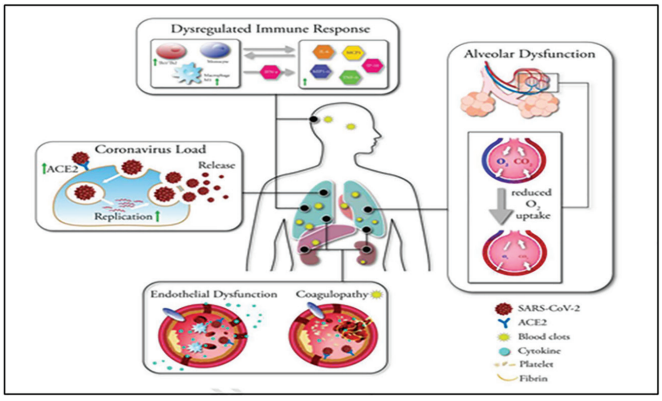

FIGURE 3 - The mechanisms associated with increased COVID-19 severity in individuals with diabetes, the source of the image is (37).

However, the possible pathways by which diabetes increases COVID-19 morbidity and death were described by Muniyappa and Gubbi as follows: improved cellular attachment affinity and viral entry efficiency (29), reduced viral clearance, alveolar dysfunction showed (30), higher sensitivity to cytokine storm and hyper-inflammation (31), and coagulopathy (32). According to a study conducted in Italy during the present COVID-19 pandemic, diabetes mellitus scores high among the comorbidities in COVID-19 patients compared with healthy people (33). Systemic hypertension and ischemic heart disease were also shown to be common, as illustrated in (Fig. 3).

Besides, Angiotensin II receptor blockers (ARBs) medications did not increase the risk of adverse outcomes in hypertensive patients and even provided a benefit in terms of heart failure. This suggests that ARB medications should be continued in COVID-19 patients, and the statistics showed that of the people were hypertensive. Patients on ACE inhibitors (ACEIs) and angiotensin receptor blockers (ARBs) showed reduced mortality rates compared to those taking other antihypertensive medicines. Also, it was found that patients aged 20-40 who had acute respiratory distress syndrome, and some of them died because of no treatment after injury.

Laboratory Findings

Diabetes patients showed greater white blood cell count, neutrophil count, levels of ‘‘C-Reactive Protein (CRP),” blood urea nitrogen, lower red blood cell count, hemoglobin level, and lymphocyte count when compared to patients without diabetes, according to laboratory test results. The results indicate that in COVID-19 patients with coexisting hypertension,

maintaining a low and stable blood pressure is ideal for a favorable prognosis. Subsequently, in the absence of other comorbidities, a similar analysis was conducted to assess whether diabetes independently affects disease severity and mortality.

In patients with COVID-19, we discovered a substantial link between D-dimer levels and diabetes. The group with diabetes and blood pressure had significantly higher D-dimer levels (500-2000 ng/mL) than the group of healthy patients, which had levels less than 500 ng/mL.

However, it is found that diabetics had much greater white blood cell counts than non-diabetics. CRP, ESR, and LDH levels were higher than normal in diabetic patients, indicating a more severe inflammatory response. Patients developed bilateral pneumonia and patchy ground-glass opacity, according to chest radiography or CT results (Figure 4). Diabetes patients had a higher white blood cell count than non-diabetics, according to laboratory test results (34).

COVID-19 severity, outcome, and associated complications

Patients were also given plasma therapy and were treated with interferon injections. Acute respiratory distress syndrome (ARDS), shock, and secondary infection were the most prevalent consequences. Among the 150 patients, 10 (6.6%) died during follow-up, 30 (20%) remained hospitalized, and 110 were discharged. Patients with diabetes require more oxygen than individuals without the disease. Furthermore, ARDS was more common in diabetic patients than in non-diabetic and high blood pressure patients. When compared to the non-diabetic group, the diabetic group had a significantly higher prevalence of complications such as sepsis, ARDS, cardiovascular disease, heart failure, and kidney injury.

Diabetes has been detected in COVID-19 as a major predictor of disease severity. Diabetes patients may also be at an increased risk of thrombotic events due to the link between diabetes, clotting factors, and fibrinolysis imbalance.

Furthermore, COVID-19 patients with uncontrolled diabetes had a higher risk of death than other patients. Uncontrolled diabetes, with a focus on hyperglycemia, appears to be a consistent predictor of a worse COVID-19 outcome. Therefore, hyperglycemia may play a negative role in the overproduction of interleukin-6 (IL-6), which has been linked to increased lung infiltration and the severity of COVID-19 (35). The data imply that for COVID-19 patients with coexisting hypertension, having a low and stable blood pressure is indeed the best way to achieve a positive prognosis. The diabetes group had a significantly higher percentage of deaths compared with the blood pressure and healthy patients' groups. This could be owing to the fact that diabetes is linked to other risk factors such as age and obesity. This could possibly be owing to the fact that persons with diabetes have a dysregulated innate and adaptive immune response, as well as persistent low-grade inflammation, making them more vulnerable to cytokine storm. People with diabetes could also be at higher risk for thrombotic events because diabetes is linked to a clotting factor and fibrinolysis imbalance.

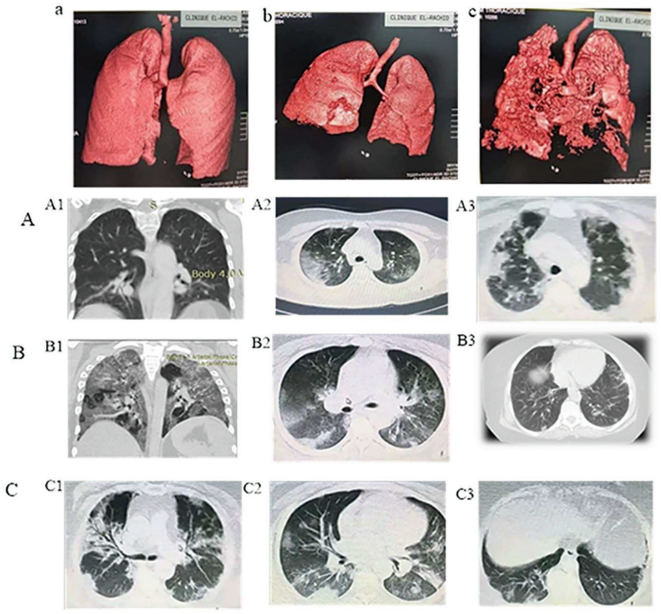

FIGURE 4 - The chest CT images of infected patients with COVID-19 during their hospitalization. **A:** healthy patient. **B:** blood pressure patients. **C:** diabetes patient. A) Healthy patients and their ages range from 28 to 50 with mild to severe injury. B) Patients with blood pressure with ages range from 35 to 70 with mild to severe injury**.** C) Patients with diabetes, ages ranging from 40 to 75, with severe injury.

Drugs Uses and Vaccines

Patients infected with SARS-CoV-2 are now being treated mostly through the repurposing of available therapeutic medications and a focus on symptomatic symptoms (36). Antibiotics, antiviral medicines, systemic corticosteroids, and anti-inflammatory pharmaceuticals (including anti-arthritis therapy) are widely used to treat ARDS, which is sometimes complicated by secondary infection. In addition to antiviral interferers and antibiotics, COVID-19 has been treated with neuraminidase inhibitors, RNA synthesis inhibitors, convalescent plasma, and traditional herbal medicines, as shown in Figure 5. Diabetes patients with COVID-19 should have adequate glycemic control, medical teams should ensure this. This involves a thorough assessment of all possible problems caused by the therapies that will be used for those patients. Insulin therapy is a treatment that is used to treat both forms of diabetes. Although insulin therapy for severe COVID-19 individuals with diabetes has been recommended, it should be determined based on the severity of COVID-19, and those patients should be constantly followed (37).

Vaccines work in a variety of ways to provide protection. However, with every vaccine (Fig. 6), the body is left with a supply of memory T- and B-lymphocytes that will remember how to fight that virus in the future. T-lymphocytes and B-lymphocytes are typically produced a few weeks after vaccination. As a consequence, a person may become infected with the virus that causes COVID-19 just before or shortly after immunization and subsequently become sick as a result of the vaccine failing to provide sufficient protection.

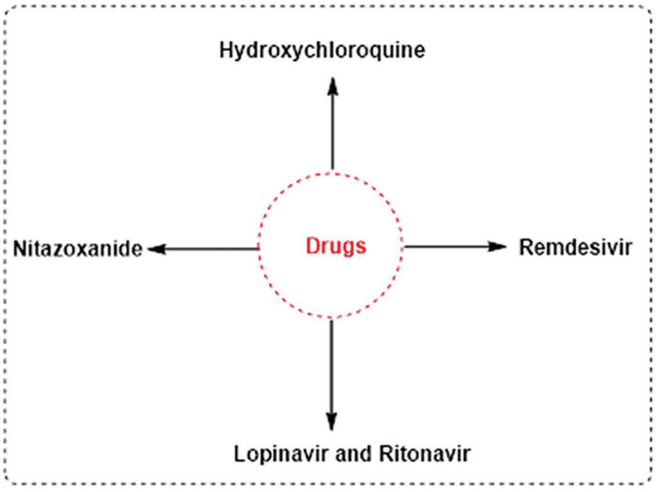

FIGURE 5 - An overview of the drugs used and their mode of action in the treatment of SARS-CoV-2 infection. The diagram was modified from (38).

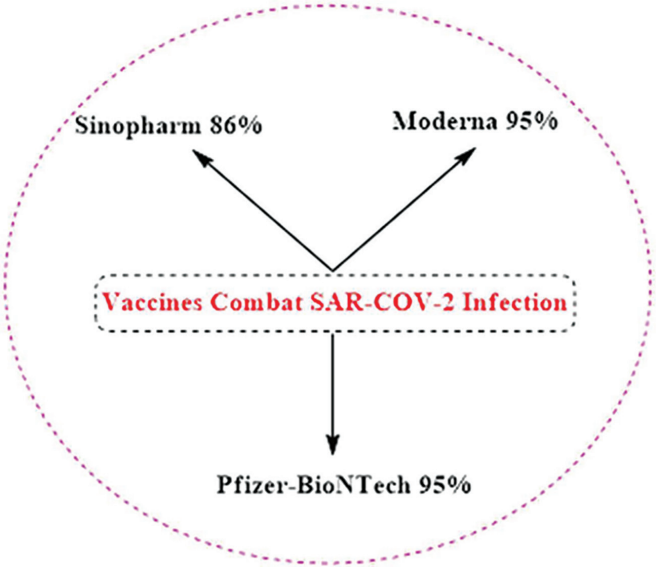

FIGURE 6 - Types of vaccines used to protect humans against SARS-CoV-2 infection. The diagram was adapted from (39).

Symptoms such as fever can occur after vaccination due to the process of building immunity. These symptoms are typical and indicate that the body is strengthening its defenses.

Conclusion

In conclusion, diabetes has been exhibited in studies to be highly prevalent in critically ill patients with severe coronavirus disease, which led to heart attacks in some cases. Diabetes patients who were infected with COVID-19 showed more severe illness and a worse prognosis than non-diabetic patients. After diabetes, COVID-19 patients with hypertension have a considerably higher mortality risk. Furthermore, the study showed that the severely ill patients have higher maximal viral concentrations and a slower decline of viral concentration compared to mildly affected patients. Diabetes may be a risk factor for disease progression and an increase in COVID-19 patients' in-hospital mortality. The results of this study emphasized the necessity of understanding COVID-19 clinical characteristics in order to put in place effective control strategies.

Disclosures

Conflict of interest: The authors declare no conflict of interest.
Financial support: This research received no specific grant from any funding agency in the public, commercial, or not-for-profit sectors
Data availability statement: The authors confirm that the data supporting the findings of this study are available within the supplementary materials.
Ethical Statement: Our study did not require ethical board approval because it did not involve human or animal trials.
Author Contributions: All the authors contributed to the conceptualization, writing the original draft, and preparation. The authors have read and agreed to the published version of the manuscript.

References

1. Zhu N, Zhang D, Wang W, et al.; China Novel Coronavirus Investigating and Research Team. A novel coronavirus from patients with pneumonia in China. N Engl J Med. 2020;382(8):727-733. CrossRef PubMed
2. Chong WH, Saha BK, Ramani A, et. al. State-of-the-art review of secondary pulmonary infections in patients with COVID-19 pneumonia 2021. Infection, 49(4): 591-605. CrossRef
3. Wong CK, Lam CW, Wu AK, et al. Plasma inflammatory cytokines and chemokines in severe acute respiratory syndrome. Clin Exp Immunol. 2004;136(1):95-103. CrossRef PubMed
4. Ahmed MN, Aziz LM, Muhaidi MJ. Inspection of some causes of renal calculi in children under the age of 15 years. Journal of Pharmaceutical Sciences and Research. 2018;10(5):1148-1152.
5. Al-Jumaili MHA. The Impact of COVID-19 on Iraqi Community: a descriptive study based on data reported from the Ministry of Health in Iraq. J Infect Dev Ctries. 2021;15(9):1244-1251. CrossRef PubMed
6. Badawi A, Ryoo SG. Prevalence of diabetes in the 2009 influenza A (H1N1) and the Middle East respiratory syndrome coronavirus: a systematic review and meta-analysis. J Public Health Res. 2016;5(3):733. CrossRef PubMed
7. Sprenkeler EGG, Webbers SDS, Kuijpers TW. When Actin is not actin' like it should: a new category of distinct primary immunodeficiency disorders. J Innate Immun. 2021;13(1):3-25. CrossRef PubMed
8. Lampl BMJ, Buczovsky M, Martin G, et al. Clinical and epidemiological data of COVID-19 from Regensburg, Germany: a retrospective analysis of 1084 consecutive cases. Infection. 2021;49(4):661-669. CrossRef PubMed
9. Tufan A, Avanoğlu Güler A, Matucci-Cerinic M. COVID-19, immune system response, hyperinflammation and repurposing antirheumatic drugs. Turk J Med Sci. 2020;50(SI-1):620-632. CrossRef PubMed
10. Thibeault C, Mühlemann B, Helbig ET, et al.; Pa-COVID Study Group. Clinical and virological characteristics of hospitalized COVID-19 patients in a German tertiary care centre during the first wave of the SARS-CoV-2 pandemic: a prospective observational study. Infection. 2021;49(4):703-714. CrossRef PubMed

11. Hine JL, de Lusignan S, Burleigh D, et. al. Association between glycaemic control and common infections in people with type 2 diabetes: a cohort study. Diabetic Medicine 2017; 34(4): 551-557. CrossRef
12. Drucker DJ. Coronavirus infections and type 2 diabetes—shared pathways with therapeutic implications. Endocr Rev. 2020;41(3):457-470. CrossRef PubMed
13. Monteil V, Kwon H, Prado P, et al. Inhibition of SARS-CoV-2 infections in engineered human tissues using clinical-grade soluble human ACE2. Cell. 2020;181(4):905-913.e7. CrossRef PubMed
14. Boadu AA, Yeboah-Manu M, Osei-Wusu S, et al. Tuberculosis and diabetes mellitus: the complexity of the comorbid interactions. Int J Infect Dis. 2024;146:107140. CrossRef PubMed
15. Hussein AD, Bakr EA, Al-Jumaili MHA. Association between ABO blood groups and the risk of infection with SARS-CoV-2 in Iraq. J Int Med Res. 2022;50(11):3000605221133147. CrossRef PubMed
16. Shah H, Khan MSH, Dhurandhar NV, et al. The triumvirate: why hypertension, obesity, and diabetes are risk factors for adverse effects in patients with COVID-19. Acta Diabetol. 2021;58(7):831-843. CrossRef PubMed
17. Misra A, Bloomgarden Z. Diabetes during the COVID-19 pandemic: a global call to reconnect with patients and emphasize lifestyle changes and optimize glycemic and blood pressure control. J Diabetes. 2020;12(7):556-557. CrossRef PubMed
18. Erener S. Diabetes, infection risk and COVID-19. Mol Metab. 2020;39:101044. CrossRef PubMed
19. Rajput V, Mulay P. Bibliometric survey on impact of sound therapy on blood pressure and COVID-19. Library Philosophy and Practice; 2020:1-20.
20. AbdulKhaliq RJ, Ahmed MN, Ali AY, et al. Assessment of some immunological and physiological indicators for infected and uninfected coronavirus disease patients. Medical Journal of Babylon. 2023;20(4):861-866. CrossRef
21. Ibrahim RK, Abdullah QK, Muhaidi MJ, et al. Study of cellular immune response and some of the blood variables in children with celiac disease. Journal of Physics: Conference Series. 2021;1818(1):012011 CrossRef
22. Chen R, Yang J, Gao X, et al. Influence of blood pressure control and application of renin-angiotensin-aldosterone system inhibitors on the outcomes in COVID-19 patients with hypertension. J Clin Hypertens (Greenwich). 2020;22(11):1974-1983. CrossRef PubMed
23. Shen L, Wang C, Zhao J, et al. Delayed specific IgM antibody responses observed among COVID-19 patients with severe progression. Emerg Microbes Infect. 2020;9(1):1096-1101. CrossRef PubMed
24. Huang C, Wang Y, Li X, et al. Clinical features of patients infected with 2019 novel coronavirus in Wuhan, China. Lancet. 2020;395(10223):497-506. CrossRef PubMed
25. Zhou F, Yu T, Du R, et al. Clinical course and risk factors for mortality of adult inpatients with COVID-19 in Wuhan, China: a retrospective cohort study. Lancet. 2020;395(10229):1054-1062. CrossRef PubMed
26. Roca-Ho H, Riera M, Palau V, et al. Characterization of ACE and ACE2 expression within different organs of the NOD mouse. Int J Mol Sci. 2017;18(3):563. CrossRef PubMed
27. Leung JM, Yang CX, Tam A, et al. ACE-2 expression in the small airway epithelia of smokers and COPD patients: implications for COVID-19. Eur Respir J. 2020;55(5):2000688. CrossRef PubMed
28. Farsalinos K, Barbouni A, Poulas K, et al. Current smoking, former smoking, and adverse outcome among hospitalized COVID-19 patients: a systematic review and meta-analysis. Ther Adv Chronic Dis. 2020;11:2040622320935765. CrossRef PubMed
29. Muniyappa R, Gubbi S. COVID-19 pandemic, coronaviruses, and diabetes mellitus. Am J Physiol Endocrinol Metab. 2020;318(5):E736-E741. CrossRef PubMed
30. Tay MZ, Poh CM, Rénia L, et al. The trinity of COVID-19: immunity, inflammation and intervention. Nat Rev Immunol. 2020;20(6):363-374. CrossRef PubMed
31. Reading PC, Allison J, Crouch EC, et al. Increased susceptibility of diabetic mice to influenza virus infection: compromise of collectin-mediated host defense of the lung by glucose? J Virol. 1998;72(8):6884-6887. CrossRef PubMed
32. Gentile S, Strollo F, Ceriello A. COVID-19 infection in Italian people with diabetes: lessons learned for our future (an experience to be used). Diabetes Research and Clinical Practice. 2020;162:108137. CrossRef
33. Ran J, Song Y, Zhuang Z, et al. Blood pressure control and adverse outcomes of COVID-19 infection in patients with concomitant hypertension in Wuhan, China. Hypertens Res. 2020;43(11):1267-1276. CrossRef PubMed
34. Ebrahim H, Fiseha T, Ebrahim Y, et al. Comparison of hematological parameters between type 2 diabetes mellitus patients and healthy controls at Dessie comprehensive specialized hospital, Northeast Ethiopia: comparative cross-sectional study. PLoS One. 2022;17(7):e0272145. CrossRef PubMed
35. Marfella R, Paolisso P, Sardu C, et al. Negative impact of hyperglycaemia on tocilizumab therapy in COVID-19 patients. Diabetes Metab. 2020;46(5):403-405. CrossRef PubMed
36. Nitulescu GM, Paunescu H, Moschos SA, et al. Comprehensive analysis of drugs to treat SARS-CoV-2 infection: mechanistic insights into current COVID-19 therapies (Review). Int J Mol Med. 2020;46(2):467-488. CrossRef PubMed
37. Yu B, Li C, Sun Y, et al. Insulin treatment is associated with increased mortality in patients with COVID-19 and type 2 diabetes. Cell Metab. 2021;33(1):65-77.e2. CrossRef PubMed
38. Valle C, Martin B, Touret F, et al. Drugs against SARS-CoV-2: what do we know about their mode of action? Rev Med Virol. 2020;30(6):1-10. CrossRef PubMed
39. Cai H. Sex difference and smoking predisposition in patients with COVID-19. Lancet Respir Med. 2020;8(4):e20. CrossRef PubMed

JCB
J Circ Biomark 2025; 14: 46-47
ISSN 1849-4544 | DOI: 10.33393/jcb.2025.3657
ERRATUM

Erratum in "Diagnostic value of carcinoembryonic antigen, cancer antigen 15-3, and cell-free DNA as blood biomarkers in early detection of canine mammary tumor"

Diksha Singh[1], Prashant P Rokade[1], Neeraj K Gangwar[1], Mukul G Gabhane[1], Sunil Malik[1], Kavisha Gangwar[1], Shyama N Prabhu[1], Renu Singh[1], DD Singh[1], Sonam Kumari[2], Soumen Chaudhary[2], Jitendra K Choudhary[3]

[1]Department of Veterinary Pathology, College of Veterinary Science & Animal Husbandry, Veterinary University, Mathura, Uttar Pradesh - India
[2]Department of Veterinary Pharmacology and Toxicology, College of Veterinary Science & Animal Husbandry, Veterinary University, Mathura, Uttar Pradesh - India
[3]Animal Genetics and Breeding, College of Veterinary Science & Animal Husbandry, Veterinary University, Mathura, Uttar Pradesh - India

In the article "Diagnostic value of carcinoembryonic antigen, cancer antigen 15-3, and cell-free DNA as blood biomarkers in early detection of canine mammary tumor" (1), which appeared in Volume 14, Issue 1 of Journal of Circulating Biomarkers, the weights reported for the Beagle, Indian Spitz and Pomeranian breeds in Table 1 were incorrect. The correct Table 1 is reported here:

TABLE 1 - Clinical history of cases showing occurrence of canine mammary tumor (n = 36)

Case No.	Breed	Age	Body wt.	No. of glands affected	Gland effected	Size (cm)	Consistency
1.	Labrador	11 yrs.	41 Kg	2	Right inguinal & right caudal abdominal	5-6 cm	Hard
2.	Rottweiler	4 yrs.	36 Kg	4	Left & right Inguinal	4-5 cm	Soft
					Left & right caudal abdominal	2-3 cm	
3.	Beagle	8 yrs.	11 Kg	2	Left & right Inguinal	6-7 cm	Soft
4.	German Shepherd	9 yrs.	39 Kg	1	Left caudal abdominal	4-5 cm	Semi-hard
5.	German Shepherd	12 yrs.	42 Kg	2	Left & right caudal thoracic	12-13 cm	Semi-hard
6.	Rottweiler	9 yrs.	45 Kg	1	Left inguinal	4-5 cm	Semi-hard
7.	Indian Spitz	11 yrs.	10 Kg	1	Left inguinal	7-8 cm	Semi-hard
8.	Pomeranian	9 yrs.	6 Kg	1	Right inguinal	9-10 cm	Soft
9.	Indian Spitz	11 yrs.	9 Kg	1	Left inguinal	5-6 cm	Soft
10.	German Shepherd	3 yrs.	38 Kg	1	Left cranial abdominal	4-5 cm.	Semi-hard
11.	Indian Spitz	10 yrs.	8 Kg	1	Right inguinal	5-6 cm.	Hard
12.	Labrador	2.5 yrs.	41 Kg	1	Left inguinal	7-8 cm.	Semi-hard
13.	German Shepherd	3 yrs.	41 Kg	1	Left caudal abdominal	5-7 cm.	Semi-hard
14.	Labrador	4 yrs.	46 Kg	1	Left inguinal	7-8 cm.	Hard

(*Continued*)

Received: September 29, 2025
Accepted: September 29, 2025
Published online: October 10, 2025

Corresponding author:
Neeraj Kumar Gangwar
email: neerajgangwarvet@gmail.com

TABLE 1 - (*Continued*)

Case No.	Breed	Age	Body wt.	No. of glands affected	Gland effected	Size (cm)	Consistency
15.	Non-descript	12 yrs.	36 Kg	1	Left inguinal	2-3 cm.	Semi-hard
16.	German Shepherd	6 yrs.	47 Kg	2	Right inguinal & caudal abdominal	15-18 cm.	Semi-hard to hard
17.	German Shepherd	9 yrs.	38 Kg	2	Left & right inguinal	9-10 cm.	Soft
18.	German shepherd	10 yrs.	43 Kg	1	left inguinal	8-9 cm.	Semi-hard
19.	Indian Spitz	8 yrs.	10 Kg	1	Right cranial abdominal	2-3 cm.	Soft
20.	German shepherd	6 yrs.	44 Kg	2	Left cranial abdominal	7-8 cm.	Semi-hard
21.	Pomeranian	5 yrs.	8 Kg	1	Right inguinal	5-6 cm.	Hard
22.	Pomeranian	8 yrs.	9 Kg	1	Left inguinal	8-9cm.	Semi-hard
23.	Non-descript	8 yrs.	42 Kg	2	Left inguinal & caudal abdominal	6-7 cm.	Semi-hard
24.	Non-descript	7 yrs.	21 Kg	2	Right inguinal & caudal abdominal	10-11 cm.	Semi-hard
25.	German shepherd	9 yrs.	40 Kg	1	Right caudal abdominal	3-4 cm.	Soft
26.	Rottweiler	4 yrs.	32 Kg	1	Left inguinal	6-7 cm.	Soft
27.	Non-descript	8 yrs.	19 Kg	1	Right cranial thoracic	5-6 cm.	Hard
28.	Non-descript	13 yrs.	39 Kg	1	Right caudal thoracic	4-5 cm.	Semi-hard
29.	Great dane	1.5 yrs.	34 Kg	1	Right cranial thoracic	7-8 cm.	Soft
30.	Rottweiler	8 yrs.	42 Kg	1	Left cranial thoracic	5-7 cm	Soft to semi-hard
31.	Non-descript	8 yrs.	37 Kg	1	Left cranial abdominal	3-4 cm	Soft
32.	Rottweiler	8 yrs.	41 Kg	2	Left & right caudal abdominal	8-9 cm	Semi-hard
33.	Labrador	10 yrs.	46 Kg	1	Right cranial abdominal	3-4 cm	Semi-hard
34.	Non-descript	7 yrs.	17 Kg	4	Right & left caudal thoracic	7-8 cm	Semi-hard
					Left cranial & caudal abdominal	2-3 cm	
35.	Pomeranian	7 yrs.	9 Kg	1	Left inguinal	4-5 cm	Soft to semi-hard
36.	German shepherd	9 yrs.	65 Kg	2	Right inguinal & caudal abdominal	13-15 cm	Semi-hard

We apologize for any inconvenience caused to the readers by these errors, which do not affect the overall results or conclusions of the study.

The final version of this article is available online and includes a reference to this correction.

References

1. Singh D., Rokade P., Gangwar N.,et al. Diagnostic value of carcinoembryonic antigen, cancer antigen 15-3, and cell-free DNA as blood biomarkers in early detection of canine mammary tumor. Journal of Circulating Biomarkers. 2025; *14*(1), 30-38. CrossRef

JCB
J Circ Biomark 2025; 14: 48-53
ISSN 1849-4544 | DOI: 10.33393/jcb.2025.3597
ORIGINAL RESEARCH ARTICLE
Open Access

Transcriptome biomarkers of colon cancer liver metastasis response to neoadjuvant triplet chemotherapy: a case series

Nataliya Babyshkina[1,2], Tatyana Dronova[1], Dmitry Eremin[1], Alexey Dobrodeev[4], Dmitry Kostromitskiy[4], Sergey Vtorushin[3], Polina Gervas[1], Sergey Afanasiev[4], Nadejda Cherdyntseva[1]

[1]Department of Molecular Oncology and Immunology, Cancer Research Institute, Tomsk National Research Medical Center, Russian Academy of Sciences, Tomsk - Russian Federation
[2]Siberian State Medical University, Tomsk - Russian Federation
[3]Department of General and Molecular Pathology, Cancer Research Institute - Tomsk National Research Medical Center, Russian Academy of Sciences, Tomsk - Russian Federation
[4]Department of Abdominal Oncology, Cancer Research Institute - Tomsk National Research Medical Center, Russian Academy of Sciences, Tomsk - Russian Federation

ABSTRACT

Introduction: The triplet FOLFOXIRI (fluorouracil, leucovorin, oxaliplatin, and irinotecan) may be considered an effective option in the neoadjuvant setting for metastatic colon cancer (mCRC). To investigate potential molecular criteria for treatment response, we evaluate the transcriptome of paired primary colon tumors and liver metastases.

Method: Two sets of quadruple-matched specimens (primary colon tumor, liver metastasis, normal colon and liver tissues) from five patients with resectable mCRC before and after neoadjuvant FOLFOXIRI were selected for RNA sequencing (RNA-seq).

Results: RNA-seq data showed that liver metastases exhibited a higher number of differentially expressed genes (DEGs) than colon tumors (FDR < 0.05, 301 vs. 62, respectively). Up-regulation of *IL1RN, MTCO1P12, RN7SL1, ALDH1A1, DUSP1, COX1*, and *FOS* may be associated with colon tumor sensitivity to FOLFOXIRI. *HBB, GADD45B, DUSP1, FOSB, HBA2, TSC22D3, TAGLN, PER1, CSRP1, CCN2, NAMPT, ZBTB16, SERPINE1, ISG20, SRGN, ATF3, IL7R, IFITM2*, and *KLF2* may potentially be involved in the partial liver metastasis response. *EPS8L2* was the only gene highly expressed in pre-treatment liver tissue of the complete responder patient compared to others (|Log2FC| = 3.84, FDR < 0.05).

Conclusion: Data obtained indicate transcriptional discordance between the primary tumors and liver metastases during neoadjuvant FOLFOXIRI, with the pattern of DEGs involved in their response being distinct. The EPS8L2 transcript could be regarded as a candidate biomarker of liver complete response; however, prognostic conclusions cannot be drawn from this cohort.

Keywords: Colon cancer liver metastasis, Metastatic colon cancer, Neoadjuvant FOLFOXIRI, RNA-seq, Transcriptome biomarkers

Introduction

Initially, metastatic colon cancer (mCRC) accounts for up to 30% of all colorectal cancers with a highly heterogeneous nature (1). Colon cancer distant metastases are observed in multiple sites; however, the liver is the only site of distant disease in one third of mCRC patients (2). Current NCCN and ESMO guidelines establish multimodal treatment, including surgery, chemotherapy, targeted therapy, and immunotherapy as the standard care for resectable mCRC (1,3).

FOLFOXIRI is a combination of three cytotoxic agents, such as fluorouracil, leucovorin, oxaliplatin, and irinotecan, that are considered in the neoadjuvant setting for resectable mCRC according to consensus statements (1,3). In the initial GONO clinical trial, neoadjuvant FOLFOXIRI improved response rates, progression-free survival, and overall survival compared with FOLFIRI (fluorouracil, leucovorin, and irinotecan) with manageable toxicity in unresectable mCRC patients (4). Subsequent randomized trials confirmed that 6 months of induction treatment with FOLFOXIRI provides a clinically

Received: July 9, 2025
Accepted: October 27, 2025
Published online: November 10, 2025

Corresponding author:
Nataliya Babyshkina
email: nbabyshkina@mail.ru

relevant improvement in 5-year survival compared with 6 months of induction treatment with FOLFIRI (5). Recent studies suggest that neoadjuvant FOLFOXIRI has a favorable safety profile and down-staging effect on locally advanced resectable rectal cancer (6).

The combination of FOLFOXIRI with anti-vascular endothelial growth factor antibody, such as bevacizumab, in patients with unresectable mCRC was investigated by several trials and demonstrated improved survival and response rates compared with doublet chemotherapy regimens (7,8). The addition of cetuximab, an anti-epidermal growth factor receptor antibody, to triplet chemotherapy also showed encouraging results (9,10).

It is important to note that the use of neoadjuvant chemotherapy with FOLFOXIRI for resectable mCRC remains undocumented. However, potential molecular criteria for choosing the optimal treatment regimen that would significantly improve patient outcomes have not been developed. Here we report a transcriptome of primary colon tumors and their matched liver metastatic lesions that were associated with treatment response in a group of mCRC patients who were treated with neoadjuvant FOLFOXIRI plus targeted drug.

Materials and methods

Patient Selection

The prospective study enrolled 5 patients with resectable mCRC who received neoadjuvant treatment in combination with a targeted agent at the Tomsk Cancer Research Institute between 2021 and 2022. All patients were males aged between 40 and 66 years. The inclusion criteria were as follows: resectable mCRC with liver-only metastases, pathologically confirmed adenocarcinoma, Eastern Cooperative Oncology Group performance status of 0-2, and known *RAS* status. In all patients, the primary tumor was located on the left side of the colon. Patients with more than one primary tumor and deficient mismatch repair, or a high microsatellite instability phenotype, were excluded. The patient characteristics are listed in Table 1.

Treatment regimens and response evaluation

All patients received 3 cycles of neoadjuvant FOLFOXIRI chemotherapy followed by synchronous or staged colectomy and liver metastases resection. FOLFOXIRI consisted of irinotecan 165 mg/m^2 on day 1, oxaliplatin 85 mg/m^2 on day 1, leucovorin 200 mg/m^2 on days 1 and 2, and 3200 mg/m^2 48 h continuous infusion of 5-fluorouracil on days 1 and 2. A combination regimen with FOLFOXIRI and cetuximab (500 mg/m^2 on day 1) was given to 2 patients. Three patients received the FOLFOXIRI-only regimen. After surgical resection, all patients received three cycles of adjuvant treatment with FOLFOXIRI within 6 weeks.

Tumor response was assessed by contrast-enhanced computed tomography (CT) of the chest, abdomen and pelvis or contrast-enhanced magnetic resonance imaging (MRI) of the pelvis according to RECIST (version 1.1) guidelines. All 5 patients (100.0%) achieved a partial response of the primary colon tumor. Four of them (80.0%) also had a partial response of metastatic liver lesions, and one patient (20.0%) had a complete response of metastatic lesions. Additional metastatic lesions assessment by intraoperative ultrasound (IOUS) was performed to confirm the complete liver response. Pathological response evaluation of colon tumor and liver metastasis was assessed by the Mandard grading system (11). No serious adverse events (grades III–IV) occurred.

Patient Specimens

A first set of biopsy specimens, including colon tumor and liver metastasis, as well as normal colon and liver tissue, was obtained from each patient before treatment (pre-treatment specimens). The second set included the same specimen's type obtained after surgical resection of both the primary lesion and metastasis (post-treatment specimens). However, one patient had a complete response of the metastatic focus in the liver and, thus, there was an incomplete second specimen set. The tumor cell content in the studied specimens was at least 40%. Normal tissue specimens were obtained at a distance of at least 0.5 cm from the tumor. All specimens were placed in RNAlater solution (Ambion, USA), incubated for 24 hours at +4°C and stored at –80°C.

RNA Isolation and Sequencing

Two sets of quadruple-matched specimens (primary colon carcinoma, liver metastases, normal colon and liver tissues) from each patient before and after treatment were selected for high-throughput RNA sequencing (RNA-seq). Total RNA was extracted using a PureLink RNA Mini Kit (Invitrogen, USA). Sequencing libraries were prepared using the MGIEasy rRNA Depletion V1.3 (MGI, China). RNA-seq library was sequenced on the DNBSeq G400 (MGI, China), using DNBSEQ-G400RS High-throughput Sequencing Kit (MGI, China).

TABLE 1 - Patient characteristics

Case	Specimen sets	Age at diagnosis, years	Sex	Primary tumor site	Histopathology type	Targeted therapy	Response colon tumor/ liver metastasis
1	Complete	42	Male	Rectosigmoid	Mode	No	Partial/Partial
2	Complete	62	Male	Rectosigmoid	Well	Cetuximab	Partial/Partial
3	Complete	39	Male	Rectosigmoid	Mode	No	Partial/Partial
4	Complete	53	Male	Rectosigmoid	Mode	Cetuximab	Partial Partial
5	Incomplete	66	Male	Rectosigmoid	Well	No	Partial/Complete

Statistical analysis

Quality control of sequencing was assessed using FastQC, QoRTs and MultiQC software Online. The DEGs were analyzed by the software package DESeq2. Adjusted P values/false discovery rates (FDR) were calculated using the Benjamini–Hochberg procedure (12). Data visualized by Phantasus Online as well as by the R 4.0.2 package Online.

A Kaplan Meier plotter Online tool was used to examine the relapse-free survival of colon cancer patients for the validation of *EPS8L2* (13). The analysis of *EPS8L2* expression was focused on a cohort of stage 3 and 4 colon cancer patients with left-sided tumors, stable or low microsatellite phenotype based on GEO, EGA and TCGA databases. The hazard ratio with 95% confidence intervals and log-rank test were used to compare differences among survival curves. A p-value of less than 0.05 was considered statistically significant.

Results

DEGs association with primary colon tumor response

In total, 62 DEGs (FDR < 0.05) between the pre-treatment and post-treatment colon specimens were identified (Fig. 1A). The top 20 up-regulated genes of pre-treatment tumors included the *CCR4, FER1L4, AMH, RHOV, GALT, CELSR3, DRAM1, RHPN1, PKMYT1, PCSK9, GRM8, MMP11, WDR62, ALG8, PABPC1L, DNM1, TMEM132A, ARHGAP39, CDH3*, and *MELTF* (|Log2FC|>1.00, FDR<0.05). Only seven up-regulated genes were found in the post-treatment colon tumors, namely *IL1RN, MTCO1P12, RN7SL1, ALDH1A1, DUSP1, COX1*, and *FOS* (|Log2FC| > 1.00, FDR<0.05; Fig. 1B). Given the partial response of the primary colon tumor in all patients, the up- or down-regulation of these genes identified after the treatment may be implicated in the colon tumor sensitivity to FOLFOXIRI alone or in combination with targeted drug.

DEGs association with partial liver metastasis response

Similar to the primary colon tumors, the transcriptome profile of liver metastases was also modulated by neoadjuvant treatment. Cluster analysis revealed a broader range of DEGs (FDR < 0.05, 301 vs. 62) compared to colon tumors (Fig. 1C). We selected the top 20 up-regulated genes *MUC3A, CDCA7, SATB2, XPNPEP2, EPCAM, SCNN1A, TONSL, AIFM3, ENTPD8, GAL3ST2, EPPK1, ANO9, SPIRE2, PTK6, SLC17A1, IQANK1, DGAT1, WNK2, FAM83E,* and *TJP3* that were in the pre-treatment liver tissue (|Log2FC| > 1.00, FDR<0.05). *HBB, GADD45B, DUSP1, FOSB, HBA2, TSC22D3, TAGLN, PER1, CSRP1, CCN2, NAMPT, ZBTB16, SERPINE1, ISG20, SRGN, ATF3, IL7R, IFITM2*, and *KLF2* were up-regulated in the post-treatment liver lesions (|Log2FC| > 1.00, FDR<0.05; Fig. 1D). Since all patients had metastatic liver lesions that responded to treatment, the detected transcripts may also be potentially associated with the efficacy of FOLFOXIRI used alone or in combination with cetuximab.

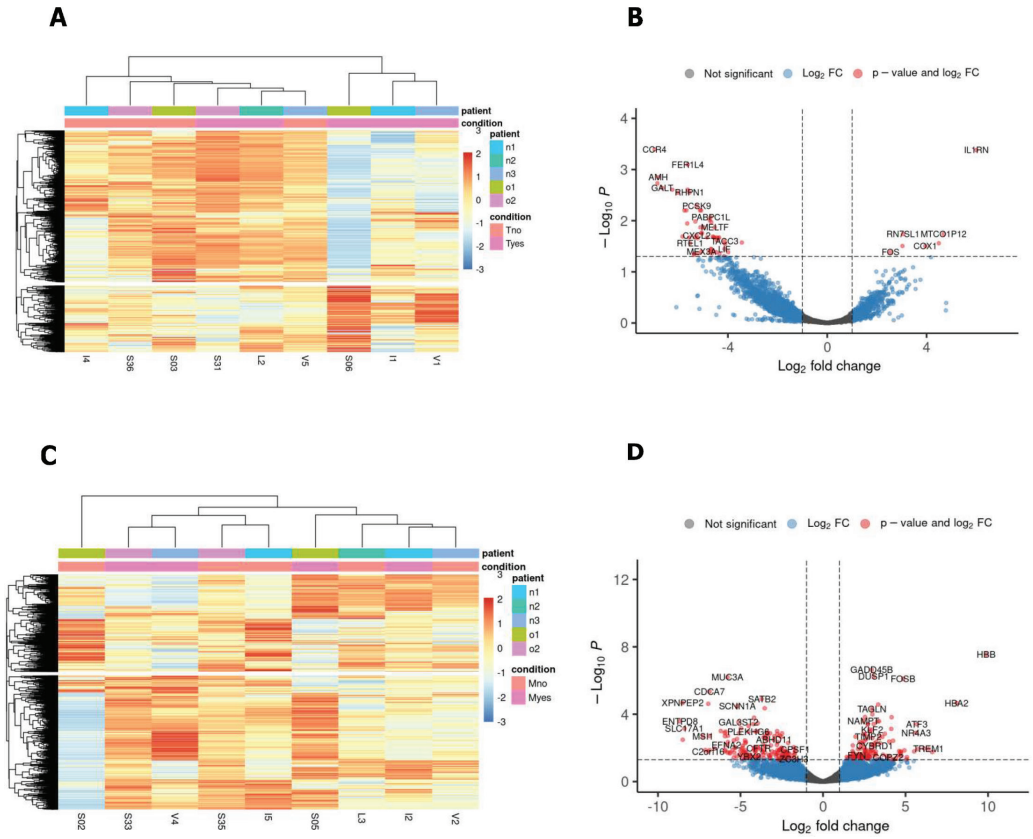

FIGURE 1 - Comparative transcriptome of primary colon tumors and matched liver metastases in mCRC patients during neoadjuvant FOLFOXIRI. Cluster analysis of differentially expressed genes (DEGs) between the pre-treatment and post-treatment colon specimens. Up-regulated genes are represented in red, and down-regulated genes are represented in blue (A); Volcano plot for DEGs in primary colon tumors (B); Cluster analysis of DEGs between the pre-treatment and post-treatment liver lesions. Up-regulated genes are represented in red, and down-regulated genes are represented in blue (C); Volcano plot for DEGs in liver metastases (D).

DEGs association with complete liver metastasis response

To identify genes predicting complete liver metastasis response after FOLFOXIRI, we performed additional transcriptome analysis in a patient who achieved a complete regression of liver metastatic lesions. Interestingly, *EPS8L2* was the only highly expressed in this patient's liver tissue before treatment compared to other patients (|Log2FC| = 3.84, FDR<0.05; Fig. 2A).

In addition, according to a public data set, low *EPS8L2* expression was associated with better relapse-free survival in colon cancer patients (HR = 3.41, 95% CI = 0.92–12.68, Log rank p = 0.052, Fig. 2B). The encoded protein is thought to be involved in regulating actin cytoskeleton remodeling. These observations suggest that *EPS8L2* expression can be modulated by FOLFOXIRI, and subsequent inhibition of cell migration may contribute to metastasis-suppressing function and increased sensitivity to therapy.

Discussion

In this study, we attempted to identify biomarkers associated with FOLFOXIRI response by comparing the transcriptome of primary colon tumors and their matched liver metastatic lesions in mCRC patients. Our data suggested that the use of neoadjuvant FOLFOXIRI, either as a single agent or with cetuximab, had a significant impact on gene expression changes in both primary tumor and metastases.

Previous studies have mainly examined the molecular changes at the genomic level that occur during doublet first-line systemic therapy in mCRC patients. In particular, the comparison of the copy number aberration landscape in liver metastases before and after chemotherapy revealed genomic variations that have a direct impact on the transcriptome (14). A pilot Japanese study indicated that the mutation rate and mutation spectrum were nearly identical regardless of FOLFOX therapy in the four recurrent colorectal cancer cases (15). However, some gene amplifications were observed only in the pre- and post-FOLFOX metastasis specimens compared to the primary tumor, suggesting that copy number variations can change during tumor progression. A recent multicenter prospective biomarker study, REVEAL, supported the differentially expressed gene data between pre-therapeutic primary tumor and post-therapeutic liver metastasis using a Nanostring assay with a 770 cancer-related gene panel (16). Although large mCRC case numbers treated with different chemotherapy regimens were recruited in this study, including six patients who received FOLFOXIRI with either bevacizumab or panitumumab, the impact of each regimen on the

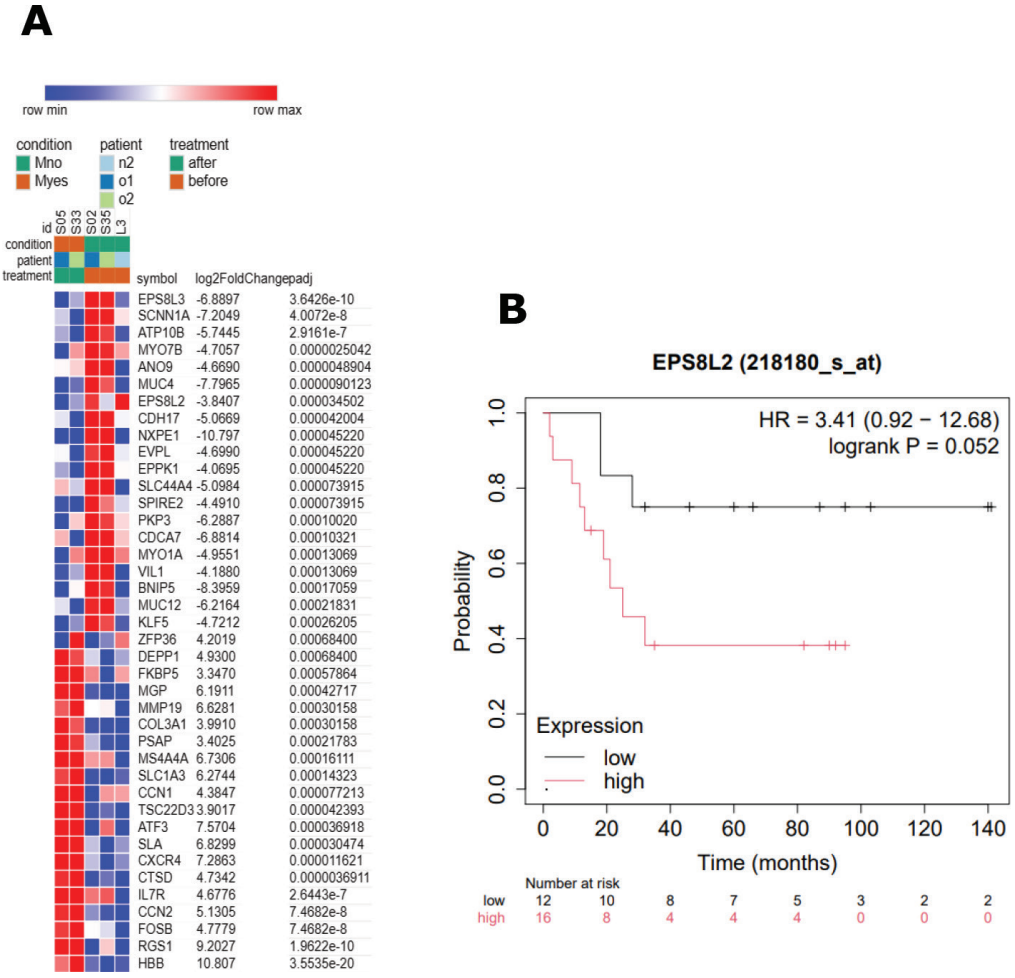

FIGURE 2 - Comparative transcriptome of liver metastases associated with complete response and validation of *EPS8L2* expression based on Kaplan Meier plotter. Heatmap with differentially expressed genes (DEGs) in a patient with complete response of liver metastatic lesions (A); Relapse-free survival stratified by *EPS8L2* expression for colon cancer patients (B).

gene expression signature was not assessed (16). In contrast to the REVEAL study, our results indicate transcriptional differences between primary tumors and liver metastases during neoadjuvant FOLFOXIRI, with the DEGs pattern changing between paired pre- and post-treatment specimens.

We identified an EPS8L2 transcript that could potentially be associated with the complete liver metastasis response and mCRC prognosis. It was recently known to be involved in nuclear movement and cell migration (17). Furthermore, there is clear evidence of the epidermal growth factor receptor pathway substrate 8 (Eps8) involvement in drug response in cell lines (18,19), and it is possible that EPS8L2 will also play a role in regulating drug resistance. The correlation between *EPS8L2* expression and patient survival based on publicly available data suggests its potential utility as a prognostic marker.

It is important to note a number of limitations of this study. Despite the prospective data set, we were able to analyze only a small number of cases. Also, the lack of non-responders in our cohort limits the study's predictive power. Indeed, selecting patients with resectable mCRC who are eligible for neoadjuvant chemotherapy appears to be challenging. However, to our knowledge, this is the first prospective study comparing the transcriptome of primary colon tumors and their matched liver metastatic lesions in resectable mCRC patients who were treated with neoadjuvant FOLFOXIRI. In addition, one of the strengths of this study was the systematic collection of two specimen sets, including colon tumor and liver metastasis, as well as normal colon and liver tissue before treatment, and the same data set after resection. Although we demonstrated a significant impact of FOLFOXIRI on gene expression in both primary tumor and liver metastases and identified *EPS8L2* as a potential biomarker of liver metastasis response, our data was preliminary; therefore, further studies with larger metastatic lesion cohorts are needed.

Conclusion

In summary, our mCRC case series demonstrated that the use of neoadjuvant FOLFOXIRI, both alone or in combination with cetuximab, leads to an alteration of the transcriptomic signature of primary colon tumors and matched liver metastatic loci. The pattern of DEGs changes between paired specimens of both primary tumor and metastases before and after treatment. Distinct patterns of DEGs are involved in the primary colon tumor and liver metastasis response. The EPS8L2 transcript identified in the liver metastatic lesion could serve as a candidate biomarker of liver complete response; however, prognostic conclusions cannot be drawn from this cohort.

Acknowledgments

The authors would like to thank Pavel Iamshchikov for technical assistance of RNA sequencing.

Disclosures

Conflict of interest: The authors have no conflicts of interest to declare that are relevant to the content of this article.
Financial support: The study was supported by the Russian Science Foundation, grant #22-15-00212; Online.

Ethical approval: The study was approved by the Ethics Committee of the Tomsk Cancer Research Institute (Approval No. 2022–0122) and has been performed in accordance with the Helsinki Declaration and its later amendments.
Informed consent: Informed consent was obtained from all individual participants included in the study.
Data availability statement: The data that support the findings of this study are available from the corresponding author upon reasonable request.
Author Contributions: All authors contributed to the study conception and design. Material preparation, data collection and analysis were performed by DE, AD, DK, SV, PG, SA, and NC**.** The first draft of the manuscript was written by NB and TD, and all authors commented on previous versions of the manuscript. All authors read and approved the final manuscript.

References

1. Benson AB, Venook AP, Al-Hawary MM, et al. Colon Cancer, Version 2.2021, NCCN clinical practice guidelines in oncology. *J Natl Compr Canc Netw*. 2021;19(3):329-359. CrossRef PubMed
2. Vatandoust S, Price TJ, Karapetis CS. Colorectal cancer: metastases to a single organ. World J Gastroenterol. 2015;21(41): 11767–11776. CrossRef.
3. Cervantes A, Adam R, Roselló S, et al.; ESMO Guidelines Committee. Metastatic colorectal cancer: ESMO Clinical Practice Guideline for diagnosis, treatment and follow-up. *Ann Oncol*. 2023;34(1):10-32. CrossRef PubMed
4. Falcone A, Ricci S, Brunetti I, et al.; Gruppo Oncologico Nord Ovest. Phase III trial of infusional fluorouracil, leucovorin, oxaliplatin, and irinotecan (FOLFOXIRI) compared with infusional fluorouracil, leucovorin, and irinotecan (FOLFIRI) as first-line treatment for metastatic colorectal cancer: the Gruppo Oncologico Nord Ovest. *J Clin Oncol*. 2007;25(13):1670-1676. CrossRef PubMed
5. Masi G, Vasile E, Loupakis F, et al. Randomized trial of two induction chemotherapy regimens in metastatic colorectal cancer: an updated analysis. *J Natl Cancer Inst*. 2011;103(1):21-30. CrossRef PubMed
6. Zhang W, Zhou H, Jiang J, et al. Neoadjuvant chemotherapy with modified FOLFOXIRI for locally advanced rectal cancer to transform effectively EMVI and MRF from positive to negative: results of a long-term single center phase 2 clinical trial. *BMC Cancer*. 2023;23(1):592. CrossRef PubMed
7. Bond MJG, Bolhuis K, Loosveld OJL, et al.; Dutch Colorectal Cancer Study Group. First-line systemic treatment strategies in patients with initially unresectable colorectal cancer liver metastases (CAIRO5): an open-label, multicentre, randomized, controlled, phase 3 study from the Dutch Colorectal Cancer Group. *Lancet Oncol*. 2023;24(7):757-771. CrossRef PubMed
8. Cremolini C, Antoniotti C, Rossini D, et al.; GONO Foundation Investigators. Upfront FOLFOXIRI plus bevacizumab and reintroduction after progression versus mFOLFOX6 plus bevacizumab followed by FOLFIRI plus bevacizumab in the treatment of patients with metastatic colorectal cancer (TRIBE2): a multicentre, open-label, phase 3, randomized, controlled trial. *Lancet Oncol*. 2020;21(4):497-507. CrossRef PubMed
9. Hu H, Wang K, Huang M, et al. Modified FOLFOXIRI with or without cetuximab as conversion therapy in patients with RAS/BRAF wildtype unresectable liver metastases colorectal cancer: the FOCULM multicenter phase II trial. *Oncologist*. 2021;26(1):e90-e98. CrossRef PubMed
10. Folprecht G, Martinelli E, Mazard T, et al. Triplet chemotherapy in combination with anti-EGFR agents for the treatment of metastatic colorectal cancer: current evidence, advances,

and future perspectives. *Cancer Treat Rev*. 2022;102:102301. CrossRef PubMed
11. Mandard AM, Dalibard F, Mandard JC, et al. Pathologic assessment of tumor regression after preoperative chemoradiotherapy of esophageal carcinoma. Clinicopathologic correlations. *Cancer*. 1994;73(11):2680-2686. CrossRef PubMed
12. Benjamini Y, Hochberg Y. Controlling the false discovery rate: a practical and powerful approach to multiple testing. *J R Stat Soc Series B Stat Methodol*. 1995;57(1):289-300. CrossRef
13. Győrffy B. Integrated analysis of public datasets for the discovery and validation of survival-associated genes in solid tumors. *Innovation (Camb)*. 2024;5(3):100625. CrossRef PubMed
14. Gambaro K, Marques M, McNamara S, et al. Copy number and transcriptome alterations associated with metastatic lesion response to treatment in colorectal cancer. *Clin Transl Med*. 2021;11(4):e401. CrossRef PubMed
15. Harada K, Okamoto W, Mimaki S, et al. Comparative sequence analysis of patient-matched primary colorectal cancer, metastatic, and recurrent metastatic tumors after adjuvant FOLFOX chemotherapy. *BMC Cancer*. 2019;19(1):255. CrossRef PubMed
16. Calero-Cuenca FJ, Osorio DS, Carvalho-Marques S, et al. Ctdnep1 and Eps8L2 regulate dorsal actin cables for nuclear positioning during cell migration. *Curr Biol*. 2021;31(7):1521-1530.e8. CrossRef PubMed
17. Luo K, Zhang L, Liao Y, et al. Effects and mechanisms of Eps8 on the biological behaviour of malignant tumours (Review). [Review]. *Oncol Rep*. 2021;45(3):824-834. CrossRef PubMed
18. Huang R, Liu H, Chen Y, et al. EPS8 regulates proliferation, apoptosis and chemosensitivity in BCR-ABL positive cells via the BCR-ABL/PI3K/AKT/mTOR pathway. *Oncol Rep*. 2018;39(1):119-128. CrossRef PubMed
19. Gorsic LK, Stark AL, Wheeler HE, et al. EPS8 inhibition increases cisplatin sensitivity in lung cancer cells. *PLoS One*. 2013;8(12):e82220. CrossRef PubMed

JCB
J Circ Biomark 2025; 14: 54-63
ISSN 1849-4544 | DOI: 10.33393/jcb.2025.3608
ORIGINAL RESEARCH ARTICLE

Anti-CENP-A/B reactivity in samples exhibiting the centromere HEp-2 pattern is associated with a lower frequency of interstitial lung disease in limited cutaneous systemic sclerosis patients

Gerson D Keppeke[1,2], Diana Landoni[2-4], Cristiane Kayser[2], Pedro Matos[2], Larissa Diogenes[2], Jessica Keppeke[5], Silvia Helena Rodrigues[2], Luis Eduardo C Andrade[2,5]

[1]Departamento de Ciencias Biomédicas, Facultad de Medicina, Universidad Católica del Norte, Coquimbo - Chile
[2]Disciplina de Reumatologia, Departamento de Medicina, Universidade Federal de São Paulo - Brasil
[3]Escuela de Graduados, Facultad de Medicina, Universidad de la República, Montevideo - Uruguay
[4]Laboratorio de Análisis Clínicos, LAC, Montevideo - Uruguay
[5]Immunology Division, Fleury Medicine and Health Laboratories, Sao Paulo - Brazil

ABSTRACT

Introduction: Anti-centromere antibodies are associated with limited cutaneous systemic sclerosis (lcSSc) and a more favorable prognosis. The centromere HEp-2 pattern (AC-3) suggests the presence of antibodies against CENP antigens, mainly CENP-B/A. This study analyzed clinical and demographic associations of anti-centromere antibodies in a cohort of patients exclusively with the lcSSc form of SSc. The frequency of CENP-B and CENP-A reactivity in samples with the AC-3 pattern was also evaluated.

Method: Samples from 38 lcSSc patients with AC-3 were evaluated for reactivity to CENP-B/A using line-blot and ELISA. Clinical data from 68 lcSSc patients (20 AC-3 and 48 Non-AC-3) were analyzed.

Results: Of the AC-3 samples, 84% and 82% were reactive against CENP-B and CENP-A, respectively, by line-blot, and 92% were positive for CENP-B by ELISA. Concordance for CENP-B reactivity between ELISA and line-blot was 79%. Reactivity to both CENP-B and CENP-A was found in 68% of AC-3 samples, while one sample was positive only for CENP-A. Overall, 97% of AC-3 samples were reactive to CENP-B, and all were reactive to either CENP-B or CENP-A. Clinically, interstitial lung disease (ILD) was less frequent in AC-3 patients compared to Non-AC-3 (10.5% vs. 54.2%; p = 0.001). Other organ involvement frequencies were similar.

Conclusion: ILD was less frequent in lcSSc patients with a positive AC-3 pattern as compared to those with a non-AC-3 pattern, which could suggest a less severe prognosis. In addition, anti-CENP-B was the predominant autoantibody in samples yielding the AC-3 pattern, but anti-CENP-A reactivity was also prevalent, and exclusive anti-CENP-A reactivity was also observed.

Keywords: Autoantibodies, Centromere, Fluorescent antibody technique, HEp-2 cells, Immunoassay, Systemic scleroderma

Introduction

Systemic sclerosis (SSc) is a chronic, heterogeneous autoimmune rheumatic disease characterized by high mortality and morbidity. This condition involves immune dysregulation, vasculopathy in small arteries and capillaries, and excessive collagen production, resulting in fibrosis of the skin and internal organs (1-5). According to the extent of skin involvement, SSc can be classified into: a) Limited cutaneous SSc (lcSSc) that involves the face and the skin distal to the elbows and knees; b) Diffuse cutaneous SSc (dcSSc) that involves the face, chest, trunk, and the skin both distal and proximal to the elbows and knees; and c) Absent skin involvement (SSc *sine scleroderma*) (6). It is also possible to classify SSC according to the presence of autoantibodies. Some autoantibodies are more associated with lcSSc, such as anti-centromere, anti-Th/To, and anti-PM-Scl, while others are more associated with dcSSc and multi-organ involvement, such as anti-topoisomerase I, anti-RNA polymerase III, and anti-fibrillarin [a comprehensive review can be found elsewhere (3)]. Each

Received: July 18, 2025
Accepted: November 11, 2025
Published online: November 26, 2025

This article includes supplementary material.

Corresponding author:
Gerson D. Keppeke
email: gerson.keppeke@ucn.cl

of these autoantibodies is related to specific disease manifestations, which makes them valuable tools for estimating prognosis in a given patient (3). Furthermore, the 2013 American College of Rheumatology and the European League Against Rheumatism (ACR/EULAR) improved the classification criteria for SSc by introducing a scoring system that includes clinical and laboratory elements (7).

Anti-centromere antibody is one of the most frequent in SSc (8). However, these can also be found at lower frequencies in other autoimmune diseases, including Sjögren disease, primary biliary cholangitis, isolated Raynaud's phenomenon, and overlap syndromes (9). Nevertheless, they are considered highly specific for SSc (>90%) and have been reported to precede the onset of clinical disease by months or years (10). In fact, the guidelines of ACR/EULAR indicate that the overall diagnostic sensitivity and specificity of anti-centromere antibody detected by indirect immunofluorescence assay on HEp-2 cells (HEp-2 IFA) were 31% and 97.4%, respectively, compared with patients with other systemic autoimmune rheumatic diseases (SARD) (6, 11-13).

When tested by HEp-2 IFA, anti-centromere antibodies reveal a characteristic, discrete speckled nuclear pattern scattered throughout interphase cells and aligned at the chromatin mass on mitotic cells, compatible with the topography of the centromeres (Figure 1A). This pattern is classified as the AC-3 pattern according to the International Consensus on Antinuclear Antibody (ANA) Patterns (ICAP; Online) (14,15). Structurally, the centromere is the region where condensed chromatin assembles to the inner and outer kinetochore to attach to the microtubules, which are responsible for chromosome segregation during cell division. Although there are many CENP proteins (CENP-A, -B, -C, -D, -E, -F, -G, H) in the kinetochore (9,16), CENP-B and CENP-A are the main autoantigens, as they are most consistently correlated with the AC-3 positive pattern on HEp-2 IFA observed in autoimmune patients (12,17). CENP-C is also the target of autoantibodies and likely yields the AC-3 pattern, but is usually found in association with antibodies to CENP-B or CENP-A (9,18,19).

The 17kDa CENP-A and the 80kDa CENP-B share a cryptic linear epitope motif named G/A-PR/S-R-R mapped towards the C-terminal portion of CENP-B and the N-terminal charged region of CENP-A, which is the main epitope target of anti-centromere autoantibodies (16, 20-22). This may explain the nearly identical prevalence of reactivity to CENP-A and CENP-B in antigen-specific solid-phase assays among samples with the AC-3 centromere pattern in the HEp-2 IFA, leading some authors to suggest that ELISA could replace HEp-2 IFA, considering the level of expertise required for the HEp-2 IFA pattern analysis (12). However, it is important to remember that HEp-2-IFA is a screening assay and does not provide the exact specificity for the nuclear antigen. Although the correlation of the AC-3 pattern with CENP-B/A autoantibodies is high, it is not flawless, especially if the sample produces multiple HEp-2 IFA patterns that may override the AC-3 pattern (3).

The HEp-2 IFA test, previously known as antinuclear antibodies (ANA), is a highly sensitive method for the screening of anti-cellular antibodies (AC) (23). The HEp-2 IFA provides information on the antibody serum concentration (titer) and possible autoantigen target (pattern). Various techniques, including ELISA, CLIA (chemiluminescent immunoassay), immunodiffusion, and immunoblotting, can be applied to detect specific antigen reactivity (3,24). Multiplex bead-based assays and ELISAs, as well as dot/line-blots, allow for the simultaneous testing of several autoantibodies. However, these immunoassays usually use recombinant CENP-B or CENP-A proteins (12,25), which could affect sensitivity, as demonstrated for other autoantibody systems (26). Second-generation assays, like CytoBeads, combine IFA on HEp-2 cells and antigen-coated beads, creating a "2-in-1" solution for a one-step, two-level ANA test (27). This approach may be useful for diagnosing patients who might not be detected with a negative HEp-2 IFA test but are positive for CENP-B by other methods. In general, CENP-B/A-specific immunoassays tend to show good agreement rates (28).

Most studies addressing the clinical associations of anti-centromere antibodies comprise general cohorts of SSc patients. Because anti-centromere antibodies are strongly associated with the lcSSc form of the disease, the clinical traits traditionally associated with anti-centromere antibodies are those that characterize lcSSc. Therefore, it is not well established how the anti-centromere antibodies correlate with the clinical spectrum of lcSSc. In this study, the clinical associations of anti-centromere antibodies were analyzed in a pure cohort of lcSSc patients. In addition, the anti-centromere reactivity in HEp-2 IFA (AC-3 pattern) was compared with the results of specific immunoassays for anti-CENP-B and anti-CENP-A antibodies.

Objective

We analyzed the possible clinical and demographic associations of anti-centromere antibodies in a cohort of patients exclusively with the limited cutaneous form of SSc (lcSSc). In addition, we evaluated the frequency of reactivity to CENP-B and CENP-A in samples with the AC-3 pattern on the HEp-2 IFA test.

Methods

Patient samples

The patients were consecutively recruited from the Systemic Sclerosis Outpatient Clinic at Escola Paulista de Medicina, Federal University of São Paulo (UNIFESP), Brazil. Patients should meet the American College of Rheumatology/European League Against Rheumatism (ACR/EULAR) 2013 classification criteria for the limited cutaneous form of Systemic Sclerosis (lcSSc) (7). In accordance with the Declaration of Helsinki, the patients signed an informed consent form to participate in the study and the research was approved by the Ethics Committee at UNIFESP (Plataforma Brasil CAAE: 59126320.1.0000.5505).

Demographic and clinical features were cross-sectionally obtained from electronic medical records and reviewed by rheumatologists with expertise in SSc (C.K. and P.M.) as previously described (26,29,30). In brief, clinical data included age, sex, disease subtype, and disease duration (defined as the time between the first non-Raynaud symptom and the enrollment visit). Interstitial lung disease (SSc-ILD) was defined as the presence of interstitial abnormalities in chest

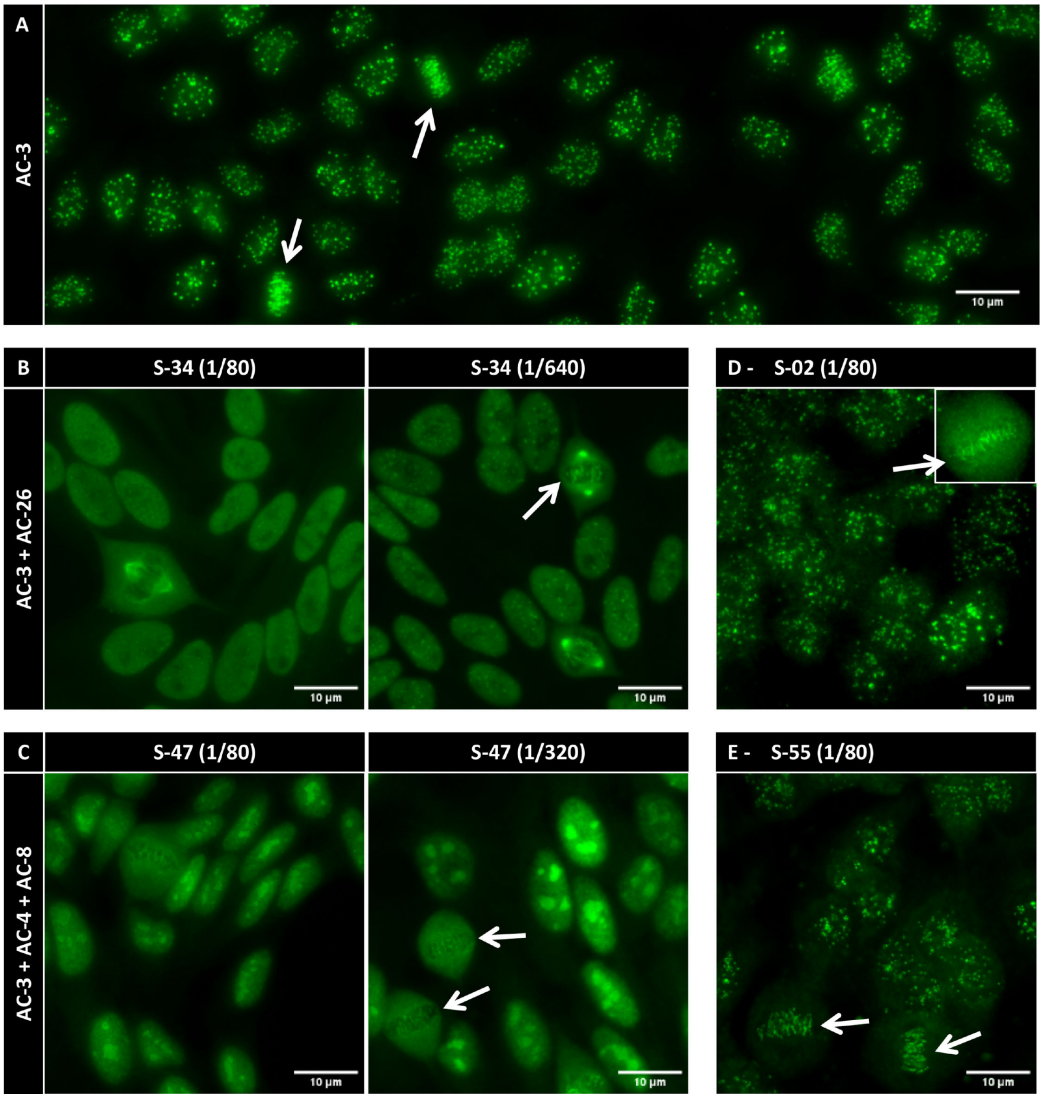

FIGURE 1 - Representative images of the HEp-2 IFA for samples with the AC-3 centromere pattern. (A) The typical AC-3 pattern. (B) Sample S34 with multiple patterns combining the centromere AC-3 and the NuMA-like AC-26 patterns; the AC-3 became evident at higher dilution. (C) Sample S47 with multiple patterns combining the nuclear fine speckled AC-4, the nucleolar homogeneous AC-8, and the centromere AC-3 patterns; the AC-3 became evident at higher dilution. (D-E) Sample S02 had reactivity to CENP-B in the line-blot but not in the ELISA. Sample S55 was negative for CENP-B in both methods, but was positive for anti-CENP-A in the line-blot (Figure 3D). Arrows in all panels indicate the characteristic metaphase plate of the AC-3 pattern. Scale bar = 10 µm.

high-resolution computerized tomography (HRCT) and a forced vital capacity (FVC) on pulmonary function test lower than 80%. Pulmonary arterial hypertension (PAH) was considered in patients with group I PAH confirmed by right heart catheterization, according to previously established criteria (31). Esophageal dysmotility was considered when confirmed in an esophagogram or esophageal manometry.

The lcSSc patients were tested in the HEp-2 IFA test and subdivided into two groups according to the presence of the AC-3 pattern in the HEp-2 IFA test respectively, the AC-3 group and the Non-AC-3 group.

Assays

The pattern and titer of the HEp-2-IFA were determined using commercial HEp-2 cell slides (#FA 1520-2010, Euroimmun; #51.100, AESKU), following the manufacturer's protocol, with a 1/80 starting dilution and serial dilutions up to 1/2560. The slides were analyzed and images captured at 400x magnification using a fluorescent microscope (Axio Imager.M2, Carl Zeiss).

Anti-CENP-B reactivity was assessed using an indirect ELISA kit (#ORG 633, Orgentec), following the manufacturer's protocol. A four-parameter logistic curve with four known concentration standards was applied (Figure 2B), and the interpolation of the samples' optical density allowed the determination of anti-CENP-B reactivity in each sample in arbitrary units (U/mL). Samples with >10 U/mL were considered positive for anti-CENP-B, as recommended by the manufacturer. In addition, reactivity to CENP-A and CENP-B was determined by immunoblot (Euroline Systemic Sclerosis Nucleoli profile kit; Cat# DL 1532-6401 G, Euroimmun) following the manufacturer's protocol (Figure 3). Although this kit can determine reactivity to other antigens, for this study, we only considered reactivity to the CENP antigens. The manufacturer recommends interpretation of the line-blot result as: (-) negative; (+) one plus as *borderline*; (≥++) two "pluses" or more, as positive. Because one plus (*borderline*) may not represent true positives, as we have shown for other autoantigens (26), we considered positive samples only those with the immunostaining intensity (≥++) two or more "pluses" (Fig. 3).

Data analysis

Immunofluorescence images were processed and panels assembled using ImageJ v1.53r software. Statistical analyses were performed using the software GraphPad Prism v7.0 or JASP v0.19.1. When comparing proportions, the two-tailed Fisher's exact test was applied. Quantitative and semi-quantitative parameters were assessed for normality distribution with the Shapiro–Wilk test, followed by comparison with Mann–Whitney or Student t-test according to the distribution pattern. Correlations were evaluated with the Spearman r-test. P values were considered significant when below 0.05. A Venn diagram was built with the Venny 2.1 online tool.

Results

There were 76 lcSSc patients, 38 classified into the AC-3 group and 48 classified into the Non-AC-3 group according to the presence of circulating anti-centromere antibodies. Concerning the AC-3 group, 29 (76%) patients showed a pure AC-3 pattern (Figure 1A) and nine (24%) patients showed a combination of the AC-3 pattern and other HEp-2 IFA patterns (Table 1). In this multiple pattern configuration, the centromere component tended to become more evident as the samples were further diluted (Figure 1B-C).

All samples were evaluated for anti-CENP-B reactivity in an indirect ELISA (Figure 2). Surprisingly, two samples that were originally not classified in the AC-3 group also tested positive, with reactivity above the cutoff of 10 U/mL (blue data-points in Fig. 2A). These two samples (S34 and S47) were re-evaluated by serial dilution HEp-2 IFA and showed the discrete speckles at the metaphase plate typical of the centromere pattern at 1/640 and 1/320, respectively (arrows in Figure 1B and 1C). Consequently, we reclassified these two samples as containing more than one pattern, including the AC-3, and thus part of the AC-3 group (n = 38). The AC-3 titer ranged from 1/80 to the highest dilution of 1/2560, with a median of 1/640 and a mean of 1/987 (Table 1 and Supplementary Fig. 1B).

As for the HEp-2 IFA pattern in the Non-AC-3 group, there were five negative samples (AC-0) and 43 with various patterns, such as nuclear fine speckled (AC-4; n = 12), nuclear coarse speckled (AC-5; n = 9), nucleolar (AC-8/9/10; n = 15), DNA topoisomerase I (topo I)-like (AC-29; n = 7), and miscellaneous patterns (AC-11, AC-18, AC-19, AC-21, AC-25; n = 5), including six samples (14%) with more than one pattern.

Regarding the anti-CENP-B reactivity measured by ELISA, three (8%) of the 38 samples with AC-3 had results below the cutoff (Fig. 2A), although all three samples had the AC-3 pattern at moderate intensity (titer 1/320; examples in Figures 1D and 1E). Therefore, 35 (92%) of the AC-3 samples were positive for anti-CENP-B by ELISA (Table 1).

Reactivity to CENP-B and CENP-A was also evaluated using a line-blot assay (Fig. 3). Most samples reacted with CENP-A and CENP-B (Fig. 4), and one sample reacted only with CENP-A (Fig. 3D). Seven samples reacted only with CENP-B (Figures 3E and 4). Altogether, the line-blot assay with the 38 AC-3 samples showed that 32 (84%) were reactive against CENP-B and 31 (82%) were reactive against CENP-A (Table 1 and Fig. 4). From the three samples negative for anti-CENP-B antibodies in ELISA (Fig. 2A), two were positive for anti-CENP-B

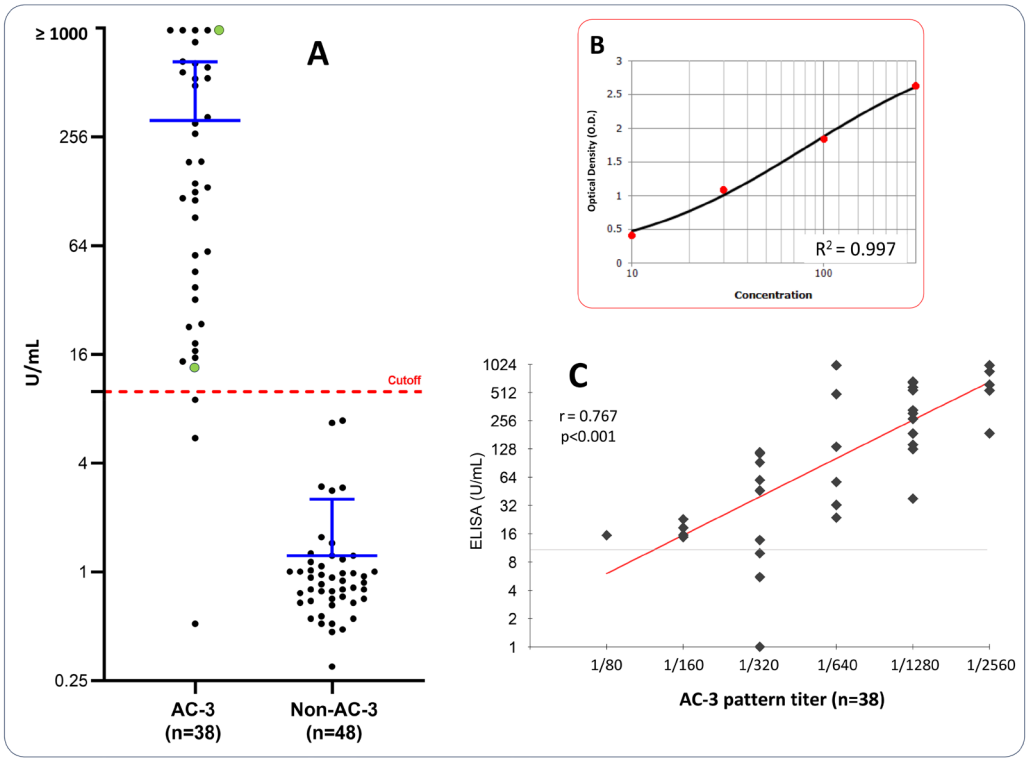

FIGURE 2 - Reactivity to CENP-B in ELISA. (A) Anti-CENP-B reactivity tested by indirect ELISA. Distribution of anti-CENP-B reactivity in U/mL. The cutoff (red dotted line) was set at 10 U/mL as recommended by the manufacturer. The two data points in green indicate the two samples in which AC-3 was not initially reported, but it was observed in the HEp-2-IFA upon re-evaluation with serial dilution, as detailed in Figures 1B and C. The blue line indicates the mean ±SD. (B) A representative standard four-parameter logistic curve for the ELISA with anti-CENP-B standards. (C) Correlation between Anti-CENP-B reactivity by ELISA and the AC-3 pattern titer.

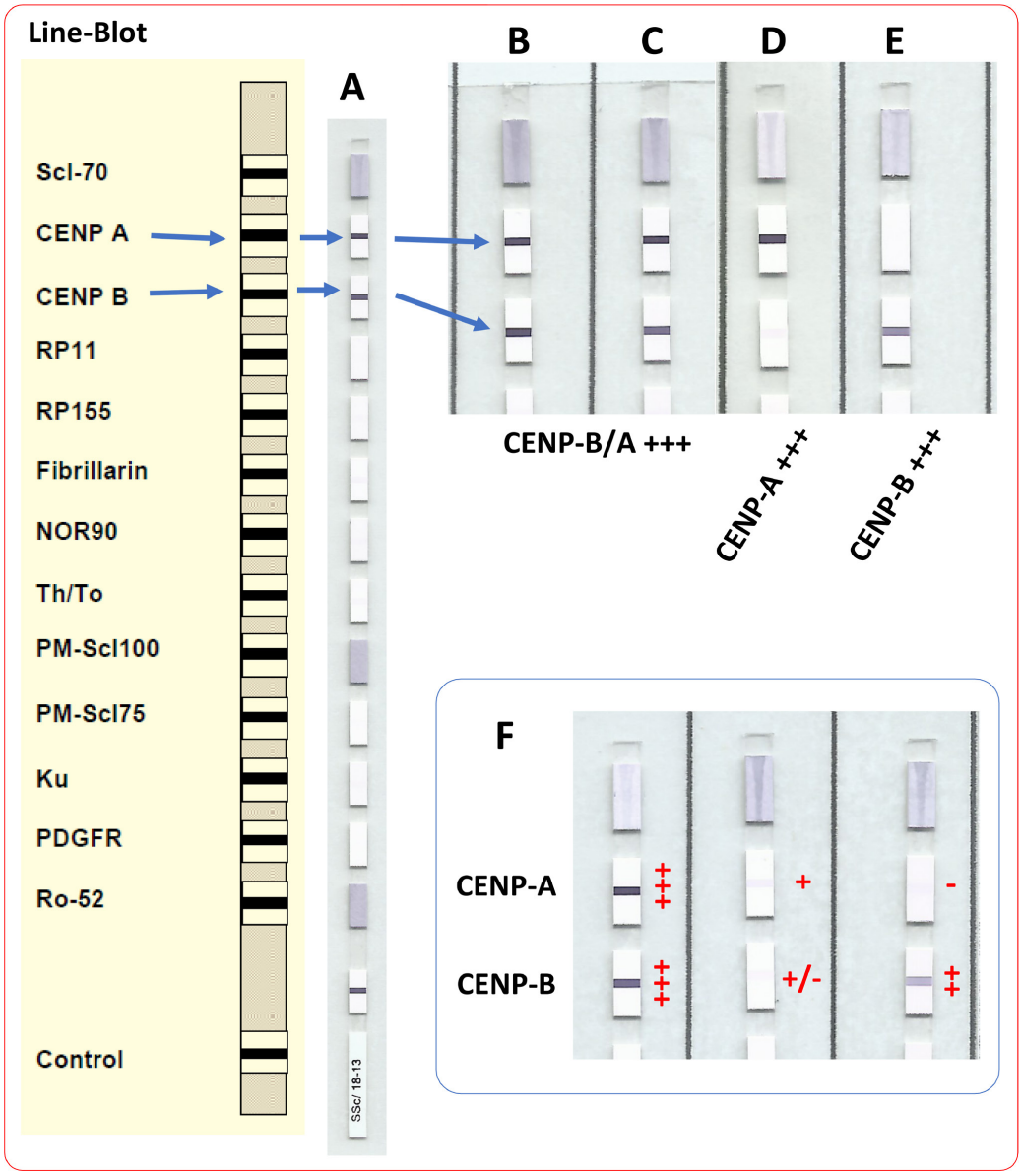

FIGURE 3 - Anti-CENP reactivity in line-blot. (A-E) Euroline Systemic Sclerosis profile, (A-C) representative samples with 3 pluses (+++) reactivity to anti-CENP-A and B, (D) representative sample with anti-CENP-A reactivity (+++) and CENP-B (+/-) considered negative, and (E) representative sample with anti-CENP-B reactivity (+++) only. (F) Examples for interpretation of line-blot results, only reactivity (≥++) was considered a true positive, as detailed in the methods.

in the line-blot assay, and one (S55, Fig. 1E) was positive only for anti-CENP-A (Figs 3D and 4).

When comparing the reactivity to CENP-B in ELISA and line-blot assay, 30 (79%) samples were reactive against CENP-B in ELISA and line-blot methods (Figure 4). One sample was reactive against CENP-B only in ELISA, and two samples were reactive against CENP-B only in line-blot. Altogether, all 38 AC-3 samples (100%) showed reactivity against either CENP-B or CENP-A in at least one of the antibody-specific immunoassays. Only one sample was reactive exclusively against CENP-A, meaning that 37 (97%) were reactive against CENP-B in at least one method (Figure 4).

The correlation between the AC-3 titer in the HEp-2-IFA and the CENP-B reactivity in U/mL levels obtained in ELISA in the 38 AC-3 samples was high, r = 0.767 (95% Confidence Interval 0.587-0.875; $p < 0.001$). The correlation between the intensity of CENP-B reactivity in ELISA and the line-blot assay was satisfactory, r = 0.594 (95% CI 0.330-0.772; $p < 0.001$) (Table 1, Fig. 2C and Supplementary Figs 1C-F).

Clinical information was available for 20 patients from the AC-3 group (of whom 19 showed positive anti-CENP-B reactivity in ELISA and/or line-blot, and one showed reactivity only to CENP-A) and for 48 patients from the Non-AC-3 group. The demographic data and clinical characteristics of these 68 lcSSc patients are depicted in Table 2. Patients in the AC-3 group were significantly older than those in the Non-AC-3 group, but the duration of the disease was similar in the two groups (Table 2 and Supplementary Fig. 1A). Regarding organ involvement, interstitial lung disease (ILD) was less frequently observed in patients in the AC-3 group (n = 2, 10.5%) compared to those in the Non-AC-3 group (n = 26, 54.2%; p = 0.001), but the other parameters of organ involvement had similar frequency in the two groups (Table 2).

TABLE 1 - Anti-CENP-B/A reactivity in 38 samples with the AC-3 pattern

HEp-2 IFA	Single pattern	Multiple patterns (AC-3 + others[§])	
AC-3 pattern	29 (76.3%)	9 (23.7%)	
Titer range	1/80 (n = 1) to 1/2560 (n = 6)		
Median titer	1/640		
Mean AC-3 titer (±SD)	1/987 (±1/809)		
CENP-B ELISA	Positives ≥10 U/mL	Negatives <10 U/mL	
Proportions	35 (92.1%)	3 (7.9%)	
Median reactivity	141.5	5.5	
Mean reactivity (±SD)	323.3 (±340.8)	5.3 (±4.7)	
Line-Blot	Positive (≥++)	Negative (–) and ***Borderline*** (+)	
CENP-B	32 (84.2%)	6 (15.8%)	
CENP-A	31 (81.6%)	7 (18.4%)	
Correlation [#]	CENP-B ELISA	Line-Blot CENP-B	Line-Blot CENP-A
AC-3 pattern titer	0.767***	0.432**	0.419**
CENP-B ELISA	–	0.594***	0.578***
Line-Blot CENP-B	–	–	0.676***

§ AC-4, AC-7, AC-8, AC-11, AC-21, AC-26. # Spearman r; **p < 0.01; ***p < 0.001

Discussion

In this study, we analyzed the clinical and demographic characteristics of lcSSc patients according to the presence of anti-centromere autoantibodies and investigated the anti-CENP-B/A reactivity in samples displaying the AC-3 pattern in the HEp-2-IFA test. We showed that even among patients with the lcSSc subtype, the presence of antibodies against centromere was associated with a lower frequency of lung involvement, specifically ILD, which could suggest a better prognosis and less severe disease. As expected, we confirmed the strong association between the AC-3 pattern and anti-CENP-B/A, as 100% of the AC-3 samples were reactive against CENP-B and/or CENP-A in at least one of the used immunoassays. Interestingly, however, the concordance rate between the solid phase assays themselves was weaker, as the agreement in anti-CENP-B reactivity between the ELISA and line-blot methods was only 79% as opposed to 100% concordance between HEp-2 AC-3 pattern and anti-CENP-B/A reactivity in solid-phase immunoassays. We also confirmed previous findings indicating that CENP-B is the dominant centromere autoantigen, as 37 (97%) of the AC-3 samples recognized CENP-B in at least one solid phase immunoassay, whereas 31 (82%) of the AC-3 samples recognized CENP-A. In addition, among the 38 samples tested for antibodies to CENP-B and CENP-A, seven (~18%) reacted exclusively with CENP-B, and one (~3%) was reactive solely against CENP-A. This result aligns with the concept that the AC-3 pattern in the HEp-2 IFA test is strongly associated with autoantibodies to CENP-B and/or CENP-A, CENP-B being the dominant autoantigen (12,19,32).

The first publications describing the targets of autoantibodies that recognize centromeric antigens, namely the CENP proteins, as well as their association with lcSSc, date back almost half a century, resulting from studies conducted in Dr Eng Tan's laboratory in the early 1980s. At that time, lcSSc was classified by the presence of calcinosis, Raynaud's phenomenon, esophageal dysmotility, sclerodactyly, and telangiectasia, collectively known as the CREST syndrome (33-35). In SSc, as mentioned, the main autoantigens in samples with the AC-3 pattern are CENP-A and CENP-B (21). Interestingly, the primary epitope on CENP-A, the G/A-PR/S-R-R motif, is also present on CENP-B and CENP-C. In fact, anti-CENP-A/B/C are frequently found in association in the same patient (18,19). It is important to note that the G/A-PR/S-R-R motif is not the only target, as these autoantibodies likely recognize other non-shared antigenic regions, providing strong evidence of intra- and intermolecular epitope spreading (22). This is supported by our findings, where one patient showed reactivity only to CENP-A and seven showed reactivity only to CENP-B (and not to CENP-A), although we cannot rule out the presence of autoantibodies against other CENP antigens in these samples. Autoantibodies against CENP-A/B/C, as well as the less common CENP-D and CENP-E, and the very rare CENP-O (36), are all associated with lcSSc or the CREST syndrome (21,22,37). CENP-D is primarily of the IgM type and tends to disappear over time (38). Anti-CENP-E has been found in approximately 40% of patients with anti-CENP (39). Autoantibodies against CENP-H are associated with Sjögren disease, particularly in patients without anti-Ro/La antibodies (40). Finally, perhaps the most distinctive among the non-CENP-A/B antigens is

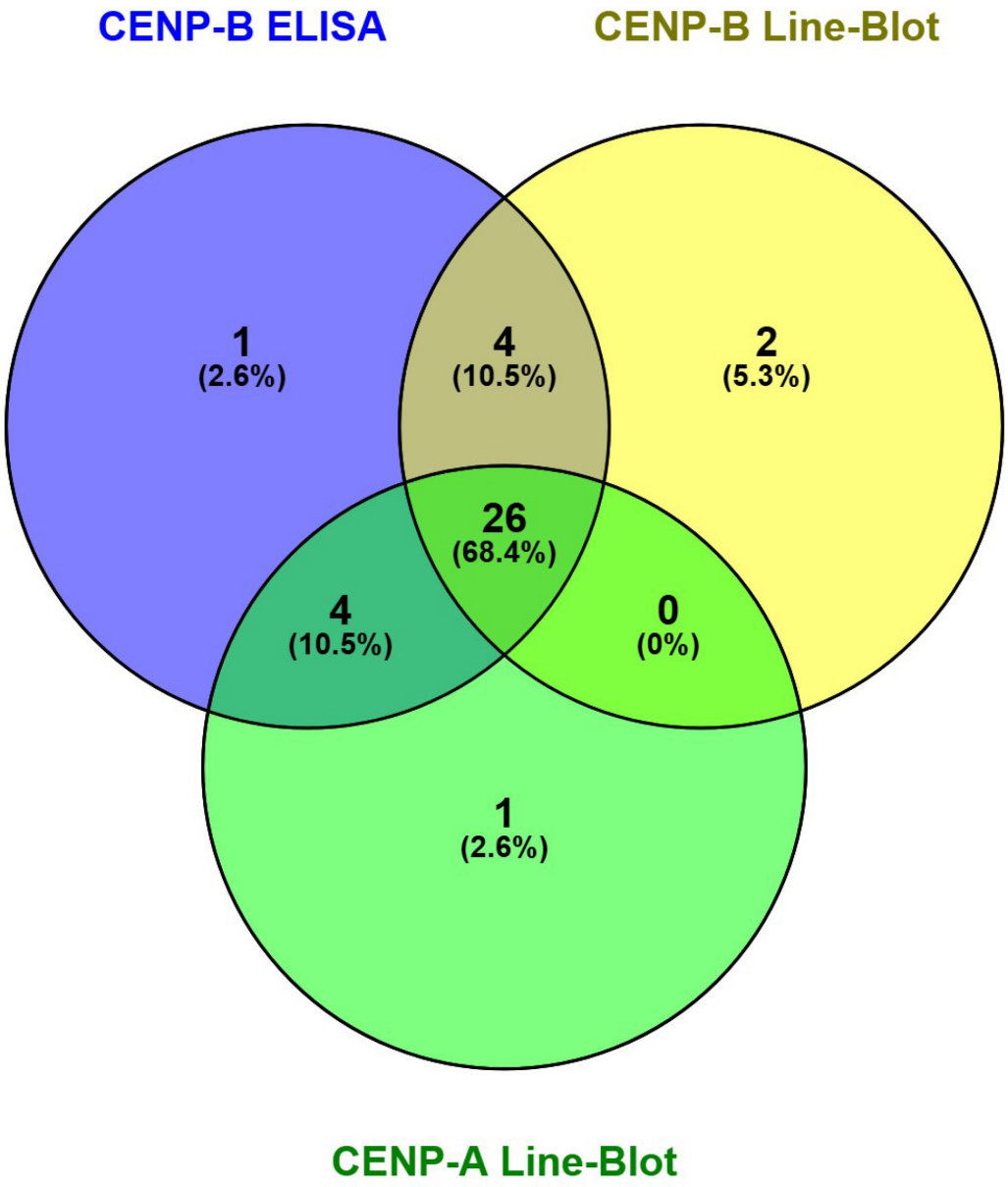

FIGURE 4 - Venn diagram for anti-CENP-B/A reactivity in ELISA and line-blot assays in samples from the AC-3 group.

CENP-F, a 330 kDa protein essential for cell cycle progression (41). Anti-CENP-F antibodies are associated with various types of malignancies rather than SSc, primary biliary cholangitis or Sjögren disease (42,43). These autoantibodies produce a different HEp-2 IFA pattern from the AC-3, referred to as the CENP-F-like pattern (AC-14) (41). The presence of anti-CENP-F antibodies may serve as a marker for cancer (44).

Choosing the most appropriate method to determine anti-centromere antibodies in patient samples is essential to ensure reliable results. In this study, no sample exhibited reactivity against CENP-B or CENP-A in the absence of the AC-3 pattern on the HEp-2 IFA. Conversely, all samples with the AC-3 pattern demonstrated reactivity against CENP-B/A in at least one assay. However, in some cases, the AC-3 pattern was visible only at higher dilutions and required a keen eye to identify the characteristic metaphase plate. Furthermore, we observed that some samples with the AC-3 pattern were negative in at least one of the solid-phase immunoassays. The concordance for CENP-B reactivity between ELISA and line-blot was less than 80%. Since clinical laboratories often use only one type of kit, they may fail to report samples with anti-centromere antibodies when relying solely on a solid-phase immunoassay. Thus, the data presented here provide additional evidence supporting the ACR/EULAR recommendation to use the indirect immunofluorescence assay on HEp-2 cells as the screening method for autoantibodies in rheumatic diseases, as commented elsewhere (45,46), and to consider the reported pattern when interpreting solid-phase immunoassay results.

TABLE 2 - Demographic and clinical features of the lcSSc patients according to the presence of anti-centromere pattern (AC-3) in HEp-2 IFA

Variable	AC-3 pattern (n = 20)	Non-AC-3 (n = 48)	*P*
Age, mean ± SD (years)	59.4 ± 12.5	50.5 ± 12.9	0.011
Female, n (%)	20 (100.0)	41 (85.4)	0.096
Disease duration, mean ± SD (years)	8.7 ± 6.3	6.6 ± 5.9	0.197
Organ involvement			
Digital ulcers, n (%)	5 (26.3)*	17 (35.4)	0.571
Esophageal dysmotility, n (%)	14 (73.7)*	38 (79.2)	0.747
Arthritis, n (%)	6 (31.6)*	19 (39.6)	0.588
FVC% of predicted, mean ± SD	84.5 ± 13.5	84.7 ± 19.9	0.967
ILD, n (%)	2 (10.5)*	26 (54.2)	0.001
PAH, n (%)	2 (10.5)*	7 (14.6)	1.000
Cardiac involvement, n (%)	0 (0.0)	2 (4.2)	1.000
Scleroderma renal crisis, n (%)	0 (0.0)	2 (4.2)	1.000

FVC: forced vital capacity; ILD: interstitial lung disease; PAH: pulmonary arterial hypertension
*Data available for 19 patients

Previous studies have demonstrated that anti-centromere autoantibodies display a less severe SSc disease and better prognosis (11,32). In fact, anti-centromere autoantibodies correlate with less frequent elevations in serum creatine kinase, digital ulcers, joint contractures, interstitial lung disease (ILD), scleroderma renal crisis, arthritis, and myositis, among others (12,32). However, these studies have inferred these associations in cohorts of patients with both forms of SSc, raising the possibility that the obtained associations are secondary to the primary association of anti-centromere antibodies to lcSSc, the more benign form of the disease. In our cohort constituted exclusively by lcSSc patients, we could confirm a lower frequency of ILD among lcSSc patients with anti-centromere antibodies compared with those without these autoantibodies. This finding suggests that the presence of anti-centromere antibodies further discriminates a subgroup of lcSS patients with a more favorable prognosis. In a cohort comprising exclusively lcSSc patients, anti-centromere antibodies were associated with better prognosis and less severe disease. As proposed by a recent publication, individual autoantibodies associate with specific SSc characteristics (32). Since ILD is the leading cause of death in SSc patients (47,48), our results suggest a less severe disease, indicated by the less frequent ILD in SSc patients with anti-centromere autoantibodies.

This study has some limitations that should be acknowledged. First, it was a cross-sectional analysis, which does not allow for assessment of the longitudinal evolution of patients, including potential reclassification of the lcSSc over time. This, as well as the relatively short disease duration in many patients, may partially explain the presence of some autoantibodies typically associated with dcSSc in the Non-AC-3 group. Second, clinical data were not available for all of the patients with a positive AC-3 pattern; however, the clinical findings were consistent with previous cohorts from our region (29, 47). Third, while we compared HEp-2 IFA with two solid-phase immunoassays, there are other platforms, such as the bead-based assays. Notably, we did not evaluate reactivity to CENP-A by ELISA. Finally, the relatively modest sample size may limit the generalizability of the findings, particularly regarding the frequency of less common lcSSc manifestations such as pulmonary hypertension, suggesting longitudinal studies with larger cohorts may be appropriate.

Conclusion

In conclusion, ILD was less frequent in lcSSc patients with positive AC-3 pattern as compared to those with no anti-centromere reactivity, which could suggest a less severe prognosis within the lcSSc spectrum for those patients with anti-CENP reactivity. All samples with the AC-3 centromere pattern in HEp-2 IFA displayed reactivity to CENP-B or CENP-A in at least one of the applied tests, meaning the HEp-2 IFA method was 100% sensitive in detecting antibodies to CENP-A and CENP-B. One sample showed reactivity only to CENP-A, and of the 38 samples with AC-3, ~82% were positive for CENP-A. Regarding CENP-B reactivity, ~84% were positive by line-blot and ~92% by ELISA, but only 30 samples were positive for CENP-B in both the ELISA and line-blot methods, with a concordance of <80%. This means that anti-CENP-B is the predominant autoantibody in samples yielding the AC-3 pattern, but exclusive anti-CENP-A reactivity can also occur less frequently, as observed in only one sample in our cohort.

Acknowledgments

Parts of the manuscript (introduction/discussion) were originally written in Portuguese or Spanish, the mother

language of the authors, and translated to English with the help of online tools such as ChatGPT with GPT-4-turbo (by OpenAI). The final text underwent proofreading for the English language; therefore, after using the online tools, the authors reviewed and edited the content and took full responsibility for the content of the publication.

Part of these data were previously presented at: "V Congreso de la Sociedad Médica de Laboratório Clínico", organized by SMLC in Santiago, Chile, September 26-27, 2024; "IFCC-EFLM EuroMedLab Congress" in Brussels, Belgium, May 18-22, 2025; "17th Dresden Symposium on Autoantibodies" in Germany, September 09-12, 2025. Additionally, part of the data was deposited as a preprint on medRxiv <CrossRef>.

Author contributions

G.D.K.: Conceptualization; Methodology; Investigation; Writing – Original Draft.; D.L.: Writing – Original Draft; C.K. and P.M.: Data Curation; Formal Analysis; Validation.; L.D., J.K., and S.H.R.: Investigation; Resources; Data Curation; Formal Analysis.; L.E.C.A.: Conceptualization; Supervision; Writing – Review & Editing. All authors read and approved the final manuscript.

Disclosures

Conflict of interest: The authors declare that they have no competing interests.

Financial support: This work was supported by the São Paulo Government agency FAPESP (São Paulo State Research Foundation) grant numbers #2017/20745-1, #2021/04588-9 and #2023/17946-6, granted to GDK, LD and CK, respectively. Additionally, LECA was supported by the Brazilian research agency National Council for Research (CNPq), grant #PQ-1D 310334/2019-5. GDK also received support during the development of this work from Agencia Nacional de Investigación y Desarrollo de Chile (ANID), project No. [86220018].

Ethics approval and consent to participate: In compliance with the Helsinki Declaration, the patients signed an informed consent form to participate in the study before donating their samples. The research was approved by the Local Ethics Committee at the Federal University of São Paulo (Plataforma Brasil CAAE: 59126320.1.0000.5505).

Data Availability Statement: The data presented in this study are available upon reasonable request from the corresponding author.

References

1. Denton CP, Khanna D. Systemic sclerosis. Lancet. 2017; 390(10103):1685-1699. CrossRef PubMed
2. Roofeh D, Khanna D. Management of systemic sclerosis: the first five years. Curr Opin Rheumatol. 2020;32(3):228-237. CrossRef PubMed
3. Stochmal A, Czuwara J, Trojanowska M, et al. Antinuclear antibodies in systemic sclerosis: an update. Clin Rev Allergy Immunol. 2020;58(1):40-51. CrossRef PubMed
4. van Leeuwen NM, Boonstra M, Bakker JA, et al. Anticentromere antibody levels and isotypes and the development of systemic sclerosis. Arthritis Rheumatol. 2021;73(12):2338-2347. CrossRef PubMed
5. Kowalska-Kępczyńska A. Systemic scleroderma-definition, clinical picture and laboratory diagnostics. J Clin Med. 2022; 11(9):2299. CrossRef PubMed
6. Johnson SR. New ACR EULAR guidelines for systemic sclerosis classification. Curr Rheumatol Rep. 2015;17(5):32. CrossRef PubMed
7. van den Hoogen F, Khanna D, Fransen J, et al. 2013 classification criteria for systemic sclerosis: an American College of Rheumatology/European League Against Rheumatism collaborative initiative. Ann Rheum Dis. 2013;72(11):1747-1755. CrossRef PubMed
8. Chepy A, Collet A, Launay D, et al. Autoantibodies in systemic sclerosis: from disease bystanders to pathogenic players. J Transl Autoimmun. 2025;10:100272. CrossRef PubMed
9. Kajio N, Takeshita M, Suzuki K, et al. Anti-centromere antibodies target centromere-kinetochore macrocomplex: a comprehensive autoantigen profiling. Ann Rheum Dis. 2021;80(5):651-659. CrossRef PubMed
10. Koenig M, Joyal F, Fritzler MJ, et al. Autoantibodies and microvascular damage are independent predictive factors for the progression of Raynaud's phenomenon to systemic sclerosis: a twenty-year prospective study of 586 patients, with validation of proposed criteria for early systemic sclerosis. Arthritis Rheum. 2008;58(12):3902-3912. CrossRef PubMed
11. Reveille JD, Solomon DH.; American College of Rheumatology Ad Hoc Committee of Immunologic Testing Guidelines. Evidence-based guidelines for the use of immunologic tests: anticentromere, Scl-70, and nucleolar antibodies. Arthritis Rheum. 2003;49(3):399-412. CrossRef PubMed
12. Hudson M, Mahler M, Pope J, et al.; Investigators of the Canadian Scleroderma Research Group. Clinical correlates of CENP-A and CENP-B antibodies in a large cohort of patients with systemic sclerosis. J Rheumatol. 2012;39(4):787-794. CrossRef PubMed
13. Matos P, Keppeke GD, Kayser C. Autoanticorpos específicos e associados na esclerose sistêmica: investigação e diagnóstico. Revista Paulista de Reumatologia. 2024;23(3):41-50. CrossRef
14. Chan EKL, Damoiseaux J, Carballo OG, et al. Report of the First International Consensus on standardized nomenclature of antinuclear antibody HEp-2 cell patterns 2014-2015. Front Immunol. 2015;6:412. CrossRef PubMed
15. Andrade LEC, Klotz W, Herold M, et al. Reflecting on a decade of the international consensus on ANA patterns (ICAP): accomplishments and challenges from the perspective of the 7th ICAP workshop. Autoimmun Rev. 2024;23(9):103608. CrossRef PubMed
16. Akbarali Y, Matousek-Ronck J, Hunt L, et al. Fine specificity mapping of autoantigens targeted by anti-centromere autoantibodies. J Autoimmun. 2006;27(4):272-280. CrossRef PubMed
17. Prasad RM, Bellacosa A, Yen TJ. Clinical and Molecular Features of Anti-CENP-B Autoantibodies. J Mol Pathol. 2021;2(4): 281-295. CrossRef
18. Earnshaw WC, Rothfield N. Identification of a family of human centromere proteins using autoimmune sera from patients with scleroderma. Chromosoma. 1985;91(3-4):313-321. CrossRef PubMed
19. Earnshaw W, Bordwell B, Marino C, et al. Three human chromosomal autoantigens are recognized by sera from patients with anti-centromere antibodies. J Clin Invest. 1986;77(2):426-430. CrossRef PubMed
20. Muro Y, Azuma N, Onouchi H, et al. Autoepitopes on autoantigen centromere protein-a (CENP-A) are restricted to the N-terminal region, which has no homology with histone H3. Clin Exp Immunol. 2000;120(1):218-223. CrossRef PubMed
21. Mahler M, Fritzler MJ. Epitope specificity and significance in systemic autoimmune diseases. Ann N Y Acad Sci. 2010; 1183(1):267-287. CrossRef PubMed

22. Fritzler MJ, Rattner JB, Luft LM, et al. Historical perspectives on the discovery and elucidation of autoantibodies to centromere proteins (CENP) and the emerging importance of antibodies to CENP-F. Autoimmun Rev. 2011;10(4):194-200. CrossRef PubMed
23. Damoiseaux J, Andrade LEC, Carballo OG, et al. Clinical relevance of HEp-2 indirect immunofluorescent patterns: the International Consensus on ANA patterns (ICAP) perspective. Ann Rheum Dis. 2019;78(7):879-889. CrossRef PubMed
24. Keppeke GD, Agustinelli RA, Landoni DM, et al. Chapter 88 – Future Direction of Laboratory Testing for Autoimmune Diseases. In: Schmitz JL, Detrick B, O'Gorman MRG, editors. Manual of Molecular and Clinical Laboratory Immunology, 9th Edition. 2. 9 ed. Washington, DC: Wiley & ASM Press; 2024. p. 968-82. CrossRef
25. Mahler M, You D, Baron M, et al.; Canadian Scleroderma Research Group (CSRG). Anti-centromere antibodies in a large cohort of systemic sclerosis patients: comparison between immunofluorescence, CENP-A and CENP-B ELISA. Clin Chim Acta. 2011;412(21-22):1937-1943. CrossRef PubMed
26. Keppeke GD, Satoh M, Kayser C, et al. A cell-based assay for detection of anti-fibrillarin autoantibodies with performance equivalent to immunoprecipitation. Front Immunol. 2022;13:1011110. CrossRef PubMed
27. Sowa M, Hiemann R, Schierack P, et al. Next-generation autoantibody testing by combination of screening and confirmation—the CytoBead® Technology. Clin Rev Allergy Immunol. 2017;53(1):87-104. CrossRef PubMed
28. Jang J, Kim S, Kim HS, et al. Comparison of antinuclear antibody profiles obtained using line immunoassay and fluorescence enzyme immunoassay. J Int Med Res. 2021;49(6):3000605211014390. CrossRef PubMed
29. de Oliveira SM, Martins LVO, Lupino-Assad AP, et al. Severity and mortality of COVID-19 in patients with systemic sclerosis: a Brazilian multicenter study. Semin Arthritis Rheum. 2022;55:151987. CrossRef PubMed
30. Kayser C, de Oliveira Delgado SM, Zimmermann AF, et al. 2023 Brazilian Society of Rheumatology guidelines for the treatment of systemic sclerosis. Adv Rheumatol. 2024;64(1):52. CrossRef PubMed
31. Humbert M, Kovacs G, Hoeper MM, et al.; ESC/ERS Scientific Document Group. 2022 ESC/ERS Guidelines for the diagnosis and treatment of pulmonary hypertension. Eur Respir J. 2023;61(1):2200879. CrossRef PubMed
32. Żebryk P, Przymuszała P, Nowak JK, et al. Autoantibodies and clinical correlations in Polish systemic sclerosis patients: a cross-sectional study. J Clin Med. 2023;12(2):657. CrossRef PubMed
33. Fritzler MJ, Kinsella TD, Garbutt E. The CREST syndrome: a distinct serologic entity with anticentromere antibodies. Am J Med. 1980;69(4):520-526. CrossRef PubMed
34. Moroi Y, Peebles C, Fritzler MJ, et al. Autoantibody to centromere (kinetochore) in scleroderma sera. Proc Natl Acad Sci USA. 1980;77(3):1627-1631. CrossRef PubMed
35. Tan EM, Rodnan GP, Garcia I, et al. Diversity of antinuclear antibodies in progressive systemic sclerosis. Anti-centromere antibody and its relationship to CREST syndrome. Arthritis Rheum. 1980;23(6):617-625. CrossRef PubMed
36. Saito A, Muro Y, Sugiura K, et al. CENP-O, a protein localized at the centromere throughout the cell cycle, is a novel target antigen in systemic sclerosis. J Rheumatol. 2009;36(4):781-786. CrossRef PubMed
37. Earnshaw WC, Machlin PS, Bordwell BJ, et al. Analysis of anticentromere autoantibodies using cloned autoantigen CENP-B. Proc Natl Acad Sci USA. 1987;84(14):4979-4983. CrossRef PubMed
38. Ford AL, Kurien BT, Harley JB, et al. Anti-centromere autoantibody in a patient evolving from a lupus/Sjögren's overlap to the CREST variant of scleroderma. J Rheumatol. 1998;25(7):1419-1424. PubMed
39. Rattner JB, Rees J, Arnett FC, et al. The centromere kinesin-like protein, CENP-E. An autoantigen in systemic sclerosis. Arthritis Rheum. 1996;39(8):1355-1361. CrossRef PubMed
40. Hsu TC, Chang CH, Lin MC, et al. Anti-CENP-H antibodies in patients with Sjögren's syndrome. Rheumatol Int. 2006;26(4):298-303. CrossRef PubMed
41. Casiano CA, Landberg G, Ochs RL, et al. Autoantibodies to a novel cell cycle-regulated protein that accumulates in the nuclear matrix during S phase and is localized in the kinetochores and spindle midzone during mitosis. J Cell Sci. 1993;106(Pt 4):1045-1056. CrossRef PubMed
42. Landberg G, Erlanson M, Roos G, et al. Nuclear autoantigen p330d/CENP-F: a marker for cell proliferation in human malignancies. Cytometry. 1996;25(1):90-98. CrossRef PubMed
43. Rattner JB, Rees J, Whitehead CM, et al. High frequency of neoplasia in patients with autoantibodies to centromere protein CENP-F. Clin Invest Med. 1997;20(5):308-319. PubMed
44. Welner S, Trier NH, Frisch M, et al. Correlation between centromere protein-F autoantibodies and cancer analyzed by enzyme-linked immunosorbent assay. Mol Cancer. 2013;12(1):95. CrossRef PubMed
45. Bossuyt X, Fieuws S. Detection of antinuclear antibodies: added value of solid phase assay? Ann Rheum Dis. 2014;73(3):e10. CrossRef PubMed
46. Pisetsky DS, Lipsky PE. Role of antinuclear antibody determinations in classification criteria for systemic lupus erythematosus: comment on the article by Leuchten et al. Arthritis Care Res (Hoboken). 2019;71(5):696. CrossRef PubMed
47. de Oliveira Martins LV, Oliveira SM, Silvatti J, et al. Mortality in systemic sclerosis-associated interstitial lung disease in Brazil: a real-life, long-term follow-up observational study. J Clin Rheumatol. 2022;28(2):e532-e538. CrossRef PubMed
48. Hoffmann-Vold AM, Petelytska L, Fretheim H, et al. Predicting the risk of subsequent progression in patients with systemic sclerosis-associated interstitial lung disease with progression: a multicentre observational cohort study. Lancet Rheumatol. 2025;7(7):e463-e471. CrossRef PubMed

Journal of Circulating Biomakers

www.aboutscience.eu

ISSN 1849-4544

ABOUTSCIENCE